BAŞKENT UNIVERSITY
INSTITUTE OF SCIENCE
DEPARTMENT OF MOLECULAR BIOLOGY AND GENETICS
MASTER OF SCIENCE IN
MOLECULAR BIOLOGY AND GENETICS

SINGLE-CELL RNA SEQUENCING IN ROOTS OF *ARABIDOPSIS THALIANA* EXPOSED TO BORON TOXICITY AT SEEDLING STAGE

BY

HİKMET YILMAZ

MASTER OF SCIENCE THESIS

ANKARA - 2023

BAŞKENT UNIVERSITY
INSTITUTE OF SCIENCE
DEPARTMENT OF MOLECULAR BIOLOGY AND GENETICS
MASTER OF SCIENCE IN
MOLECULAR BIOLOGY AND GENETICS

SINGLE-CELL RNA SEQUENCING IN ROOTS OF *ARABIDOPSIS THALIANA* EXPOSED TO BORON TOXICITY AT SEEDLING STAGE

BY

HİKMET YILMAZ

MASTER OF SCIENCE THESIS

ADVISOR

ASSOC. PROF. DR. CEYHUN KAYIHAN

ANKARA - 2023

BAŞKENT UNIVERSITY

INSTITUTE OF SCIENCE

This study, which was prepared by Hikmet YILMAZ, for the program of Master of science with Thesis (English), has been approved in partial fulfillment of the requirements for the degree of MASTER OF SCIENCE IN MOLECULAR BIOLOGY AND GENETICS Department by the following committee.

Date of Thesis Defense: 05/01/2023

Thesis Title: Single-Cell RNA Sequencing in Roots of *Arabidopsis thaliana* Exposed to Boron Toxicity at Seedling Stage

Examining Committee Members	**Signature**
Prof. Dr. Füsun EYİDOĞAN (Başkent University)	……..
Assoc. Prof. Dr. Ceyhun KAYIHAN (Başkent University)	……..
Asst. Prof. Dr. Emre AKSOY (Middle East Technical University)	……..

APPROVAL
Prof. Dr. Ömer Faruk ELALDI
Director, Institute of Science
Date: … / …

BAŞKENT UNIVERSITY
INSTITUTE OF SCIENCE
YÜKSEK LİSANS TEZ ÇALIŞMASI ORİJİNALLİK RAPORU

Date: … / … / 20…

Öğrencinin Adı, Soyadı : Hikmet YILMAZ
Öğrencinin Numarası : 22010447
Anabilim Dalı : Moleküler Biyoloji ve Genetik
Programı : Yüksek Lisans
Danışmanın Unvanı/Adı, Soyadı : Doç. Dr. Ceyhun KAYIHAN
Tez Başlığı : Single-cell RNA sequencing in roots of *Arabidopsis thaliana* exposed to boron toxicity at seedling stage

Yukarıda başlığı belirtilen Yüksek Lisans tez çalışmamın; Giriş, Ana Bölümler ve Sonuç Bölümünden oluşan, toplam 68. sayfalık kısmına ilişkin, 19/01/2023 tarihinde şahsım/tez danışmanım tarafından Tunitin adlı intihal tespit programından aşağıda belirtilen filtrelemeler uygulanarak alınmış olan orijinallik raporuna göre, tezimin benzerlik oranı % 19 'dur. Uygulanan filtrelemeler:

1. Kaynakça hariç
2. Alıntılar hariç
3. Beş (5) kelimeden daha az örtüşme içeren metin kısımları hariç

"Başkent Üniversitesi Enstitüleri Tez Çalışması Orijinallik Raporu Alınması ve Kullanılması Usul ve Esaslarını" inceledim ve bu uygulama esaslarında belirtilen azami benzerlik oranlarına tez çalışmamın herhangi bir intihal içermediğini; aksinin tespit edileceği muhtemel durumda doğabilecek her türlü hukuki sorumluluğu kabul ettiğimi ve yukarıda vermiş olduğum bilgilerin doğru olduğunu beyan ederim.

Öğrenci İmzası:…….

ONAY
Tarih: … / … / 20…
Öğrenci Danışmanı Unvan, Adı, Soyadı, İmza:
……..

ACKNOWLEDGEMENTS

I would like to express my endless thanks to my thesis advisor, Assoc. Prof. Dr. Ceyhun KAYIHAN who never spared his support and contributions to me at every stage of my thesis work, and who made great efforts by following every stage of my thesis with care and meticulousness. I would like to thank my lab mates Halis Batuhan ÜNAL and Oğuzhan YAPRAK for their hard work and contributions.

Finally, I would like to thank my dear wife Gönül VAY YILMAZ for sharing my worries with patience, my happiness with the same excitement, and for being with me at all times during this process.

ÖZET

Hikmet YILMAZ

FİDECİK AŞAMASINDA BOR TOKSİSİTİNE MARUZ BIRAKILAN *ARABIDOPSIS THALIANA* KÖKLERİNDE TEK HÜCRE RNA DİZİLEMESİ

Başkent Üniversitesi Fen Bilimleri Enstitüsü

Moleküler Biyoloji ve Genetik Anabilim Dalı

2023

Bu tez kapsamında, bor (B) toksisite tolerans mekanizmasının moleküler temellerini yüksek verimde ve tek hücre düzeyinde aydınlatmak için literatürde ilk kez *Arabidopsis thaliana* kökleri ile tek hücreli RNA dizileme çalışması yapılmıştır. Bu kapsamda, *Arabidopsis thaliana* kökleri tohum çimlenmesi aşamasında farklı konsantrasyonlarda B toksisitesine maruz bırakılmıştır. Strese maruz bırakılan köklerden protoplastlar izole edilmiştir ve sonrasında tek-hücre RNA dizilemesi yapılmıştır. Kontrol, 1 mM B ve 2 mM B gruplarından oluşan 8 numune Illumina NovaSeq 6000 ile dizilenmiştir. Üç kopya boyunca toplam 1554 hücre popülasyonu geri kazanıldı. Bu tek hücreli transkriptomda quiescent center, endodermis, kaliptra (root cap), kolumella, korteks ve trikoblast dahil olmak üzere ana dokular tanımlanmıştır. B toksisitesi uygulamalarında trikoblast ve korteks tanımlanmamıştır. Ayrıca, literatürde sunulan genler ve B toksisitesi tolerans mekanizmaları ile ilgili benzer yolaklar tespit edilmekle birlikle hücre tipleri özelinde birçok yeni gen belirlenmiştir. Örneğin; çok yeni bir şekilde esasları ortaya konulan antosiyanin ve GST'lerin birincil rolü bulunan internal B toksisitesi tolerans mekanizmasının kolumella hücre kümesinde olabileceği öngörülmüştür. Ayrıca, B toksisitesi altında hücre özelinde 13 TF ailesi tanımlanmıştır. Son olarak, daha önce tespit edilen ve bu projede bulunan yeni yolakların hücre kümeleri özelinde literatüre sunulması B toksisitesi toleransıyla ile ilgili yeni transgenik ve ıslah çalışmalarına yön vermesi beklenmektedir.

ANAHTAR KELİMELER: *Arabidopsis thaliana,* Bor Toksisitesi, Tek Hücre RNA Dizileme

Bu proje, TUBİTAK tarafından (121Z029 no'lu proje) desteklenmiştir.

ABSTRACT

Hikmet YILMAZ

SINGLE-CELL RNA SEQUENCING IN ROOTS OF *ARABIDOPSIS THALIANA* EXPOSED TO BORON TOXICITY AT SEEDLING STAGE

Başkent University Graduate School of Natural and Applied Sciences

Department of Molecular Biology and Genetics

2023

In this thesis, a single-cell RNA sequencing study was performed for the first time in the literature to reveal the molecular basis of boron (B) toxicity tolerance mechanism in *Arabidopsis thaliana* with high efficiency and at the single cell level. In this context, the roots of *Arabidopsis thaliana* were exposed to different concentrations of B toxicity at seedling stage. Protoplasts were isolated from stress-exposed roots and then single-cell RNA was sequenced. Total of 8 samples from control, 1 mM and 2 mM B groups were sequenced with Illumina NovaSeq 6000. Accordingly, a total population of 1554 cells were recovered across three replicates. Major tissues have been identified in this single-cell transcriptome, including the quiescent center, endodermis, root cap, columella, cortex, and trichoblast. Trichoblast and cortex had not been defined under B toxicity treatment. In addition, although similar pathways related to the genes and B tolerance mechanisms presented in the literature have been detected, many new cell-type specific genes were also identified. For example, the internal B toxicity tolerance mechanism, via the role of anthocyanins and GSTs may be in the columella cell cluster. Moreover, we found cell specific 13 TF families under B toxicity. Finally, the new pathways identified previously and new ones at cell cluster level will lead to new transgenic and breeding studies for B toxicity tolerance mechanism.

KEYWORDS: *Arabidopsis thaliana,* Boron Toxicity, Single Cell RNA Sequencing

This thesis was supported by TUBİTAK (project number 121Z029).

FOREWORD

In this study for the first time in the literature, single cell RNA sequencing was performed in the roots of *Arabidopsis thaliana* exposed to different concentrations of B toxicity. With this study, new pathways and candidate marker genes related to B tolerance mechanism at cell basis were presented to the literature for the first time.

TABLE OF CONTENTS

LIST OF TABLES

LIST OF FIGURES

LIST OF SYMBOLS AND ABBREVIATIONS

ATP	Adenosine triphosphate
1B	1 mM boric acid treatment group
2B	2 mM boric acid treatment group
B	boron
BP	biological process
C	control group
CC	cellular component
GDH	glutamate dehydrogenase
GST	Glutathione S-transferase
kg	kilogram
LD	Linkage disequilibrium
MF	molecular function
mM	millimolar
NAD	nicotinamide adenine dinucleotide
NADP	nicotinamide adenine dinucleotide phosphate
ng	nanogram
PCA	principial component analysis
scRNA-seq	single cell RNA sequencing
TF	Transcription facto
t-SNE	t-distributed Stochastic Neighbor Embedding
µl	microliter
USA	United States of America

1. INTRODUCTION

B toxicity damages plant growth and development, and causes yield losses. Entering the plant, toxic B binds to the cis-hydroxyl groups of some biomolecules and causes basic damage to the cells; It causes metabolic damage by binding to ribose-containing biomolecules incluiding ATP and NADH. By binding to ribose in RNA, it may cause disruption of cell wall structure, inhibition of cell division and disruption of cell growth [1, 2]. These damages cause deterioration in developmental and metabolic activities of plants, yield losses and serious economic losses. For these reasons, elucidating the molecular mechanisms of B toxicity in high resolution is important for understanding the progression of tolerance pathways and preventing damage.

Single-cell sequencing techniques, chosen as the method of the year according to Nature Methods in 2013, are the techniques that provide the most accurate information about molecular mechanisms and dynamic changes at the cellular level. In the literature, there are transcriptome studies under various B toxicity using the model organism *Arabidopsis thaliana* and other plants [3]. The bulk methods frequently used in these studies have some notable shortcomings. Especially due to heterogeneity in tissues, cell spesific detection of differently expressed genes in these methods is very limited [4, 5]. Because the gene expression values obtained in these bulk transcriptome methods are average of the expression values of all cells in the tissue, and so profiles of up and down expression according to cell types cannot be determined by these techniques. In addition, it is not possible to find rare cell types in bulk methods [6].

Single cell RNA sequencing (scRNA-seq) studies are pioneering and efficient in overcoming all these problems. Because single-cell sequencing techniques enable expression profiles on a cell basis, solves heterogeneous problem, obtain high-resolution transcriptomic data, and allow the analysis of cell types and responses of cells to all kinds of factors with high resolution and output [6]. Since plants have high heterogeneity and highly differentiated cell diversity, single-cell RNA sequencing has the potential to yield very promising results in plants [7, 8, 9, 10, 11, 12]. *Arabidopsis thaliana* roots are useful for single-cell RNA sequencing applications because they contain few cells. Several scRNA-seq

studies were performed using *Arabidopsis thaliana* protoplast obtained by degradation of the cell wall. Almost all of these studies are about differentiation and cell type and marker gene detection [13, 9, 14].

In this thesis, a high-throughput scRNA-seq study was performed for the first time in the literature to analyze how plant cell-specific response are affected by B toxicity in the model organism *Arabidopsis thaliana*. In this context, *Arabidopsis thaliana* roots were exposed to different concentrations of B toxicity at the seedling stage. Next, protoplasts were obtained from the roots and then successfully scRNA-seq was performed using the drop-based, high-throughput 10X Genomics Chromium platform [15]. Next, preprocessing, clustering, and detailed gene expression profile analyses were performed with bioinformatics analysis. In conclusion, the molecular basis of B toxicity tolerance at cellular level were revealed by single-cell RNA sequencing at the seedling stage.

2. LITERATURE

2.1. *Arabidopsis thaliana*, A Plant Model Organism

Arabidopsis thaliana, also known as thale cress or rock cress, is a small annual or wintery, white-flowered rosette plant. It is in the Brassicaceae taxonomic family of the dicotyledonous group of angiosperm plants. It usually grows 20–25 cm [16]. *A. thaliana* began to be used frequently in plant studies since 1980s. Even though *A. thaliana* is not of direct importance for agriculture, it has important features such as short production time, small size, and self-pollination [17]. Thanks to these features, it has become a widely used model organism in many studies such as development, breeding, plant genetics, population genetics and plant evolution [18, 19].

A. thaliana research are convenient, fast, and cheap. An *A. thaliana* seed can develop into a plant bearing mature seeds in as little as 6 weeks. Compared to many plants, *A. thaliana* can grow indoors under poor fluorescent lighting, which can easily obtain in the laboratories. seeds of *A. thaliana* are small enough that they can be germinated on a single petri dish. Moreover, there is no need to co-culture with other species to thrive, facilitate aseptic growing conditions and controlling variables. The genome of *A. thaliana* is ∼132 Mbp with approximately 38,000 loci, > 20,000 protein coding genes which are dispersed among five nuclear chromosomes. This genome size is small for a plant (wheat 16,000 Mbp). Moreover, *A. thaliana* genome do not have much repetitious DNA, but it contains a complete set of genes which controls developmental, metabolisms, environmental responses, and disease resistances [20, 21].

Unlike many plants, Arabidopsis can tolerate high level of homozygosity and self-fertile; tens of thousands of offspring are produced from each individual. Moreover, plant defense is poison. Arabidopsis deters herbivores chemically by producing pungent glucosinolates [22]. Chemical defense and autotrophy generate great chemical and enzymatic diversity, which provides fertile ground for research.

Furthermore, *A. thaliana* models characteristics and specific cell types of seed plants such as simple leaves, stems, roots, root hairs, female gametophytes, pollen, apical

meristems, vascular tissue, trichomes, perfect flowers (presence of both stamens and carpel), stomata and epidermal pavement cells. The functions of the genes discovered in Arabidopsis are generally similar to those discovered in other plants. About 3 of 4 gene families found in Arabidopsis are also found in other flowering plants. In this way, Arabidopsis studies have made it understand the inner workings of many *plants* [23].

2.2. An Introduction to Boron

B was independently discovered in 1808; English chemist Sir Humphry Davy and French chemists Joseph-Louis Gay-Lussac and Louis-Jacques Thenard [24]. B is in the second period IIIA group of the periodic table. It is a semi-metal with atomic number 5. B has one missing valence electron, that is, there is a fundamental negatively charged particle in its outermost region of the B atom and this atom engages the formation of chemical bonds. In this way, B has a dominant effect on the chemical reactions it enters. It is small and has a high ionization energy and therefore forms a covalent bond rather than a metallic bond [25]. With the structural complexity of its allotropic modifications, B has a unique feature. Several B containing organic compounds are known [26, 27]. Some compounds containing B and their main core structures are shown in Figure 2.1. [28]. Among other known main properties. B can form rings, chains, and networks [29]. B reacts with simple alcohols to form esters $B(OR)_3$ [30].

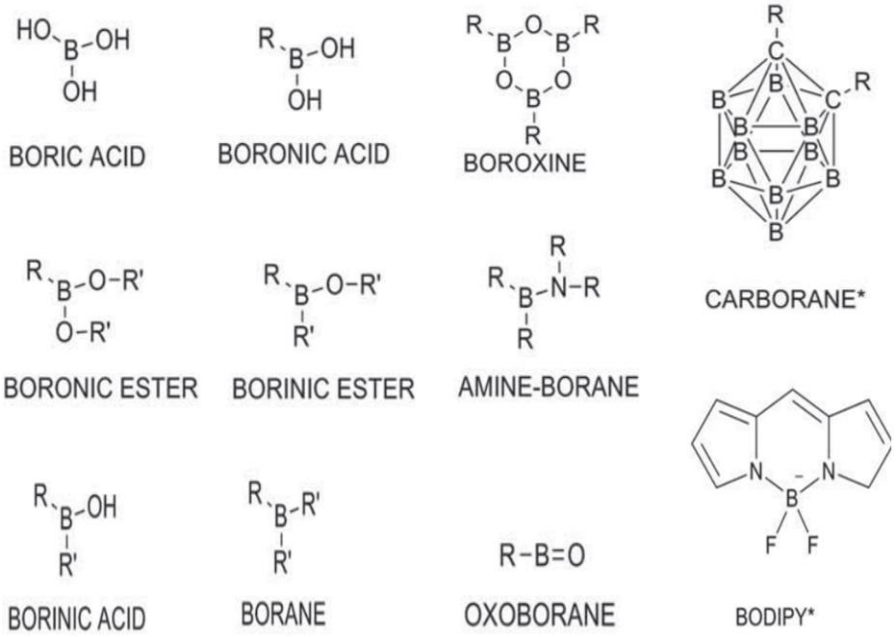

Figure 2.1. Some B containing compounds and their main core structures [28]

B is not abundant in natura [31]. The average B concentration is 10-20 mg B kg^{-1} in rocks, 1-10 mg B kg^{-1} in seas and about 1/350 of seawater concentration in rivers [32]. The concentration in soil is <10 $mgkg^{-1}$ is classified as low B content, the concentration in soil is 10-100 $mgkg^{-1}$ is classified as high B content Detailed atomic structure, chemical properties and physical properties of B are given in Table 2.1. [33].

Table 2.1. Atom structure, chemical properties, and physical properties of B [33]

Proton units	5		
Number of neutrons	6		
Electron number (no load)	5		
Electron array	$1s^2 2s^2 2p^1$		
Valence electrons	$2s^2 p^1$		
Atomic diameter	1.17 Å		
Ion diameter	0,23 Å		
Atomic volume	4.63cm^3/mol		
Crystalline	Rhombohedral		
Potential energy of valence electrons (-eV)	190		
Electronegativity (Pauling)	2,04		
Electrochemical equation	0,1344 g/amp-sa		
Ionization potential (eV)	1. İonization 8,298	2. Ionization 25,154	3. Ionization 37,93
Fusion heat value	50,02 kj/mol		
Appearance	Yellow brown ametalic and crystal		
Physical form	20°C 1atm: Solid state		
Atomic Mass	10,811		
Conductivity	Electrical: 1.0 E - 12 106 / cm		
Thermal Expansion coefficient	0.0000083 cm / °C (0°C)		
Density	2,34 g/cc - 300K		
Hardness	Mohs: 9,3 (Vickers: 49000M.N.m^{-2})		
Enthalpy	573,2 kj/mol (25°C)		
Enthalpy (Fusion)	22,18 kj/mol		
Enthalpy (Evaporation)	480 kj/mol		
Heat (Evaporation)	489,7 kj/mol		
Pressure value (Steam)	0,348Pa – 2300 °C		
Melting point	2573K - 2300°C – 4172 °F		
Specific heat value	1,02 J/gK		
Flexibility status	Bulk: 320/GPa		
Molar volume	4,68 cm^3/mol		
Boiling point	4002°C		

B is not found as a free element in nature. Mainly natural occurring form of B is Borate ($B(OH)_4$) while not common form of B is boric acid (H_3BO_3). Among the main compounds of B, the one found at Physiological pH is $B(OH)_3$. It behaves like a weak Lewis acid (Ka = $6x10^{-10}$, pKa: 9.1) (Equation 2.1.) [34]. Ribose, apiose, sorbitol, phenolics and serine are some of the biomolecules that reacts with $B(OH)_3$ [35, 34].

$$B(OH)_3 + H_20 \leftrightarrow B(OH)_4^- + H^+ \quad (2.1)$$

Although the USA and Russia are home to important B mines, Turkey is the world's largest B producer. In 2016, approximately 2.7 million tons of B_2O_3-based B were produced in the world. Turkey has the largest distribution (73.40%) of this reserve. B is widely used in the production of high-quality and sustainable products in several industrial areas. In the cleaning sector, borate has an important place due to its properties such as facilitating stain removal and bleaching, alkali buffering, stabilizing enzymes, and water softening. By using B in the production of ceramic glaze and enamel, resistant to heat, chemicals and physical effect products are obtained. Moreover, wood protection products produced with B compounds are not harmful to human health and the environment. They are easily soluble in water and easily applicable. In the glass industry, glass products are converted into a heat and chemical resistant product with the addition of B (https://www.etimaden.gov.tr/en/boron-minerals).

2.3. The Function of Boron in Plants

B is an indispensable trace micronutrient for the growth of higher plants. The role of B in vascular plants was first demonstrated in *Vicia faba* [36]. B play role in various metabolic processes [37, 38]. The relationship between B and primary cell walls was demonstrated by several researchers. Loomis and Durst found that as a component of cell wall polysaccharides and a residue in pectins, apiose may be the main sugar moiety in the borate crosslinking complex [1, 39] and Kobayashi et al., [40]. showed that apiose residue is responsible for the binding of B to the polysaccharide chains. Several studies showed that B binds to pectin polysaccharides, especially rhamnogalacturonan-II (RGII), the first B-containing compound identified in plants. It is involved in integrity of the cell walls [41, 35, 42, 43]. B is crosslinked with two RGII monomers by a borate bridge and provides stability to the cell wall matrix [38]. Kobayashi et al., [40] showed that the molecular weight of the

RG-II-B complex was halved when B was removed from the complex [40]. Furthermore, B deficiency causes abrupt cell wall size increase in *Chenopodium album L.* [44], and the larger pore is associated with dB-RG-II and the pore size appeared to decrease after B-reintroduction into these cells [45]. These results shows that dB-RG-II formation is effective in physiological processes such as plant cell wall modification, metabolism, and growth. Additionally, in 2014, Voxeur and Fry [46] emphasized the role of B in cell membranes through complex formation with glycosyl inositol phosphoryl ceramide (GIPC), which is major components of lipid rafts. B is involved in GIPCs-B-RGII complex formation through bridging the cell plasma membrane and the cell wall [47].

B is also involved in integrity of cell membranes. B deficiency causes rapid deterioration of the cell membrane stability, composition and membrane transport and the cell membrane becomes more permeable [48, 49]. By measuring membrane potentials in the roots of *Elodea densa* and *Helianthus annuus*, Blaser-Grill et al., [50] showed that B affects the proton gradient. Complexation of the glycoprotein with B on the membrane surface creates additional negative charges across the membrane that may affect electrostatics. In addition to glycoproteins, both surface glycoproteins and glycolipids in the bilayer have oligosaccharide side chains that can form borate complexes [51]. This interaction may cause changes in surface charge, stiffness, and membrane permeability. This excess cell membrane permeability due to B deficiency increases the secretory of organic compounds including sugar and amino acids outside root and leaf cells [48]. Moreover, compared to plants without B deficiency, B deficient plants have less potassium in their leaves [52]. Plants lacking B cannot take up potassium [53].

In vascular plants, B affects the root growth [54]. B deficiency results in reduced root hair formation and elongation [55, 56] and cell elongation of the primary root [54, 57]. Another physiological developmental process in plants in which B is effective generative development, particularly germination, pollen viability and pollen tube development [58, 59, 60]. B deficiency severely affects the healthy growth and function of pollen tubes. This leads to decreases or stop of fertilization. Additionally, decreases in flowering and the shedding of the resulting flowers are seen in plants under B deficiency [58].

B is also involved in many metabolic pathways as it forms complexes with various hydroxylated molecules [61]. Sugar uptake and transport is faster in normal level B

containing plants compared to B deficient ones [62]. B deficiency inhibits glucose-6-phosphate dehydrogenases resulting in increased phenol production in plants, [63, 64]. Borate is an alcohol dehydrogenase inhibitor [65, 66]. Legumes are known to have a very high demand for B. One of the main reasons for this is thought to be that B deficiency greatly affects the nitrogen fixation process and nodule formation [67, 68, 69]. Furthermore, various other roles of B have been demonstrated in plants, including of reproductive tissue stimulation, seed quality improvement, and its effect on the biosynthesis of certain metabolic compounds such as polyphenols and antioxidants [35, 70, 71]. Various studies have been conducted showing that antioxidant enzyme activity increases under high levels of B [72, 73].

2.4. Boron Toxicity in Plants

Plants are often exposed to B toxicity when grown in soils with high B content or/and irrigated with waters having high B content. [74]. Even though B toxicity is not as common as B deficiency in nature, it is a severe problem that reduces plant growth and development and causes yield losses in semi-arid and arid environments. It is difficult to recover toxic B from the soils therefore, the only sustainable solution may be to find the mechanisms of B toxicity and tolerant crops with adequate yields should be grown [75].

In plants, optimal and toxic concentrations of B are very close to each other [76] and these concentration levels may greatly vary between varieties of each species as well as from species to species. Some species are very sensitive to B while some species are high tolerant. Sensitive plants such as *Phaseolus vulgaris* safe B concentrations in irrigation water change between 0.3 to 1 mgL^{-1}.Moreover, semi-tolerant plants such as *Zea mays* and *Solanum tuberosum*, safe B concentrations in irrigation water change between 1 to 2 mgL^{-1}, tolerant plants such as *Daucus carota* and *Cuminos melo,* safe B concentrations in irrigation water change between 2 to 4 mgL^{-1}, and very tolerant plants such as *Solanum lycopersicon* safe B concentrations in irrigation water change between 4 to 6 mgL^{-1} [77].

B is unique nutrient among plants in many ways. Symptoms of B toxicity also differ between species, based on the mobility and immobility of the phloem. In phloem-motile plant species the effects of B toxicity are related to the accumulation of high B concentrations in older leaves [78]. B moves through the xylem and then accumulates in the leaves at the end of the transpiration stream. In the presence of toxic level B, these plant species such as

barley and wheat develop necrosis and chlorosis spreading from the leaf tips with brown lesions first forming at the edges, then covering most of the leaf [79]. Additionally, delay in emergence and delay in leafing, decrease in yield, number of spikes per plant, dry matter weight, grain weight and stem height were observed in several studies [80, 81, 82, 83, 84, 85, 86, 87, 88, 89]. Root weakness and reduced lateral root growth were observed in hydroponically grown barley and wheat [83]. The symptoms that occur under B toxicity can vary between genotypes. For example, it was observed that 70 durum wheat genotypes had varying dry matter weights from low to high under B toxicity [90]. On the other hand, in phloem-mobile plants such as *Malus*, *Pyrus* and *Prunus* species, B accumulates in developing sinks [91], and young shoot tip cessation, bud abscission are observed. Moreover, in celery, B toxicity causes deformed young leaves and irregular stem shape [92].

Contrary to the relationship between leaf and B toxicity, the information on the relationship between root and B toxicity is quite limited. Interestingly, visible symptoms are not seen in roots. Moreover, B concentrations in these tissues is relatively low compared to leaves, even if plants are exposed to high levels of the B [83]. Under B toxicity, the primary phenotypic effect in root tissues is inhibition of root growth, followed by a decrease in root dry weight, and then an increase in B content. [72, 93]. Additionally, abnormal cell division was observed in the bean root meristem under B toxicity [94].

B toxicity may cause severe physiological and biochemical effects including photosynthesis inhibition [95], membrane leakage increase [96], lipid peroxidation [96] and change in antioxidant enzyme activity [96]. In toxic concentrations that enter the plant, B binds to biomolecules with its cis-hydroxyl groups and may cause some major damage to cells. Cell growth may be impaired due to binding to ribose in RNA. Due to its binding to ribose in ATP, NADH and NADP, metabolic damage may occur, cell wall structure may be disrupted, and cell division may be inhibited [2]. Furthermore, toxic level B concentrations also cause significant changes in several enzymes' activities. Bonilla et al., [97] and Kastori and Petrovic [98] suggested that B alter the nitrogen metabolism.

2.5. Omics Studies on Plants Exposed to Boron Toxicity

Uncovering the molecular mechanisms of B toxicity in high resolution is critical to understand the progression of damage and tolerance pathways. For this purpose, the so-called omics; It requires multidimensional, large-scale, and detailed experiments involving all genetic, or functional components. The major types of omics are genomics, transcriptomics, proteomics, and metabolomics [99]. Particularly, transcriptomics is routinely used in B toxicity including [99, 100, 3, 101].

To understand the B response and tolerance mechanisms in the roots and leaves of wheat, physiological, transcriptomic and biochemical studies were performed in toxic B treated cultivars [3]. Despite the high B content, neither the root nor the leaves of either cultivar showed reduced viability or delayed growth. 957 and 1248 1248 of the expressed genes were susceptible to B toxicity in the roots of Bolal and Atay, respectively. Moreover, 892 and 995 of the expressed genes were significantly expressed at least two-fold under B toxicity in the leaves of Bolal and Atay, respectively. Compared to Bolal cultivar, in Atay cultivar, protein degradation genes induced under B toxicity were more expressed in both root and leaf tissues. These contrasts in the transcriptome pattern are the result of higher B accumulation needing a high degree of metabolic adjustment in the sensitive variety. Furthermore, B toxicity altered genes expression related to hormone and kinases signalling, ROS scavenging, and TFs including WRKY and MYB. The nodulin-26-like intrinsic proteins (NIP4;1) and Glutathione S-transferase (GST) and genes were key B stress response factors among the genes commonly regulated in Atay and Bolal [3].

Kayıhan et al., [101] examined B-treated seeds of *Arabidopsis thaliana* to determine gene expression patterns related to anthocyanin biosynthesis and transport, and related TFs under B toxicity. 3 mM boric acid treatment caused upregulation of anthocyanin biosynthesis genes (*4CL3* and *C4H)* and TFs (*MYB114* and *MYB75*) and anthocyanin transporter genes (*TT19* and *TT13*). Furthermore, since the B-anthocyanin complex conjugated with GSH participates in the B tolerance mechanism in plants and SLIM1 TF activates sulfate uptake for cysteine producing sulfate-initiated S assimilation that is the substrate for GSH, Anthocyanin accumulation level was calculated in both wild type and *slim1* mutant *Arabidopsis thaliana* under both normal and toxic B conditions. As expected, toxic B conditions increased anthocyanin accumulation both WT and *slim1* mutant Arabidopsis, and

slim1 mutant had higher anthocyanin accumulation compared to WT under all conditions. From these results, it is seen that anthocyanin have a critical role in B tolerance.

In the leaves of *C. grandis*, an intolerant cultivator, and *Citrus sinensis*, a tolerant cultivator, miRNAs were found via Illumina sequencing. B treatment induced differential expression of 20 miRNAs in *C. sinensis* and 51 miRNAs in *C. grandis*. Interestingly, miR397a and miR395a were downregulated in the leaves of *C. sinensis* whereas, they were the significantly upregulated in the leaves of *C. grandis*. miR160a and miR397a targets were confirmed by the 5′-RACE method as two laccase genes and four auxin response factor genes, respectively. Downregulation of AC4 and LAC17 in *C. grandis* caused, and upregulation of LAC4 in *C. sinensis* caused poorly developed vessel elements and secondary deposition of cell wall polysaccharides in vessel elements, respectively. These results indicate that miR397a has a crucial role in B-toxicity tolerance in Citrus vis targeting LAC17 and LAC4 [102]. Moreover, in another study, they showed that B treatment caused differential expression of 37 miRNAs in *C. grandis and*11 miRNAs in *C. sinensis* [103]. The targets of miR171, miR319, and miR396g-5p were confirmed via 5'-RACE and qRT-PCR as SCARECROW-like protein gene, myeloblastosis (MYB) TF gene and cation transporting ATPase gene, respectively. From these results, downregulation of MYB as a result of upregulation of miR319 in roots can reduce root tip number and thus significantly alter the root system architecture. Moreover, since B-treated *Citrus* roots allow normal root elongation despite B toxicity, SCARECROW expression may be required for dormant centre specification, stem cell maintenance and endodermis specification. In conclusion, miR171 and miR319 have a key role in the long-term B toxicity adaptation of *Citrus* via targeting *SCARECROW* and *MYB89* involving development and root growth, respectively.

After measuring the expression levels of miRNAs including JA and ethylene targets (miR319, miR172, miR159, miR394) and laccase target (miR397) in *Arabidopsis thaliana* under toxic B conditions, mature miRNAs were amplified using stem-loop qRT-PCR for expression analysis. Expression levels of these miRNAs were increased under moderate level (1 mM) B toxicity treatment but not under high level (3 mM) B toxicity treatment. The most striking rearrangements occurred in miR319 and miR172. There was no notable change in the expression level of miR397. These results indicate that under B toxicity, there is no post-transcriptional regulation of laccase involved in cell wall modification. Furthermore,

miRNAs targeting TFs involved in ethylene and JA metabolisms in *Arabidopsis thaliana* may be oxidative stress-adaptive responses to B toxicity of Arabidopsis [104].

Recently, Yingna et al., [105] found AtWRKY47, a B toxicity response transcription factor in *Arabidopsis thaliana*. Under B toxicity conditions, T-DNA insertion mutants Atwrky47 increased growth parameters and B toxicity tolerance under elevated B treatment compared to WT Col-0 plants. Overexpression of AtWRKY47 in Col-0 increased B toxicity sensitivity, resulting in less chlorophyll content and less biomass. Additionally, B concentration in shoots was higher in overexpression lines but lower in Atwrky47 mutants. These results show that AtWRKY4 is a B toxicity sensitive transcription factor in *Arabidopsis thaliana* and has an effective role in regulation of B toxicity tolerance.

2.6. Single Cell RNA Sequencing

Before single cell technologies, bulk methods were standard for analysing the transcriptome and were provided a lot of molecular information to the literature. However, since different cell populations are averaged and the values of gene expressions in the bulk transcriptome methods give an average of all cells in the tissue, they are likely to give limited results, a phenomenon known as Simpson's dilemma. In addition, it is not possible to detect rare cell types in these bulk methods [106].

A recently found single cell sequencing studies are pioneering and efficient in overcoming all these problems [107]. Single-cell technology is pioneering and efficient in overcoming all these problems. Single-cell approaches are a very powerful tools that can detect cellular heterogeneity among individual cells and outlying cell maps [107]. Single cell RNA sequencing (scRNA-seq) is one of the single cell technologies. It has made it possible to profile the transcriptome of hundreds of thousands of individual cells. Through the discovery of new cell populations with different gene expression profiles, scRNA-seq enables us to understand the cell as a functional unit [4, 5]. It can identify previously known and unknown cell types [108, 109, 110] and allow to find subpopulations of a known cell type [111, 108]. It can sensitively and specifically isolate signals from rare cells in cell populations that would be lost in bulk RNA sequencing [112, 113, 114, 115]. Moreover, it can enable the discovery of potentially useful markers for cell types [108, 116]. Finally, it provides finding

differentiation and cell lineage. When a stem cell population promotes differentiation, snapshots of the differentiation process at various time points can be taken by scRNA-seq, and by using these snapshots, the trajectories and key genes can be obtained. Tajectories enable the cell to reach each differentiated state. Key genes enable cells to be arranged differently at each branch point [117, 106, 108, 118].

scRNA-seq has not been widely applied in plants unlike animals. One reason for this is that cell wall in plants prevents cells make it difficult to separate and individual cell. [12]. However, several groups have efficiently performed high-throughput scRNA-seq in plants. These studies generally focused on the Arabidopsis root system, [9, 14, 119, 120]. *Arabidopsis thaliana* root is a well-studied and understood plant organ and has relatively few cells and cell types. Moreover, there are methods to isolate individual cells through protoplast in the literature. Many tissue/cell type marker genes have been known through gene several expression studies. These reasons make Arabidopsis root a useful plant organ for scRNA-seq studies [13, 121, 9, 14].

10X Genomics is a commercially available and widely used droplet-based platform that capable of performing high-throughput scRNA-seq [15]. In this technology, approximately 3.5 million Barcodes are used to individually index the transcriptome of each cell. Interestingly, this is achieved by dividing thousands of cells into beads (GEM: Gel Beads in Emulsion). On the other hand, single cell data analysis is not easy process. First, raw data is demultiplexed and quality control analysis is performed. These data are mapped to the reference genome. Expression matrices are created by selecting UMIs for each gene and each cell barcode [15]. This matrix is filtered and cells with too little and/or too much gene expression, too many mitochondrial genes, and/or cell debris are filtered out from the datasets. Then normalization is done. Normalization makes it possible to compare cells. Then, a subset of features that show variation among cells higher in the dataset is calculated (variable genes analysis). Standardization (scaling) is done. Standardization allows gene comparison. Then, linear dimension reduction (Principal Component Analysis (PCA)) is done on the standardized data set. Selecting the optimum number of PC for downstream analysis is a critical step. Too many PCs will cause technical noise, too few PCs will cause data loss. Then clustering and nonlinear dimension reduction (UMAP, t-distributed Stochastic Neighbor Embedding (t-SNE)) are done. Differential expression analysis is performed, and gene markers are found. Finally, GSEA is performed. After the control and

condition groups are analysed separately, integration analysis can be performed, and the data sets can be compared. Thus, cell types in the datasets can be identified, rare cell clusters can be found, conserved cell type marker can be obtained, and cell responses can be found [122].

In this thesis, for the first time in the literature, high throughput scRNA-seq study was performed to find the molecular basis of the B toxicity tolerance mechanism on cellular level. In this context, Arabidopsis roots exposed to 1 mM and 2 mM B toxicity at seedling stage were used. Protoplasts were isolated from the roots. Using the 10X Genomics Chromium Controller device, cells were barcoded and libraries were constructed. After sequencig, data analyzes were performed. Gene expression profiles and clustering of cell types were carried out.

3. MATERIALS AND METHODS

3.1. Plant Growth and Boron Toxicity Treatments

In this study, wild type (WT) *Arabidopsis thaliana* cv. Columbia seeds were used. Experimental details were shown in Figure 3.1.

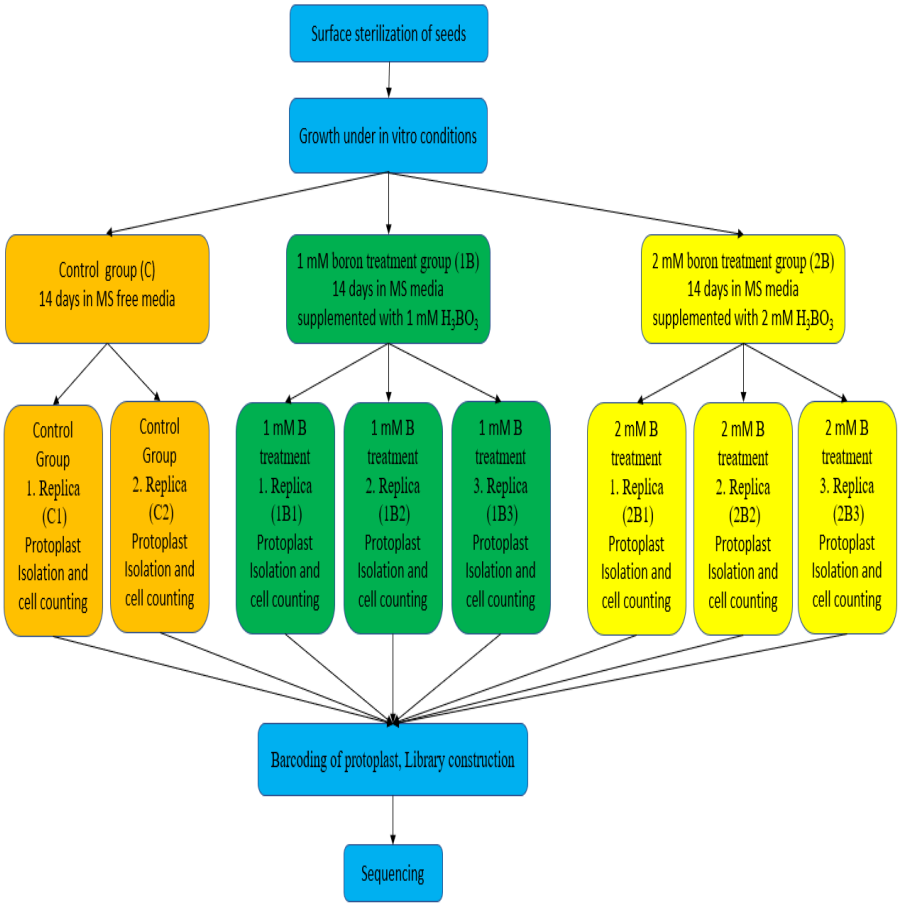

Figure 3.1. Experimental set up in detail

Arabidopsis thaliana seeds were surface sterilized before sowing on the growth media. Briefly, the seeds were placed in an Eppendorf tube containing 500 µl of 70% (v/v) EtOH, inverted for 2 minutes and EtOH was withdrawn. 500ul of 2.5% (v/v) NaOCl was added. After 10 minutes of inversion, the NaOCl was withdrawn. Then, seeds were washed three times for 30 seconds with 500 µl of distilled water.

Surface sterilized seeds were placed one by one on the line drawn on the petri dishes at intervals. Control groups were grown in half-strength MS media (Murashige and Skoog,

1962) (pH: 5.7). On the other hand, 1 mM boric acid and 2 mM boric acid treatment were chosen for the treatment of B toxicity [100, 104] and 1 mM boric acid treatment group (1B) and 2 mM boric acid treatment group 2B toxicity treatment groups were grown in MS media containing 1 mM or 2 mM boric acid, respectively. Petri dishes were first wrapped with stretch film and then with aluminium foil. After stratification at 4°C for 3 days and kept in the growth chamber at 22 ±1°C for 14 days with 16 hours of light (200 µmol $m^{-2}s^{-1}$) and 8 hours of dark photocycle at 60% relative humidity.

3.2. Protoplast Isolation and Cell Counting

After the 14-day growth period was complete, approximately 20 primary roots were chopped with a length of 2 cm, above the tips with the help of forceps. The enzyme solution containing 1.25% [w/v] Cellulase ["ONOZUKA" R10, Yakult], 0.1% [w/v] Pectolyase [P-3026, Sigma-Aldrich], 0.4 M Mannitol, 20 mM MES [pH 5.7], 20 mM KCl, 10 mM CaCl2, 0.1% [w/v] bovine serum albumin was prepared.

3 ml of enzyme solution per sample was poured in a small petri dish and then a 70 µm strainer was placed in this petri dish. Primary roots were put into a petri dish with enzyme solution and shaken in a shaker at 90 rpm for 2.5 hours, gently crushed every half hour. The liquid parts that filtered out of the petri dish were taken into 15 ml falcon and passed through a 40 µm strainer and centrifuged at 100 g at 22°C for 6 min. The pellets were dissolved in 500 µl of 8% mannitol and passed through a 40-pipette strainer (SP Bel-Art).

25 µl of solution was taken into 1.5 ml Eppendorf tube. 0.4% Trypan Blue was added to each sample in the tube (at 10:0.8 ratio) and waited for 1-2 minutes at room temperature. Samples were loaded onto a Thoma slide and viewed with a Light microscope (Zeiss Primo Star). According to Equation 3.1. and 3.2., live and dead cells in 1 ml and 1 µl of each sample were counted separately, and cell viability was calculated according to Equation 3.3.

$$\text{cell/ml} = \text{A x SF x } 10000 \quad (3.1.)$$

$$\text{cell/µl} = \text{A x SF x } 10 \quad (3.2.)$$

In here A: Number of cells in 16 squares, SF: Dilution Factor

$$\text{viability} = \frac{\text{Alive cell number}}{\text{Total Cell Number}} x\ 100 \qquad (3.3.)$$

3.3. Barcoding of protoplast, library construction and sequencing

The control group, 1mM B treatment groups, and 2mM B treatment groups were used. Since there are 8 wells in a 10X Genomics chip, 2 replicates in the control group, 3 replicates in the 1mM B treatment group and 2mM B treatment were used. In detail, experimental steps of 10X Genomics scRNA-seq and times were shown in Table 3.1.

Table 3.1. Single cell sequencing experimental steps and times

STEPS		TIMING
CELL PREPARATION	Dependent on Cell Type	1-1.5 hours
GEM GENERATION AND BARCODING	Preparing Reaction Mix	20 minutes
	Loading Chromium Next GEM Chip	10 minutes
	Running the Chromium Controller	18 minutes
	Transferring GEMs	3 minutes
	GEM-RT Incubation	55 minutes
POST GEM-RT CLEANUP & CDNA AMPLIFICATION	Post GEM RT-Clean-up	45 minutes
	cDNA Amplification	40 minutes
	cDNA Clean-up	20 minutes
	cDNA quality and quantification	50 minutes
3' GENE EXPRESSION & LIBRARY CONSTRUCTION	Fragmentation, End Repair and A-tailing	50 minutes
	Post Fragmentation, End Repair and A-tailing Double Sided Size Selection	30 minutes
	Adaptor Ligation	55 minutes
	Post Ligation Clean-up	20 minutes
	Sample Index PCR	40 minutes
	Post Sample Index PCR Double Sided Size Selection	30 minutes
	Post Library Construction QC	50 minutes

3.3.1. GEM generation and barcoding

3.3.1.1. Preparing single cell master mix

Master mix was prepared (Table 3.2.). It was pipetted and centrifuged. 31.8 µl of the mix was added to 8 PCR tubes on ice.

Table 3.2. GEM generation master mix preparation protocol

Master Mix (Reagents were added in the order listed)	8X (10% µl)
RT Reagent B	165.0
Template Switch Oligo	20.8
Reducing Agent B	17.3
RT Enzyme C	76.8
TOTAL	279.8

3.3.1.2. Loading chromium next GEM chip G

The volumes of water and single-cell mix were calculated for 75 µl in each tube (Table 3.3.) according to the Table 3.4.

Table 3.3. Single cell suspension preparation

Sample	Stock Solution (Cell/ µL)	Targeted Cell Number	Nuclease-free Water per reaction (µl)	Cell Suspension Stock (µl)
C1	500	5000	26,7	16,5
C2	320	5000	15,7	27,5
1B-1	520	5000	26,7	16,5
1B-2	720	5000	31,4	11,8
1B-3	760	5000	31,4	11,8
2B-1	680	5000	31,4	11,8
2B-2	420	5000	22,6	20,6
2B-3	520	5000	26,7	16,5

Table 3.4. Cell Suspension Volume Calculator Table. Red color: Cell suspension stock per reaction volume, blue color: Nuclease-free water per reaction volume, black color: volume exceeding the allowable volume of water in each reaction volume, yellow color: Low transfer volume, Navy Blue color: Optimal range

Cell Stock (Cells/µl)	Targeted Cell Recovery										
	500	1000	2000	3000	4000	5000	6000	7000	8000	9000	10000
100	8.3	16.5	33								
	35	26.7	10.2	n/a	n/a	n/a	n/a	n/a	n/a	n/a	n/a
200	4.1	8.3	16.5	25	33	41.3					
	39.1	35	26.7	19	10	2	n/a	n/a	n/a	n/a	n/a
300	2.8	5.5	11	17	22	27.5	33	#			
	40.5	37.7	32.2	27	21	15.7	10	#	n/a	n/a	n/a
400	2.1	4.1	8.3	12	17	20.6	25	#	33	37	41.3
	41.1	39.1	35	31	27	22.6	19	#	10.2	6.1	2
500	1.7	3.3	6.6	9.9	13	16.5	20	#	26.4	30	33
	41.6	39.9	36.6	33	30	26.7	23	#	16.8	14	10.2
600	1.4	2.8	5.5	8.3	11	13.8	17	#	22	25	27.5
	41.8	40.5	37.7	35	32	29.5	27	24	21.2	19	15.7
700	1.2	2.4	4.7	7.1	9.4	11.8	14	#	18.9	21	23.6
	42	40.8	38.5	36	34	31.4	29	#	24.3	22	19.6
800	1	2.1	4.1	6.2	8.3	10.3	12	#	16.5	19	20.6
	42.2	41.1	39.1	37	35	32.9	31	#	26.7	25	22.6
900	0.9	1.8	3.7	5.5	7.3	9.2	11	#	14.7	17	18.3
	42.3	41.4	39.5	38	36	34	32	#	28.5	27	24.9
1000	0.8	1.7	3.3	5	6.6	8.3	9.9	#	13.2	15	16.5
	42.4	41.6	39.9	38	37	35	33	#	30	28	26.7
1100	0.8	1.5	3	4.5	6	7.5	9	#	12	14	15
	42.5	41.7	40.2	39	37	35.7	34	#	31.2	30	28.2
1200	0.7	1.4	2.8	4.1	5.5	6.9	8.3	#	11	12	13.8
	42.5	41.8	40.5	39	38	36.3	35	#	32.2	31	29.5
1300	0.6	1.3	2.5	3.8	5.1	6.3	7.6	#	10.2	11	12.7
	42.6	41.9	40.7	39	38	36.9	36	#	33	32	30.5
1400	0.6	1.2	2.4	3.5	4.7	5.9	7.1	#	9.4	11	11.8
	42.6	42	40.8	40	39	37.3	36	35	33.8	33	31.4
1500	0.6	1.1	2.2	3.3	4.4	5.5	6.6	#	8.8	9.9	11
	42.7	42.1	41	40	39	37.7	37	#	34.4	33	32.2
1600	0.5	1	2.1	3.1	4.1	5.2	6.2	#	8.3	9.3	10.3
	42.7	42.2	41.1	40	39	38	37	36	35	34	32.9
1700	0.5	1	1.9	2.9	3.9	4.9	5.8	#	7.8	8.7	9.7
	42.7	42.2	41.3	40	39	38.3	37	#	35.4	35	33.5
1800	0.5	0.9	1.8	2.8	3.7	4.6	5.5	#	7.3	8.3	9.2
	42.7	42.3	41.4	41	40	38.6	38	#	35.9	35	34
1900	0.4	0.9	1.7	2.6	3.5	4.3	5.2	#	6.9	7.8	8.7
	42.8	42.3	41.5	41	40	38.9	38	#	36.3	35	34.5
2000	0.4	0.8	1.7	2.5	3.3	4.1	5	#	6.6	7.4	8.3
	42.8	42.4	41.6	41	40	39.1	38	#	36.6	36	35

The cell suspension was slowly pipetted and added to the master mix. 70 µl of solution was added to the centre of all wells in the first row of the chip. The tube strip holder was inserted into vortex. After vortexing about 30 seconds, centrifuged for approximately 5 seconds. After that, it was placed in a holder. 50 µl of Gel Beads were gently aspirated, added to the wells in the second row without forming bubbles, and left for 30 seconds at room temperature (RT). 45 µl of partitioning oil was dispensed into all wells in the third row of the chip (Figure 3.2.).

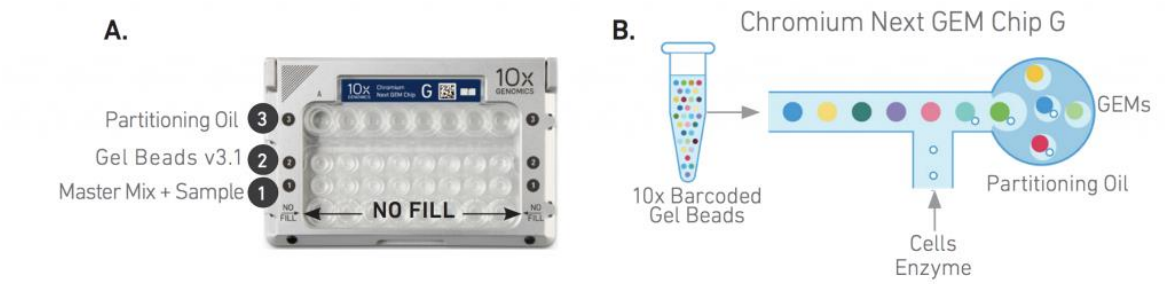

Figure 3.2. The principles of the 10X Genomics scRNA-seq library preparation

3.3.1.3. Running chromium controller, transferring GEMs and GEM-RT incubation

The chip was run on the Chromium Controller. After, it was ensured that any wells were not abnormally high. 100 µl of GEMs were slowly aspirated in the third row (Figure 3.2.). After ensuring that the GEMs appeared opaque and uniform in all channels, the GEMs were dispensed into the tube strip for approximately 20 seconds with the pipette tips and incubated with a thermal cycler under the incubation protocol provided by the company (Table 3.5.).

Table 3.5. Transferred GEM's RT incubation protocol

Lid Temperature	Reaction Volume	Run Time
53°C	125 µl	~55 min
Step	Temperature	Time
1	53°C	00:45:00
2	85°C	00:05:00
3	4°C	Hold

3.3.2. Post GEM–RT cleanup and cDNA amplification

3.3.2.1. Post GEM–RT cleanup

125 µl of recovery agent was added to the samples and waited for 2 minutes at RT and 125 µl of recovery agent + partitioning oil was slowly removed. According to Table 3.6., Dynabeads Cleanup Mix was prepared, vortexed, 200 µl was added to the sample, mixed by pipetting, and incubated at RT for 10 minutes, respectively. Then it was mixed again by pipetting approximately 5 minutes after the start of the incubation to resuspend the settled beads.

Table 3.6. Dynabeads Cleanup Mix protocol

Dynabeads Cleanup Mix (Reagents were added in the order listed)	8X (10% µl)
Cleanup Buffer	1602
Dbeads MyOne SILANE	70
Reducing Agent B	44
Nuclease-free Water	44
TOTAL	1760

Elution Solution I was prepared according to Table 3.7. and vortexed and briefly centrifuged. It was incubated for 10 minutes, then placed in the 10X Magnetic Separator in the elevated position until the solution cleared. The supernatant was removed. On the magnet, 300 µl of 80% ethanol was added to the pellet and waited approximately 30 seconds. Ethanol was removed. 200 µl of 80% ethanol was added to the pellet and left approximately 30 seconds. Ethanol was removed. Briefly centrifuged and placed on the magnet in a low position. The remaining ethanol was removed and dried about 1 minute in the air. It was removed from the magnet. 35.5 µl of Elution Solution I was immediately added and mixed with a pipette without creating bubbles. It was incubated for 2 minutes at RT. The solution was placed on the magnet in a low position until clear.

Table 3.7. Elution Solution preparing protocol

Elution Solution I (Reagents were added in the order listed)	1X (µl)	10X (µl)
Buffer EB	98	980
10% Tween 20	1	10
Reducing AgentB	1	10
Total	100	1000

3.3.2.2. cDNA amplification

The cDNA Amplification Mix was prepared according to Table 3.8. on ice. It was vortexed and centrifuged for mixing. 65 µl of mix was added to 35 µl of the sample. Pipetting was done. Centrifugation was done. It was incubated according to the protocol in Table 3.9.

Table 3.8. cDNA Amplification Reaction Mix preparing protocol

cDNA Amplification Reaction Mix (Reagents were added in the order listed)	8X 10% (µl)
Amp Mix	440
cDNA Primers	132
Total	572

Table 3.9. cDNA Amplification incubation protocol

Lid Temperature	Reaction Volume	Run Time
105°C	100 µl	~30-45 min
Step	Temperature	Time
1	98°C	00:03:00
2	98°C	00:00:15
3	63°C	00:00:20
4	72°C	00:01:00
5	15 cycles	
6	72°C	00:01:00
7	4°C	Hold

3.3.2.3. cDNA cleanup and cDNA quality control and quantification

The Ampure reagent was vortexed to resuspend, 60 µl of reagent was added to the sample and pipetted. Samples were incubated for 5 minutes at RT. They were placed in the high position of the magnet until the solution cleared. The supernatants were removed. 200 µl of 80% ethanol was added to the pellets and waited approximately 30 seconds. Ethanol was removed. Ethanol addition and removal steps were repeated for 2 washes. The samples

were centrifuged for a short time and placed in the high position of the magnet. The remaining ethanol was removed and dried for 2 minutes. 2 minutes were not exceeded as it would reduce the elution efficiency. Samples were removed from magnet. 40.5 µl of Buffer EB was added. Pipetting was done. The samples were incubated at RT for 2 minutes. The tube strip was placed on the magnet in a high position until the solution was clear. 40 µl of sample was transferred to a tube strip. The concentration and quality of the generated cDNAs were analysed by Qubit.

3.3.3. 3′ gene expression library construction

3.3.3.1. Fragmentation, end repair and A-tailing

The incubation protocol in Table 3.10. below was prepared. Fragmentation Buffer was vortexed. It was ensured that there was no precipitate. Fragmentation Mix was prepared (Table 3.11.) and mixed with a pipette and centrifuged. 10 µl of purified cDNA was transferred to a tube. 25 µl of Buffer EB and 15 µl of Fragmentation Mix were added to each sample, respectively. Pipetting was done on ice. It was briefly centrifuged. The pre-chilled thermal cycler was also started protocol.

Table 3.10. Fragmentation Mix incubation protocol

Lid Temperature	Reaction Volume	Run Time
65°C	50 µl	~35 min
Step	**Temperature**	**Time**
Pre-cool block	4°C	Hold
Fragmentation	32°C	00:05:00
End Repair & A-tailing	65°C	00:30:00
Hold	4°C	Hold

Table 3.11. Fragmentation Mix preparation protocol

Fragmentation Mix (Reagent were added in the order listed)	8X + 10% (µl)
Fragmentation Buffer	44
Fragmentation Enzyme	88
Total	132

3.3.3.2. Post fragmentation, end repair and a-tailing double sided size selection

Ampure reagent was vortexed to resuspend. 30 µl of reagent was added to sample. Pipetting was done. Sample was incubated for 5 minutes at RT. They were placed in a high position above the magnet until the solution cleared. The supernatant was removed. 75 µl of the supernatant was transferred to a tube. Ampure reagent was vortexed to suspend. 10 µl reagent was added to sample. Pipetting was done. Samples were incubated for 5 minutes at RT. They were placed in a high position above the magnet and 80 µl of supernatant was removed. The beads have been received. 125 µl of 80% ethanol was added to the pellets and held for 30 seconds. Ethanol was removed. For 2 washes, the ethanol addition and removal steps were repeated and briefly centrifuged. Samples were placed in the low position of the magnet until the solution cleared. The remaining ethanol was removed. The samples were removed from the magnet. 50.5 µl of Buffer EB was added to each sample. Pipetting was done. Samples were incubated at RT for 2 minutes. The solution was placed on the magnet in a high position until clear.

3.3.3.3. Adaptor ligation

The Adapter Ligation Mixture was prepared according to Table 3.12. Mixed with a pipette and briefly centrifuged. 50 µl of Mix was added to sample. Pipetting was done. It was briefly centrifuged. The samples were incubated according to the protocol in Table 3.13.

Table 3.12. Adaptor Ligation preparing protocol

Adaptor Ligation Mix (Reagents were added in the order listed)	8X 10% (µl)
Ligation Buffer	176
DNA Ligase	88
Adaptor Oligos	173
Total	440

Table 3.13. Adaptor Ligation incubation protocol

Lid Temperature	Reaction Volume	Run Time
30°C	100 µl	15 min
Step	**Temperature**	**Time**
1	20°C	00:15:00
2	4°C	Hold

3.3.3.4. Post ligation cleanup

The ampure reagent was vortexed to resuspend and 80 µl of Ampure Reagent was added to each sample. Pipetting was done. Samples were incubated fat RT for 5 minutes. They were held in a high position on the magnet until the solution cleared. The supernatant was removed. 200 µl of 80% ethanol was added to the pellets. Waited 30 seconds. Ethanol was removed. The ethanol addition and subtraction steps were repeated for 2 washes and centrifuged. Samples were placed on the magnet in the low position. The remaining ethanol was removed and dried approximately 2 minutes. After removed from magnet. 30.5 µl of Buffer EB was added. Pipetting was done. Incubation was done at RT for 2 minutes. The solution was placed in a low position on the magnet until clear.

3.3.3.5. Sample index-PCR

Non-overlapping sample index sets were selected (Table 3.14.). Sample Index PCR Mixture was prepared (3.15.) and 60 µl Mix was added to each 30 µl of sample. 10 µl of single Index was added to each well. Pipetting was done. It was briefly centrifuged and incubated (Table 3.16.).

Table 3.14. Sample Index

Sample	Sample Index
C1	A3
C2	A4
1B-1	A5
1B-2	A6
1B-3	A7
2B-1	A8
2B-2	A9
2B-3	A10

Table 3.15. Sample Index mixture preparation protocol

Sample Index PCR Mix (Reagents were added in the order listed)	8X 10% (µl)
AmpMix	440
SI Primer	88
Total	528

Table 3.16. Sample Index PCR incubation protocol

Lid Temperature	Reaction Volume	Run Time
105°C	100 µl	~25-40 min
Step	Temperature	Time
1	98°C	00:00:45
2	98°C	00:00:20
3	54°C	00:00:30
4	72°C	00:00:20
5		15 cycles
6	72°C	00:01:00
7	4°C	Hold

3.3.3.6. Post sample index PCR double sided size selection

The ampure reagent was vortexed to resuspend. 60 µl of reagent was added to sample. Pipetting was done. Incubation was done at RT for 5 minutes. The samples were held in a high position on the magnet until cleared. The supernatant was removed. 150 µl of the supernatant from the samples was transferred to tube. The ampure reagent was vortexed to resuspend. 20 µl of reagent was added to sample. Pipetting was done. Incubation was done at RT for 5 minutes. The samples were held in a high position on the magnet until they were

cleaned. 165 µl of supernatant was removed from the samples. While the tube was inside the magnet, 200 µl of 80% ethanol was added to the pellets. Waited 30 seconds. Ethanol was removed. The ethanol addition and subtraction steps were repeated 2 more times. Samples were briefly centrifuged. The samples were placed on the magnet in the low position. The ethanol was removed. The samples were removed from the magnet. 35.5 µl of Buffer EB was added to the samples. Pipetting was done. Incubation was done at RT for 2 minutes. The solution was placed on the magnet in a low position until cleared.

3.3.3.7. Post library construction quality control

1 µl of library at 1:10 dilution was loaded on the Agilent Bioanalyzer chip and the size and quality of the library were calculated.

3.4. Sequencing

All isolated *Arabidopsis thaliana* root protoplast samples were sequenced with 5000 cells per sample and 20000 readings per cell (100.000.000 reading per sample in total with single end sequencing) by Ger Era Diagnostics A.Ş. with Illumina NovaSeq 6000.

3.4. Data Analysis

3.4.1. Preprocessing

The Cell Ranger (v3.0.0) pipeline is a set of Chromium single cell data processing programs to align reads, produce feature-barcode matrices, clustering, and other analysis. First, with the Cellranger mkfastq command, FASTQ files were generated from the baseline call (BCL) files generated by the Illumina sequencing device. Then, with the cell ranger count command, reads were mapped to the TAIR10 reference genome by STAR software. The 10X Barcode and UMI counting was done, and feature-barcode matrices were created with chromium cellular barcodes. Finally, using 10X Genomic's Cellranger aggr pipeline, sample files (datasets) were aggregated for use in Loupe Browser (v.6.2.0). In this way, all samples were not analysed together and compared. The Cellranger aggr command automatically equalizes the average read depth per cell between groups before combining

the sample files. This approach avoids artifacts that may arise due to differences in sequencing depth.

3.4.2. Data filtering, dimensionality reduction, clustering, and cluster identification and differential gene expression analysis

Downstream analyses were conducted using the Loupe Browser (v.6.2.0). Firstly, interactive filtering and reclustering workflow were used to precisely screen out possible cell multiplets, dead cells, or cells with low diversity and perform PCA and t-SNE. In this workflow, filtering was performed using violin plots of UMI counts of the currently selected barcodes, threshold by a distinct number of detected features (number of distinct genes found for each barcode) and the percentage of UMIs per barcode associated with mitochondrial genes. Then, normalization was performed with the library size parameter per cell. PCA (default 20 PCA) was performed via the num_principal_comps command using the Python implementation of the IRLBA algorithm to reduce the size of the dataset, the samples were visualized t-SNE (default 30 t-SNE). After filtering and reclustering workflow, cell clusters were then identified using specific and validated gene markers for each cell type to cluster the cells in a robust manner. Differential gene expression was performed with a negative binomial exact test using sSeq application.

3.4.3. Gene ontology and KEGG (kyoto encyclopedia of genes and genomes pathway) orthology analysis

Gene ontology (GO) and KEGG orthology (KO) analysis was performed using the web-based program ShinyGO (v.0.76.3) [123]. p-values were calculated according to the hypergeometric distribution of gene numbers. This applies to both query and background genes. False Discovery Rate (FDR) was calculated according to the nominal p value obtained from the hypergeometric test. The FDR cutoff value was chosen as 0.05, and then the important pathways (biological process, cellular component, and molecular function) were ranked according to the FDR Enrichment value and visualized with Dotplot. KEGG pathways were obtained and visualized with KEGG pathway map and Dotplot.

3.4.4. Heatmap analysis of gene expression

Lists of 50 most differentially expressed genes (DEGs) were used for the heat map analysis. Briefly, gene count was $\log_2$ normalized and scaled via the Loupe Browser (v.6.2.0).

4. RESULTS

4.1. Plant Growth

Arabidopsis seeds were grown in vitro conditions for 14 days after surface sterilization (Figure 4.1.). Arabidopsis roots were obtained by positioning the petri dishes vertically after planting. Growth results after culturing were shown in Figure 4.2.- 4.4.

Figure 4.1. Growth chamber (Poetries are positioned vertically after planting)

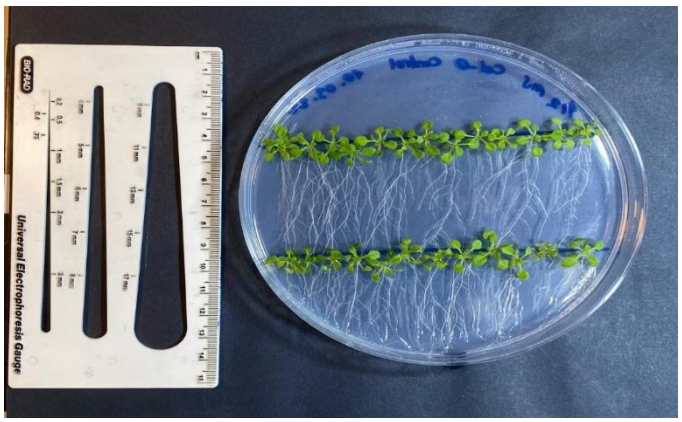

Figure 4.2. Plants grown in vitro for 14 days (control group)

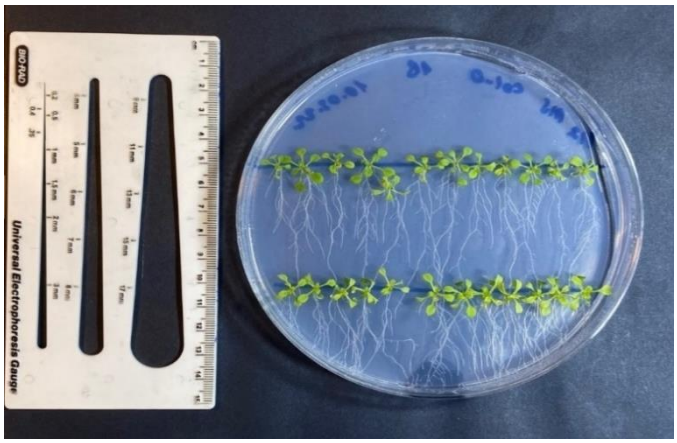

Figure 4.3. Plants grown in vitro for 14 days (1B treatment group)

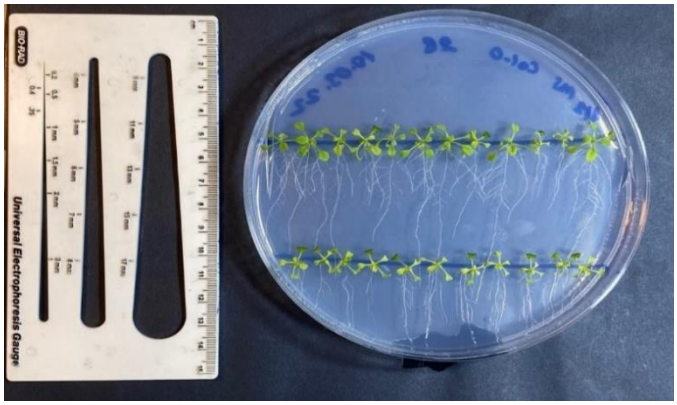

Figure 4.4. Plants grown in vitro for 14 days (2B treatment group)

4.2. Protoplast Isolation

Primary root protoplast isolation protocol has been optimized to reliably implement the 10X genomics scRNA-seq and produce residue-free single-cell suspensions at the seedling stage. In this way, pellets were found in falcons in isolated protoplasts for all experimental groups. Pellet images of the control group protoplasts are given in Figure 4.5. Isolated protoplasts were examined under a light microscope and live cells were counted separately in 1 µl of each sample and cell viability was calculated (Table 4.1.).

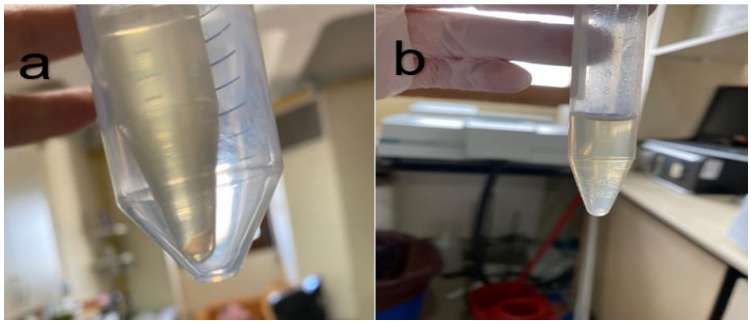

Figure 4.5. Pellet image of the precipitated protoplasts (Control group a: C1, b: C2)

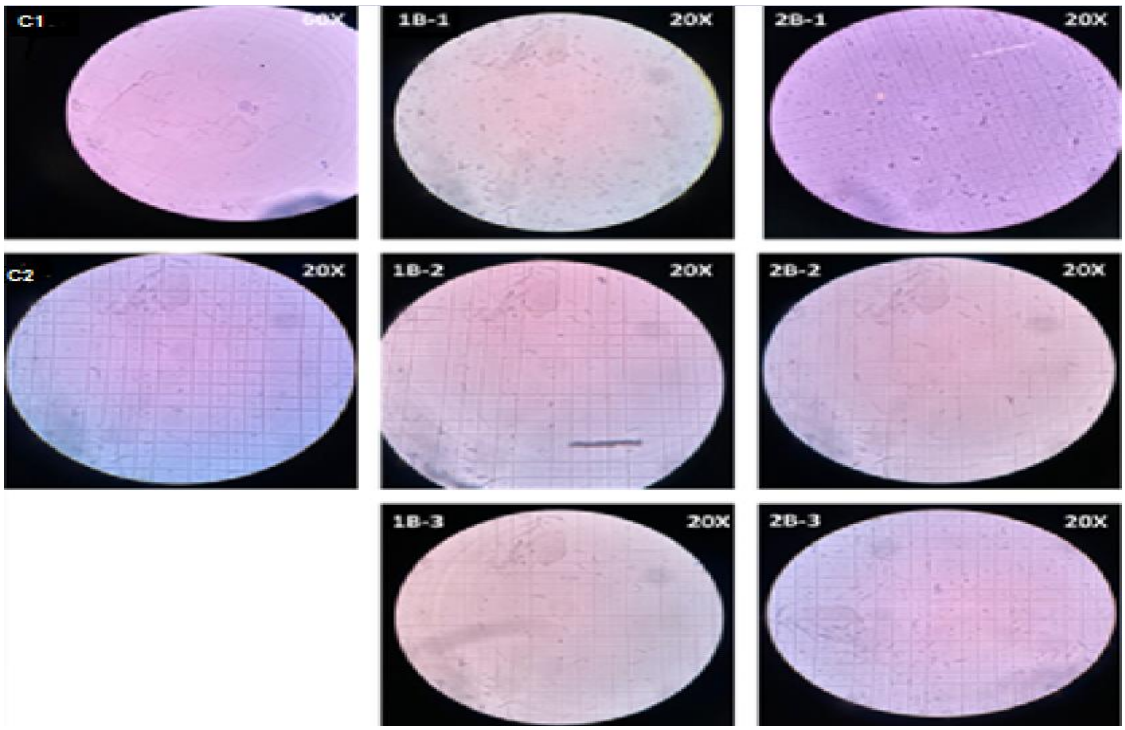

Figure 4.6. Light microscope image of *Arabidopsis thaliana* root protoplast cells (Control (C) group 1B treatment group and 2B treatment group)

Table 4.1. Cell count results of isolated protoplast solutions (cells/µl)

Condition	Replica	Alive cell number (cell/µl)
C	C1	500
	C2	320
1B	1B1	520
	1B2	720
	1B3	760
2B	2B1	680
	2B2	420
	2B3	520

4.3. Single cell library construction

In accordance with 10X Genomics Inc. instructions, single cell solutions were prepared using the Chromium Next GEM Single Cell v3.1 kit and loaded into 3' v2 chemistry Chromium microfluidic chips and barcoded with the 10X Chromium Controller device. Reverse transcription was performed from the mRNAs of barcoded cells, followed by library

constructed. The size and quality of cDNAs were analysed with Qubit device (Table 4.2.) and the size and quality of libraries with Bioanalyzer device (Figure 4.7.-4.15.).

Table 4.2. Concentration of protoplast cDNAs determined by Qubit device

Sample	Concentration (ng/µl)	Dilution Factor	Cycle
C1	4.21	40	15
C2	1.72	40	15
1B1	7.02	40	15
1B2	2.31	40	15
1B3	12.9	40	15
2B1	4.15	40	15
2B2	2.16	40	15
2B3	2.59	40	15

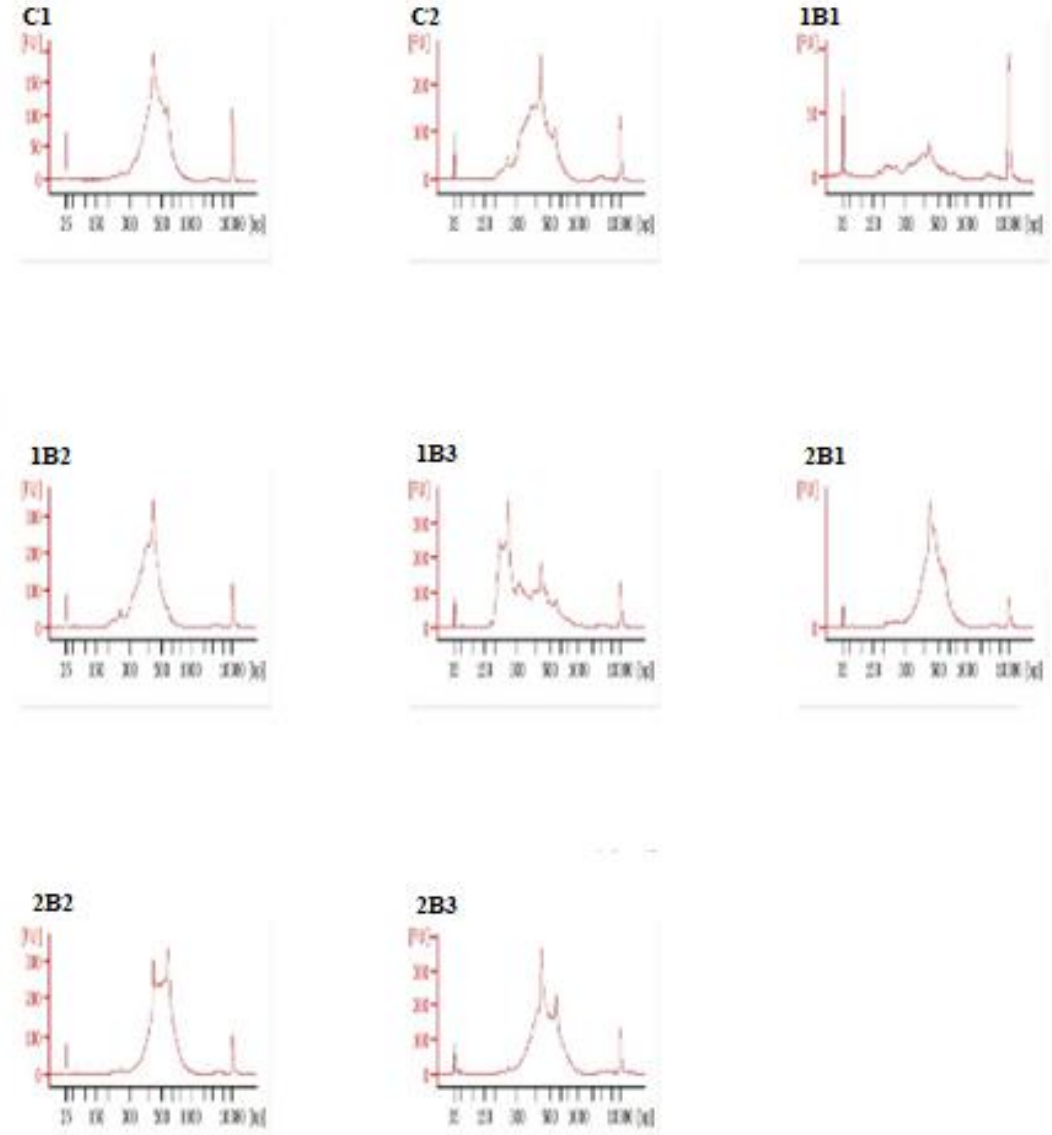

Figure 4.7. Electropherogram results of the protoplast libraries analyzed with the Bioanalyzer

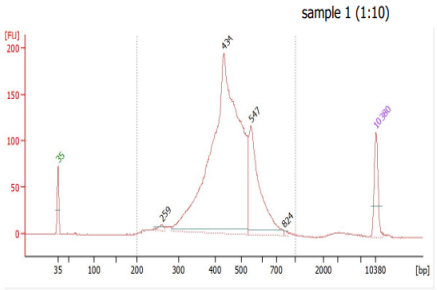

Overall Results for sample 1 : sample 1 (1:10)

Number of peaks found:	4	Corr. Area 1:	2,370.8
Noise:	0.4		

Peak table for sample 1 : sample 1 (1:10)

Peak		Size [bp]	Conc. [pg/µl]	Molarity [pmol/l]	Observations
1	◀	35	125.00	5,411.3	Lower Marker
2		259	18.42	107.9	
3		434	1,930.82	6,744.3	
4		547	411.08	1,139.4	
5		824	4.60	8.5	
6	▶	10,380	75.00	10.9	Upper Marker

Region table for sample 1 : sample 1 (1:10)

From [bp]	To [bp]	Corr. Area	% of Total	Average Size [bp]	Size distribution in CV [%]	Conc. [pg/µl]	Molarity [pmol/l]	Color
200	1,000	2,370.8	98	458	20.6	2,568.53	9,049.3	

Figure 4.8. Size and quality of the protoplast (C1) library analyzed with the Bioanalyzer

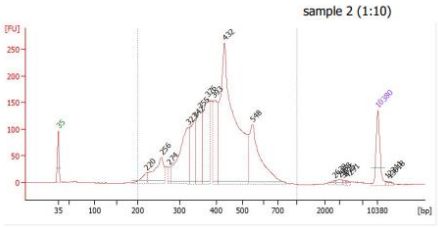

Overall Results for sample 2 : sample 2 (1:10)

Number of peaks found:	16	Corr. Area 1:	3,494.1
Noise:	0.4		

Peak table for sample 2 : sample 2 (1:10)

Peak		Size [bp]	Conc. [pg/µl]	Molarity [pmol/l]	Observations
1	◀	35	125.00	5,411.3	Lower Marker
2		220	44.86	309.6	
3		256	178.86	1,057.8	
4		274	34.57	191.2	
5		323	347.02	1,626.2	
6		342	197.05	872.9	
7		355	208.11	888.5	
8		376	290.87	1,172.3	
9		393	186.42	717.8	
10		432	1,046.98	3,668.4	
11		548	302.99	837.2	
12		2,639	5.96	3.4	
13		2,968	8.86	4.5	
14		3,625	3.10	1.3	
15		4,291	3.64	1.3	
16	▶	10,380	75.00	10.9	Upper Marker
17		12,311	0.00	0.0	
18		13,018	0.00	0.0	

Region table for sample 2 : sample 2 (1:10)

From [bp]	To [bp]	Corr. Area	% of Total	Average Size [bp]	Size distribution in CV [%]	Conc. [pg/µl]	Molarity [pmol/l]	Color
200	1,000	3,494.1	96	414	23.6	3,024.68	12,026.4	

Figure 4.9. Size and quality of the protoplast (C2) library analyzed with the Bioanalyzer

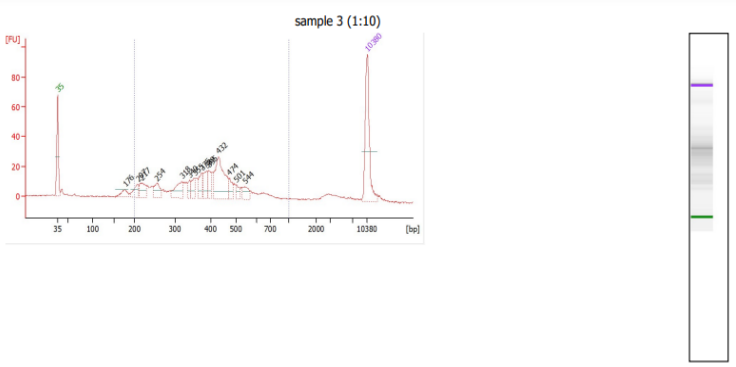

Overall Results for sample 3 : **sample 3 (1:10)**

Number of peaks found:	14	Corr. Area 1:	440.2
Noise:	0.5		

Peak table for sample 3 : **sample 3 (1:10)**

Peak	Size [bp]	Conc. [pg/µl]	Molarity [pmol/l]	Observations
1	35	125.00	5,411.3	Lower Marker
2	176	19.44	167.5	
3	207	25.87	189.1	
4	217	32.77	228.7	
5	254	30.97	184.6	
6	318	39.48	187.9	
7	340	13.43	59.9	
8	355	19.05	81.3	
9	375	23.17	93.6	
10	389	26.21	102.1	
11	395	23.99	92.1	
12	432	98.61	346.2	
13	474	16.33	52.1	
14	501	10.87	32.9	
15	544	15.97	44.5	
16	10,380	75.00	10.9	Upper Marker

Region table for sample 3 : **sample 3 (1:10)**

From [bp]	To [bp]	Corr. Area	% of Total	Average Size [bp]	Size distribution in CV [%]	Conc. [pg/µl]	Molarity [pmol/l]	Color
200	1,000	440.2	83	400	30.7	513.16	2,226.8	

Figure 4.10. Size and quality of the protoplast (1B1) library analyzed with the Bioanalyzer

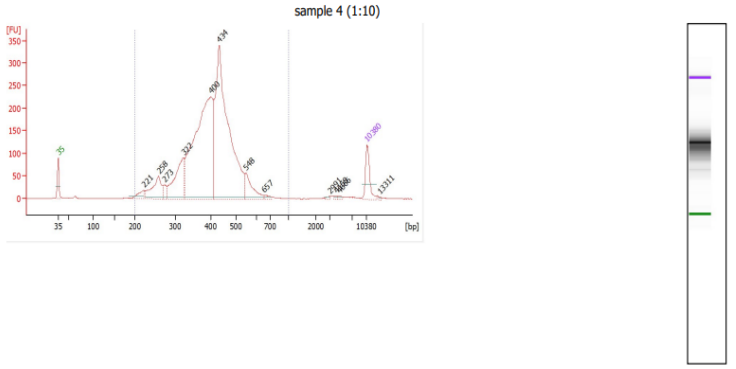

Overall Results for sample 4 : **sample 4 (1:10)**

Number of peaks found:	12	Corr. Area 1:	3,684.8
Noise:	0.4		

Peak table for sample 4 : **sample 4 (1:10)**

Peak	Size [bp]	Conc. [pg/µl]	Molarity [pmol/l]	Observations
1	35	125.00	5,411.3	Lower Marker
2	221	53.31	366.2	
3	258	193.01	1,133.4	
4	273	42.08	233.7	
5	322	292.42	1,375.6	
6	400	1,235.19	4,673.5	
7	434	1,307.11	4,561.1	
8	548	106.39	294.0	
9	657	11.46	26.4	
10	2,991	4.73	2.4	
11	4,168	4.53	1.6	
12	4,666	4.50	1.5	
13	10,380	75.00	10.9	Upper Marker
14	13,311	0.00	0.0	

Region table for sample 4 : **sample 4 (1:10)**

From [bp]	To [bp]	Corr. Area	% of Total	Average Size [bp]	Size distribution in CV [%]	Conc. [pg/µl]	Molarity [pmol/l]	Color
200	1,000	3,684.8	97	407	20.3	3,325.14	13,182.8	

Figure 4.11. Size and quality of the protoplast (1B2) library analyzed with the Bioanalyzer

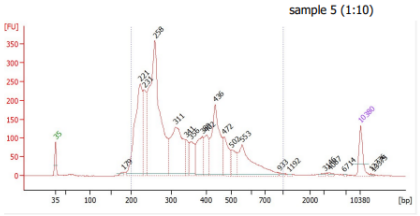

Overall Results for sample 5 : sample 5 (1:10)

Number of peaks found:	20	Corr. Area 1:	5,170.3
Noise:	0.5		

Peak table for sample 5 : sample 5 (1:10)

Peak	Size [bp]	Conc. [pg/µl]	Molarity [pmol/l]	Observations
1	35	125.00	5,411.3	Lower Marker
2	179	16.74	141.6	
3	221	836.92	5,727.2	
4	231	338.38	2,218.4	
5	258	1,579.51	9,273.5	
6	311	576.76	2,812.8	
7	341	94.53	420.0	
8	356	156.33	665.5	
9	389	209.97	817.0	
10	402	144.92	546.8	
11	436	448.40	1,557.9	
12	472	167.19	536.3	
13	502	95.22	287.4	
14	553	318.47	872.1	
15	933	8.18	13.3	
16	1,192	3.98	5.1	
17	3,146	7.28	3.5	
18	4,087	7.66	2.8	
19	6,714	2.49	0.6	
20	10,380	75.00	10.9	Upper Marker
21	12,776	0.00	0.0	
22	13,375	0.00	0.0	

Region table for sample 5 : sample 5 (1:10)

From [bp]	To [bp]	Corr. Area	% of Total	Average Size [bp]	Size distribution in CV [%]	Conc. [pg/µl]	Molarity [pmol/l]	Color
200	1,000	5,170.3	96	347	36.5	4,989.45	25,361.4	

Figure 4.12. Size and quality of the protoplast (1B3) library analyzed with the Bioanalyzer

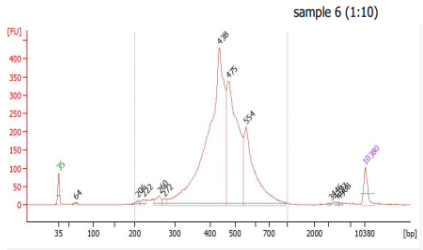

Overall Results for sample 6 : sample 6 (1:10)

Number of peaks found:	11	Corr. Area 1:	4,603.4
Noise:	0.6		

Peak table for sample 6 : sample 6 (1:10)

Peak	Size [bp]	Conc. [pg/µl]	Molarity [pmol/l]	Observations
1	35	125.00	5,411.3	Lower Marker
2	64	19.38	460.4	
3	206	29.68	218.1	
4	222	37.26	254.1	
5	260	72.06	420.6	
6	272	29.47	164.3	
7	438	2,629.50	9,104.4	
8	475	1,336.80	4,267.6	
9	554	772.08	2,112.8	
10	3,446	5.47	2.4	
11	4,327	6.26	2.2	
12	4,968	5.00	1.5	
13	10,380	75.00	10.9	Upper Marker

Region table for sample 6 : sample 6 (1:10)

From [bp]	To [bp]	Corr. Area	% of Total	Average Size [bp]	Size distribution in CV [%]	Conc. [pg/µl]	Molarity [pmol/l]	Color
200	1,000	4,603.4	97	462	20.8	5,018.53	17,557.1	

Figure 4.13. Size and quality of the protoplast (2B1) library analyzed with the Bioanalyzer

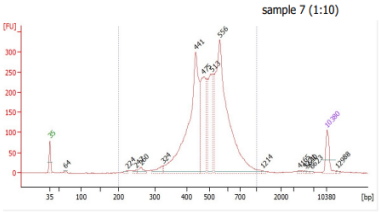

Overall Results for sample 7 : sample 7 (1:10)

Number of peaks found:	15	Corr. Area 1:	3,742.7
Noise:	0.7		

Peak table for sample 7 : sample 7 (1:10)

Peak	Size [bp]	Conc. [pg/µl]	Molarity [pmol/l]	Observations
1	35	125.00	5,411.3	Lower Marker
2	64	11.71	278.7	
3	224	11.91	80.7	
4	247	12.71	78.1	
5	260	41.15	239.6	
6	324	51.24	239.4	
7	441	1,249.37	4,296.9	
8	475	401.63	1,281.7	
9	513	365.04	1,077.8	
10	556	1,381.21	3,765.1	
11	1,214	5.26	6.6	
12	4,165	5.04	1.8	
13	5,271	2.96	0.9	
14	5,640	2.99	0.8	
15	6,623	3.11	0.7	
16	10,380	75.00	10.9	Upper Marker
17	12,988	0.00	0.0	

Region table for sample 7 : sample 7 (1:10)

From [bp]	To [bp]	Corr. Area	% of Total	Average Size [bp]	Size distribution in CV [%]	Conc. [pg/µl]	Molarity [pmol/l]	Color
200	1,000	3,742.7	98	505	19.7	3,816.99	12,134.1	

Figure 4.14. Size and quality of the protoplast (2B2) library analyzed with the Bioanalyzer

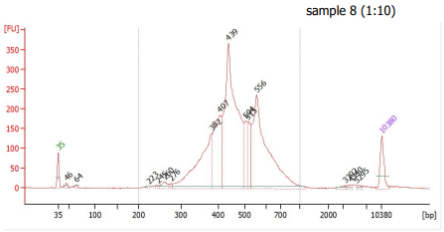

Overall Results for sample 8 : sample 8 (1:10)

Number of peaks found:	15	Corr. Area 1:	3,818.6
Noise:	0.8		

Peak table for sample 8 : sample 8 (1:10)

Peak	Size [bp]	Conc. [pg/µl]	Molarity [pmol/l]	Observations
1	35	125.00	5,411.3	Lower Marker
2	46	20.57	674.7	
3	64	10.86	258.4	
4	223	9.13	62.0	
5	245	12.20	75.3	
6	260	33.60	195.6	
7	276	11.34	62.2	
8	382	575.62	2,281.9	
9	407	407.02	1,514.5	
10	439	1,225.37	4,227.6	
11	504	141.33	425.1	
12	515	136.40	401.4	
13	556	868.14	2,366.3	
14	3,302	8.41	3.9	
15	4,340	7.76	2.7	
16	5,295	6.92	2.0	
17	10,380	75.00	10.9	Upper Marker

Region table for sample 8 : sample 8 (1:10)

From [bp]	To [bp]	Corr. Area	% of Total	Average Size [bp]	Size distribution in CV [%]	Conc. [pg/µl]	Molarity [pmol/l]	Color
200	1,000	3,818.6	96	477	22.6	3,421.87	11,633.5	

Figure 4.15. Size and quality of the protoplast (2B3) library analyzed with the Bioanalyzer

4.4. Data Analysis

4.4.1. Preprocessing and cluster annotation

With Cell ranger (v3.0.0) pipeline, raw reads were demultiplexed into FASTQ files and alignment, barcode counting were performed. Finally, datasets (*Arabidopsis thaliana* sample files) were aggregated. The sample files combined with the Cellranger aggr command were filtered and normalized using the Loupe Browser (v.6.2.0) program. In the filtering step, droplets containing multiple cells, empty droplets, low-quality cells, cells containing large numbers of mRNAs, and ambient RNAs were filtered. It was observed that some of the 8 samples (C1, 1B2, 1B3, 2B1, 2B3) had too much mRNA and ambient RNA. Too much mRNA contamination and/or dead cells are thought to be present in these samples. Therefore, these samples were not used in downstream analysis. Among other data sets, the best biological replicates (C2, 1B1 and 2B2) were selected from each experimental group (C, 1B, and 2B) according to data quality and the study was continued with these data sets. Accordingly, a total population of 1554 cells were recovered across three replicates. Approximately 179368 reads were obtained per cell, which generated a median of 1686 unique molecular identifiers per cell, more than 19000 total genes detected per each replicate, more than 82% Q30 bases in RNA read per each replicate, and more than 93% valid barcode total per each replicate (Table 4.3.).

Table 4.3. Cell ranger summary results

Groups	**C**	**1B**	**2B**
Estimated Number of Cells	542	374	638
Mean Reads per Cell	54,062	323957	160084
Median Genes per Cell	1,088	588	916
Number of Reads	29,301,440	1.21E+08	1.02E+08
Valid Barcodes	95.70%	93.90%	96.00%
Sequencing Saturation	32.90%	62.10%	71.00%
Q30 Bases in Barcode	94.70%	94.40%	94.70%
Q30 Bases in RNA Read	89.70%	82.40%	88.30%
Q30 Bases in UMI	92.40%	91.90%	92.50%
Reads Mapped to Genome	89.60%	59.40%	92.10%
Reads Mapped Confidently to Genome	62.40%	32.40%	61.60%
Reads Mapped Confidently to Intergenic Regions	7.20%	8.20%	6.20%
Reads Mapped Confidently to Intronic Regions	0.30%	0.20%	0.40%
Reads Mapped Confidently to Exonic Regions	54.90%	24.00%	55.00%
Reads Mapped Confidently to Transcriptome	47.90%	16.80%	47.50%
Reads Mapped Antisense to Gene	7.30%	7.40%	7.90%
Fraction Reads in Cells	31.30%	21.50%	36.40%
Total Genes Detected	20,786	19518	21854
Median UMI Counts per Cell	1,813	1448	1798

Plotting the single-cell transcriptomes via Louvain clustering and t-SNE projections using Loupe Browser (v.6.2.0). yielded six clusters of cell transcriptomes. We then determined tissue/cell type cluster annotation using 16 marker genes (Table 4.4.). We identified some major cell types including quiescent cells (QC), endodermis, cortex, columella, trichoblast (root-hair) and root cap. Identified clusters and organization of the Arabidopsis root were shown in Figure 4.16. [124].

Table 4.4. Arabidopsis root cell specific markers used to identify the clusters.

AGI Code	Gene Name		Location
AT5G49270	COBL9/ SHV2	COBRA-LIKE 9/ SHAVEN 2	Trichoblast
AT1G33280	BRN1/ NAC015	BEARSKIN 1/ NAC DOMAIN CONTAINING PROTEIN 15	Root Cap
AT1G79580	SMB/ ANAC033	SOMBRERO/ ARABIDOPSIS NAC DOMAIN CONTAINING PROTEIN 33	Root Cap
AT5G62165	AGL42	AGAMOUS-LIKE 42	QC
AT5G02130	SSR1	SHORT AND SWOLLEN ROOT 1	QC
AT3G54220	SCR	SCARECROW	Endodermis
AT5G14750	WER/ MYB66	WEREWOLF/ MYB DOMAIN PROTEIN 66	Epidermis and Lateral Root Cap
AT1G26870	FEZ		Epidermis LRC Stem
AT5G57620	MYB36	MYB DOMAIN PROTEIN 36	Endodermis
AT2G36100	CASP1	CASPARIAN STRIP MEMBRANE DOMAIN PROTEIN 1	Endodermis
AT1G78520			Columella
AT3G61930			Proximal and distal columella
AT1G62510	CORTEX4		Cortex
AT4G30080	ARF16	AUXIN RESPONSE FACTOR 16	Root Cap
AT1G01570			Columella
AT3G12700	Cor10		Cortex

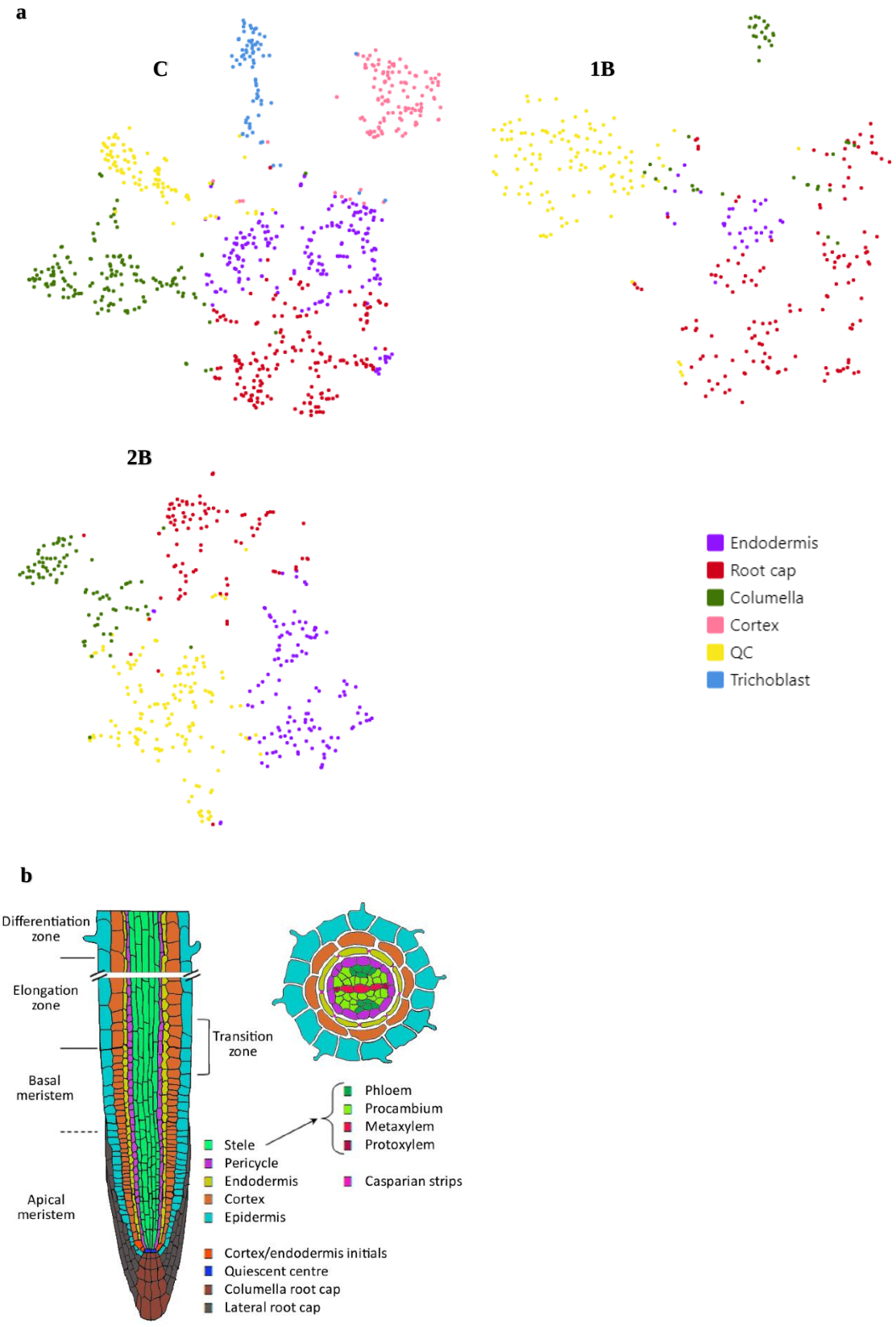

Figure 4.16. Cluster analysis of single-cell transcriptomes, a) t-SNE projection plot showing 6 major clusters of the 1554 individual Arabidopsis root cell transcriptomes. C: Control group, 1B: 1mM treatment group and 2B: 2mM treatment group b) Organization of the Arabidopsis root. Depictions of transverse (left) and longitudinal (right) sections of the Arabidopsis primary root (QC: Quiescent center) [124]

4.4.2. DEGs of single-cell transcriptome of Arabidopsis roots exposed to boron toxicity

We used Loupe software (v.6.2.0) to identify changes in gene expression profiles among all clusters and for each cluster individually in Arabidopsis roots under B toxicity. The number of overlapping DEGs between all group were shown in Figure 4.17a., 4.17b. and the number of overlapping DEGs in the clusters for each group were shown in Figure 4.17c-4.17h. and the number of overlapping DEGs between the groups for each cluster were given in Figure 4.18. by using upset plot (http://www.bioinformatics.com.cn/en). In each panel on these upset plots, the lower left horizontal bar graph labelled DEG size shows the total number of DEGs per post-treatment time point. The circles in the matrix of each panel represent the unique and overlapping DEGs. Accordingly, we found that 84, 49 and 218 genes were specifically upregulated in C, 1B and 2B, respectively (Figure 4.17a). 23 upregulated genes were commonly regulated in both 1B and 2B (Figure 4.17a.). On the other hand, 262, 46 and 148 genes were specifically downregulated in C, 1B and 2B, respectively (Figure 4.17b.). 32 genes were commonly downregulated in both 1B and 2B Figure 4.17b.).

We also determined the overlapping DEGs between clusters for each group (Figure 4.17c.-4.17l.). Accordingly, we found that 112, 109, 86, 60, 48 and 27 were specifically upregulated under C in trichoblast, columella, QC, cortex, root cap and endodermis, respectively (Figure 4.17c.). Moreover, under this condition, 76, 73, 25 and 10 genes were commonly upregulated between columella and QC, and between cortex and trichoblast, and between endodermis and root cap, and between endodermis and QC, respectively. 12 genes were commonly upregulated in endodermis, root cap and QC and 8 genes were commonly upregulated in endodermis, columella and QC, and 7 genes were commonly upregulated in endodermis, cortex and trichoblast (Figure 4.17c.). On the other hand, 15, 10, 9, 6, 4 and 3 genes were specifically downregulated under C in endodermis, QC, root cap, columella, cortex, and trichoblast, respectively (Figure 4.17d.). Furthermore, 14 genes were commonly downregulated between endodermis and root cap, and also 5 genes were commonly downregulated in cortex, trichoblast, root cap and endodermis, and 4 genes were commonly downregulated in cortex, trichoblast, QC, root cap and endodermis (Figure 4.17d.).

Under 1B condition, 151, 96, 45 and 37 genes were specifically upregulated in columella, endodermis, root cap and QC, respectively (Figure 4.17e.). Additionally, 27, 16

and 14 genes were commonly upregulated between root cap and endodermis, and between endodermis and columella, and between root cap and columella, respectively (Figure 4.17e.). On the other hand, 17 and 9 genes were specifically downregulated under 1B in root cap and endodermis, respectively (Figure 4.17f.). 7 genes commonly downregulated between root cap and endodermis (Figure 4.17f.).

Under 2B condition, 159, 146, 134 and 52 genes were specifically upregulated in endodermis, QC, columella and root cap, respectively (Figure 4.17g.). Additionally, 68, 40, 32, 18 and 14 genes were commonly upregulated between columella and QC, and between root cap and QC, and between root cap and endodermis, and between root cap and columella, and between endodermis and QC, respectively. Furthermore, 7 genes commonly upregulated in root cap, endodermis and QC (Figure 4.17g.). On the other hand, 50, 18, 11 and 8 genes were specifically downregulated under 2B in root cap, QC, columella and endodermis, respectively (Figure 4.17h.). Additionally, 20, 12 and 12 genes were commonly downregulated between QC and root cap, and between endodermis and root cap, and between columellar and root cap, respectively. Also, 8 genes commonly downregulated in endodermis, QC and root cap, and 6 genes commonly downregulated in endodermis, columella and root cap (Figure 4.17h.).

Furthermore, we determined the common and DEGs between C and B toxicity conditions for each cell cluster to find high B responsive regulations of gene expression patterns of clusters in Arabidopsis root (Figure 4.18.). Accordingly, 57, 56 and 98 genes were specifically upregulated in endodermis under C, 1B and 2B, respectively (Figure 4.18a.). Moreover, in this cluster, 66 genes were commonly upregulated between 1B and 2B (Figure 4.18a.). On the other hand, 39, 15 and 15 genes were specifically downregulated in endodermis under C, 1B and 2B, respectively (Figure 4.18b.). 24, 43 and 49 genes were specifically upregulated in root cap under C, 1B and 2B, respectively (Figure 4.18c.). Additionally, in this cluster, 14 genes were commonly upregulated 1B and 2B (Figure 4.18c.). On the other hand, 15, 4 and 63 genes were specifically downregulated in root cap. On the other hand, 15, 4 and 63 genes were specifically downregulated in root cap under C, 1B and 2B, respectively (Figure 4.18d.). Moreover, 9 genes were commonly upregulated between 1B and 2B (Figure 4.18d.). 110, 42 and 153 genes were specifically upregulated in QC under C, 1B and 2B, respectively (Figure 4.18e.). On the other hand, 29 and 44 genes were specifically downregulated in C and 2B, respectively (Figure 4.18f.). 66, 13 and 54

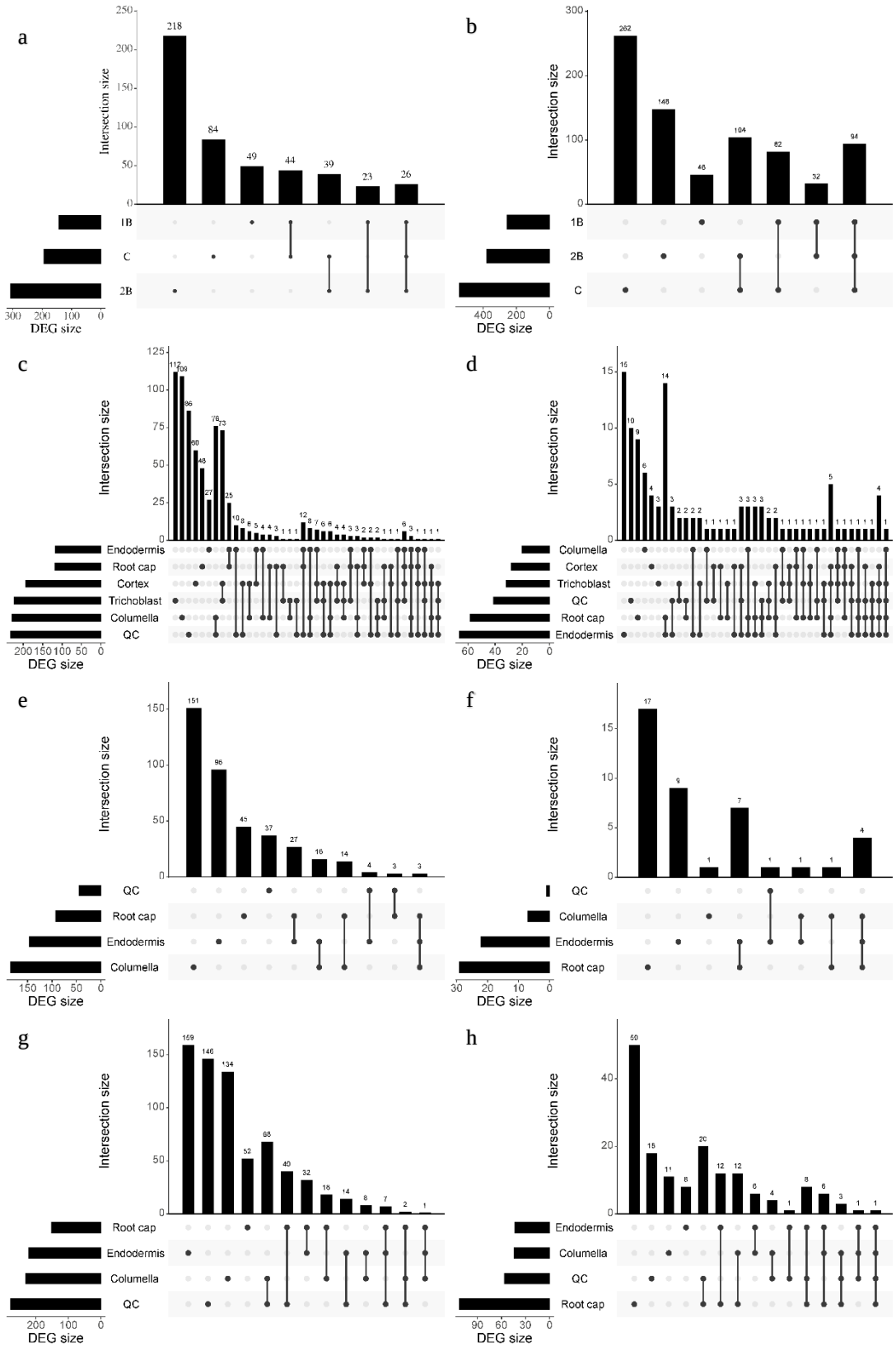

Figure 4.17. Upset plots to summarize the common and specifically regulated genes. a) The intersection of upregulated genes between C and B toxicity treatment groups, b) The intersection of downregulated genes between C and B toxicity treatment groups, c) The intersection of upregulated genes between clusters under C condition, d) The intersection of downregulated genes between clusters under C condition e) The intersection of upregulated genes between clusters under 1B condition, f) The intersection of downregulated genes between clusters under 1B condition, g) The intersection of upregulated genes between clusters under 2B condition and h) The intersection of downregulated genes between clusters under 2B condition

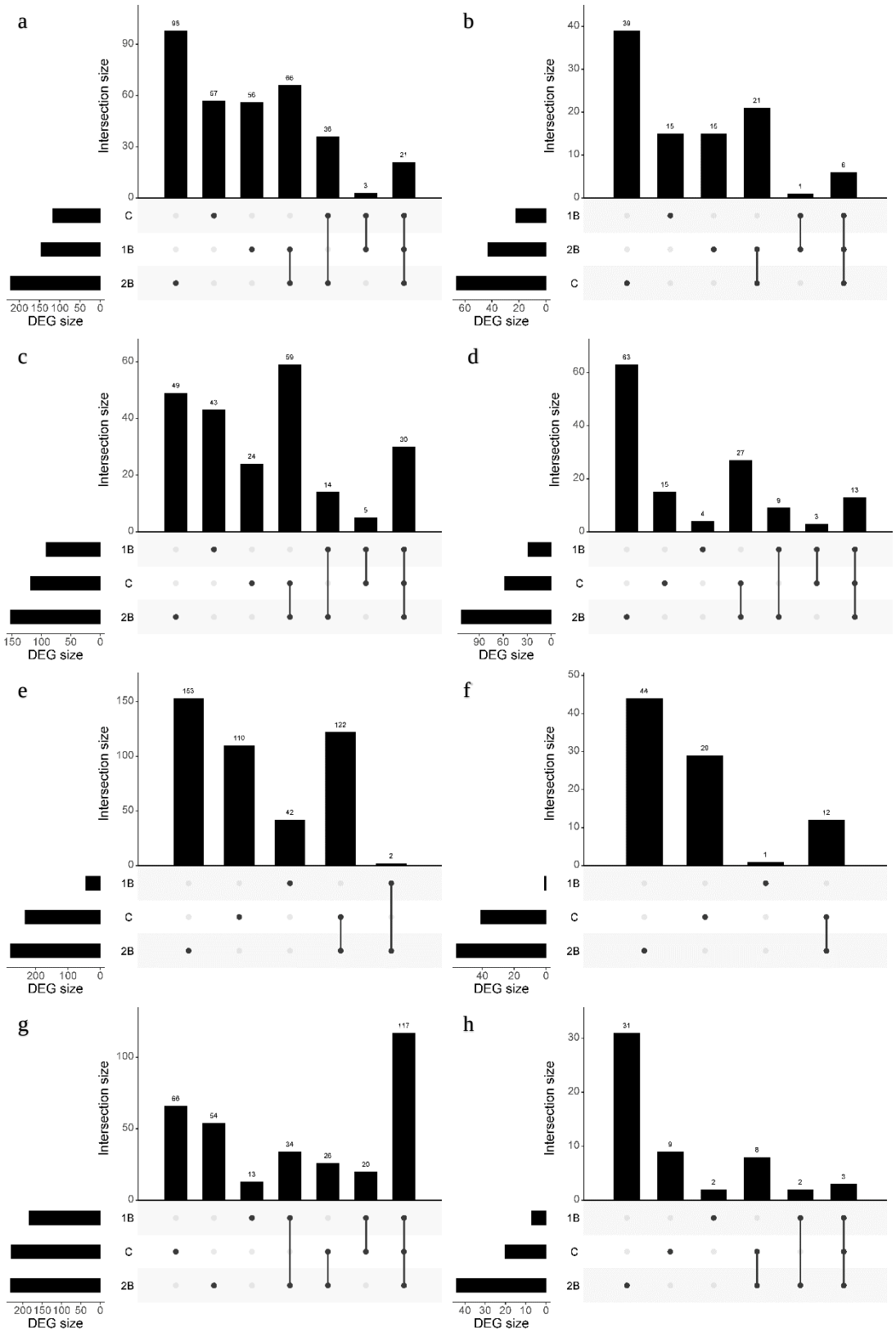

Figure 4.18. Upset plots to summarize overlaps between clusters for up and downregulated genes, a, c, e, g) The intersection of upregulated genes in endodermis, root cap, QC and columella respectively, and b, d, f, h) The intersection of downregulated genes in endodermis, root cap, QC and columella, respectively

genes were specifically upregulated in columella under C, 1B and 2B, respectively (Figure 4.18g.). Moreover, in this cluster, 34 genes were commonly upregulated between 1B and 2B (Figure 4.18g.). On the other hand, 9 and 31 genes were specifically downregulated in C and 2B, respectively (Figure 4.18h.).

4.4.3. GO and KO Analyses

To determine whether B toxicity is associated with unique GO terms (biological process, cellular component, and molecular function) at cell clusters, a GO enrichment analysis of gene expression subsets based on each cluster of B toxicity treatment groups was performed (Figure 4.19.-4.26.). Accordingly, under 1B condition in columella, top-ranked biological processes were response to hypoxia, cellular response to hypoxia, response to oxygen level and cellular response to decreased oxygen level (Figure 4.19a.), and top-ranked cellular components were cell wall and external encapsulating structure (Figure 4.19b.), and top-ranked molecular functions were serine type endopeptidase inhibitor activity, peptidase inhibitor activity, endopeptidase inhibitor activity, endopeptidase regulator activity, peptidase regulator activity and flavin adenine dinucleotide binding (Figure 4.19c.) for upregulated genes. In this cluster, top-ranked biological processes were tryptophan catabolic process to kynurenine, kynurenine metabolic process, indolalkylamine catabolic process, cellular biogenic amine catabolic process, amine catabolic process and indole-containing compound catabolic process (Figure 4.19d.), and top-ranked cellular component was mitochondrion (Figure 4.19e.), and top-ranked molecular function was RNA binding (Figure 4.19f.) for downregulated genes.

In endodermis, top-ranked biological process was ATP metabolic process (Figure 4.20a.), top-ranked cellular components were inner mitochondrial membrane protein complex, mitochondrial protein-containing complex and mitochondrial inner membrane (Figure 4.20b.), and top-ranked molecular function was protein transmembrane transporter activity (Figure 4.20c.) for upregulated genes. In this cluster, top-ranked biological processes were organonitrogen compound biosynthetic process, cellular amide metabolic process and amide biosynthetic process (Figure 4.20d.), and top-ranked cellular component was mitochondrion (Figure 4.20e.), and top-ranked molecular function was FMN binding (Figure 4.20f.) for downregulated genes.

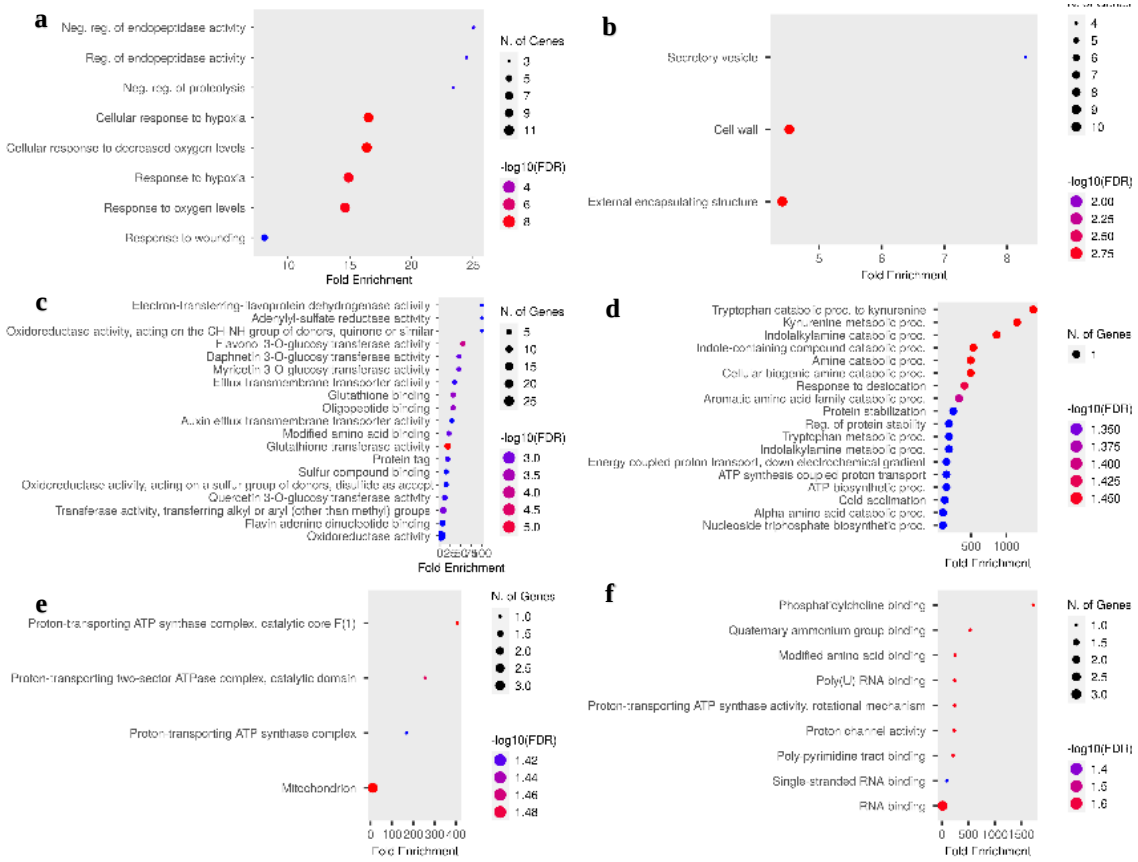

Figure 4.19. Significantly enriched GO terms in columella under 1B condition, a, b, c) BP, CC and MF for upregulated genes in columella, respectively, d, e, f) BP, CC and MF for downregulated genes in columella, respectively. BP: Biological process, CC: Cellular component, MF: Molecular Function

In QC, top-ranked biological processes were electron transport chain, ATP metabolic process and respiratory electron transport chain (Figure 4.21a.), and top-ranked cellular component was mitochondrion (Figure 4.21b.), and top-ranked molecular function was oxidoreduction-driven active transmembrane transporter activity (Figure 4.21c.) for up regulated genes.

In root cap, top-ranked biological process was response to oxygen containing component (Figure 4.22a.), top-ranked cellular component was anchored component of membrane (Figure 4.22b.), and top-ranked molecular function was mRNA (Figure 4.22c.) for up regulated genes. In this cluster, top-ranked, biological processes were peptide metabolic process and cellular amide metabolic process (Figure 4.22d.), and top-ranked cellular component was mitochondrion (Figure 4.22e.), and top-ranked molecular functions were protein transmembrane transporter activity, glutathione transferase activity and oxidoreduction-driven active transmembrane transporter activity (Figure 4.22f.) for downregulated genes.

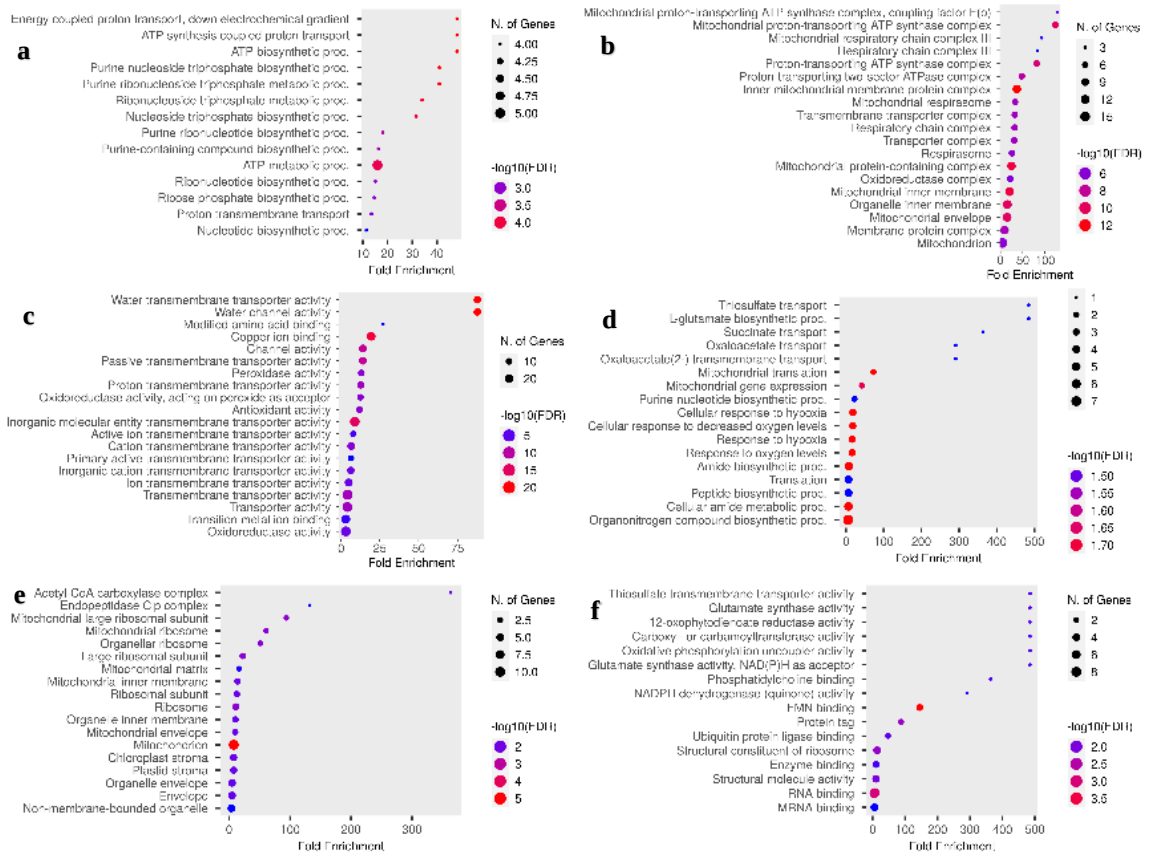

Figure 4.20. Significantly enriched GO terms in endodermis under 1B condition, a, b, c) BP, CC and MF for upregulated genes in endodermis, respectively, d, e, f) BP, CC and MF for downregulated genes in endodermis, respectively. BP: Biological process, CC: Cellular component, MF: Molecular Function

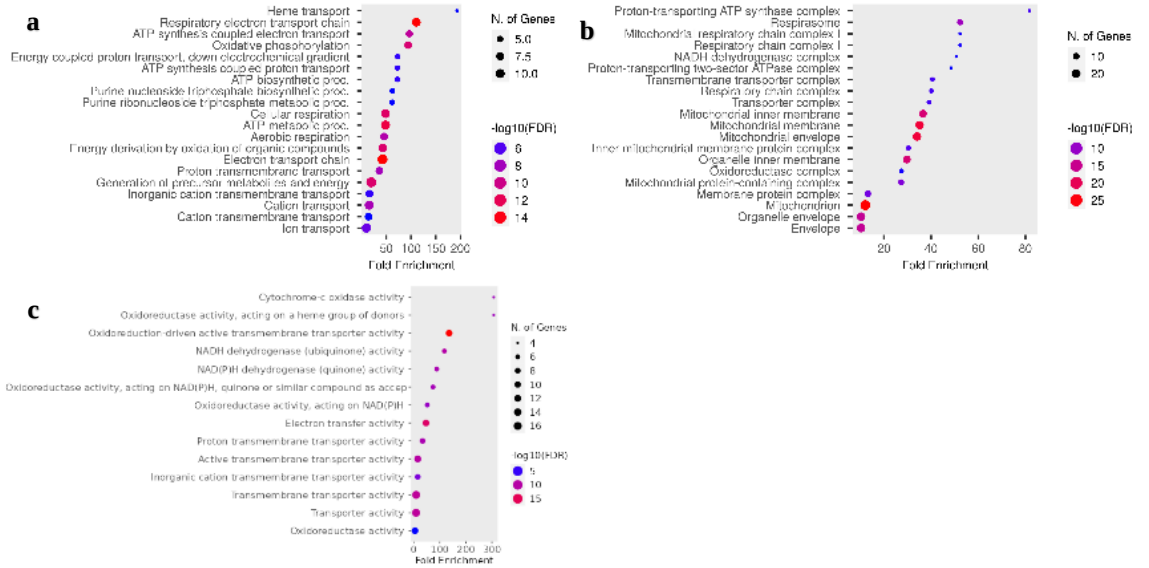

Figure 4.21. Significantly enriched GO terms in QC under 1B condition, a, b, c) BP, CC and MF for upregulated genes in QC, respectively. BP: Biological process, CC: Cellular component, MF: Molecular Function

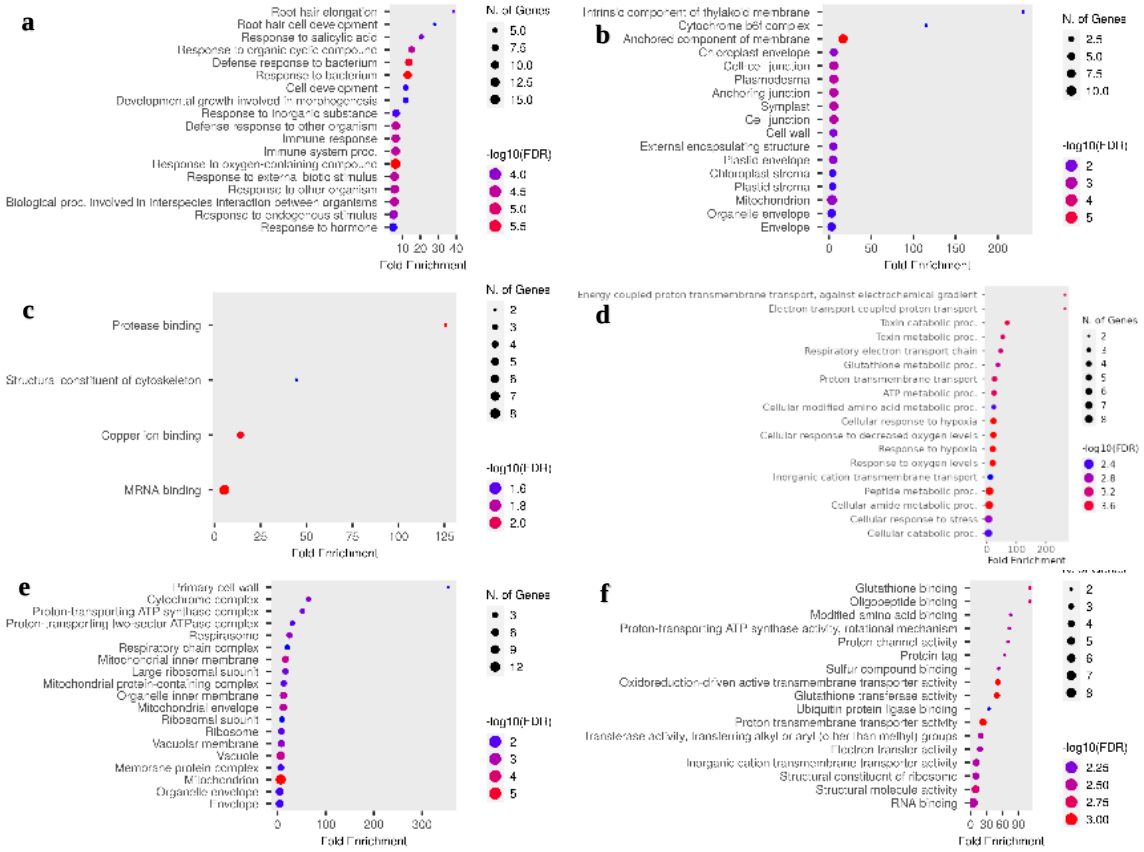

Figure 4.22. Significantly enriched GO terms in root cap under 1B condition, a, b, c) BP, CC, and MF for upregulated genes in root cap, respectively, d, e, f) BP, CC and MF for downregulated genes in root cap, respectively. BP: Biological process, Cellular component, MF: Molecular Function

Moreover, under 2B condition in columella, top-ranked biological processes were response to hypoxia, cellular response to hypoxia, response to oxygen level and cellular response to decreased oxygen level (Figure 4.23a.), and top-ranked cellular components were cell wall and external encapsulating structure (Figure 4.23b.), and top-ranked molecular functions were serine type endopeptidase inhibitor activity, peptidase inhibitor activity, endopeptidase inhibitor activity, endopeptidase regulator activity and peptidase regulator activity (Figure 4.23c.) for upregulated genes. In this cluster, top-ranked biological processes were response to hypoxia, cellular response to hypoxia, response to oxygen level and cellular response to decreased oxygen level (Figure 4.23d.), and top-ranked cellular components were cell-cell junction, plasmodesma, anchoring junction, symplast and cell junction (Figure 4.20e.), and top-ranked molecular function was copper ion binding (Figure 4.23f.) for downregulated genes.

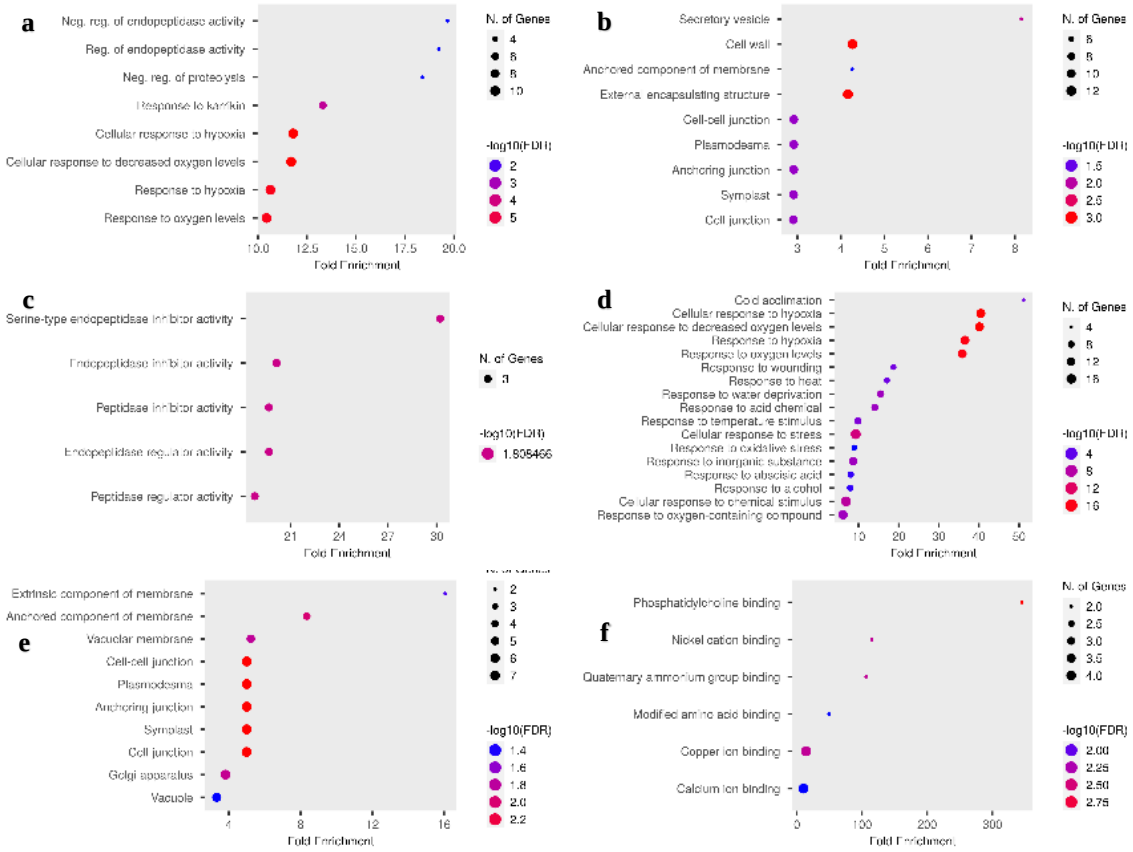

Figure 4.23. Significantly enriched GO terms in columella under 2B condition, a, b, c) BP, CC and MF for upregulated genes in columella, respectively, d, e, f) BP, CC and MF for downregulated genes in columella, respectively. BP: Biological process, CC: Cellular component, MF: Molecular Function

In endodermis, top-ranked biological processes were response to metal ion, response to inorganic substance and response to cadmium ion (Figure 4.24a.), and top-ranked cellular components were cell-cell junction, plasmodesma, anchoring junction, symplast and cell junction (Figure 4.24b.), and top-ranked molecular function was copper ion binding (Figure 4.24c.) for upregulated genes. In this cluster, top-ranked biological processes were response to hypoxia, cellular response to hypoxia, response to oxygen level and cellular response to decreased oxygen level (Figure 4.24d.), and top-ranked cellular component was vacuole (Figure 4.24e.), and top-ranked molecular function was modified amino acid binding (Figure 4.24f.) for downregulated genes.

In QC, top-ranked biological processes were response to hypoxia, cellular response to hypoxia, response to oxygen level and cellular response to decreased oxygen level (Figure 4.25a.), and top-ranked cellular components were cell-cell junction, plasmodesma, anchoring junction, symplast and cell junction (Figure 4.25b.), and top-ranked molecular functions were glutathione transferase activity and oxidoreductase activity (Figure 4.25c.)

for upregulated genes. In this cluster, top-ranked biological processes were response to inorganic substance, response to metal ion and response to cadmium ion (Figure 4.25d.), and top-ranked cellular components were vacuole and mitochondrion (Figure 4.25e.), and top-ranked molecular functions were protein tag and ubiquitin protein ligase binding (Figure 4.25f.) for downregulated genes.

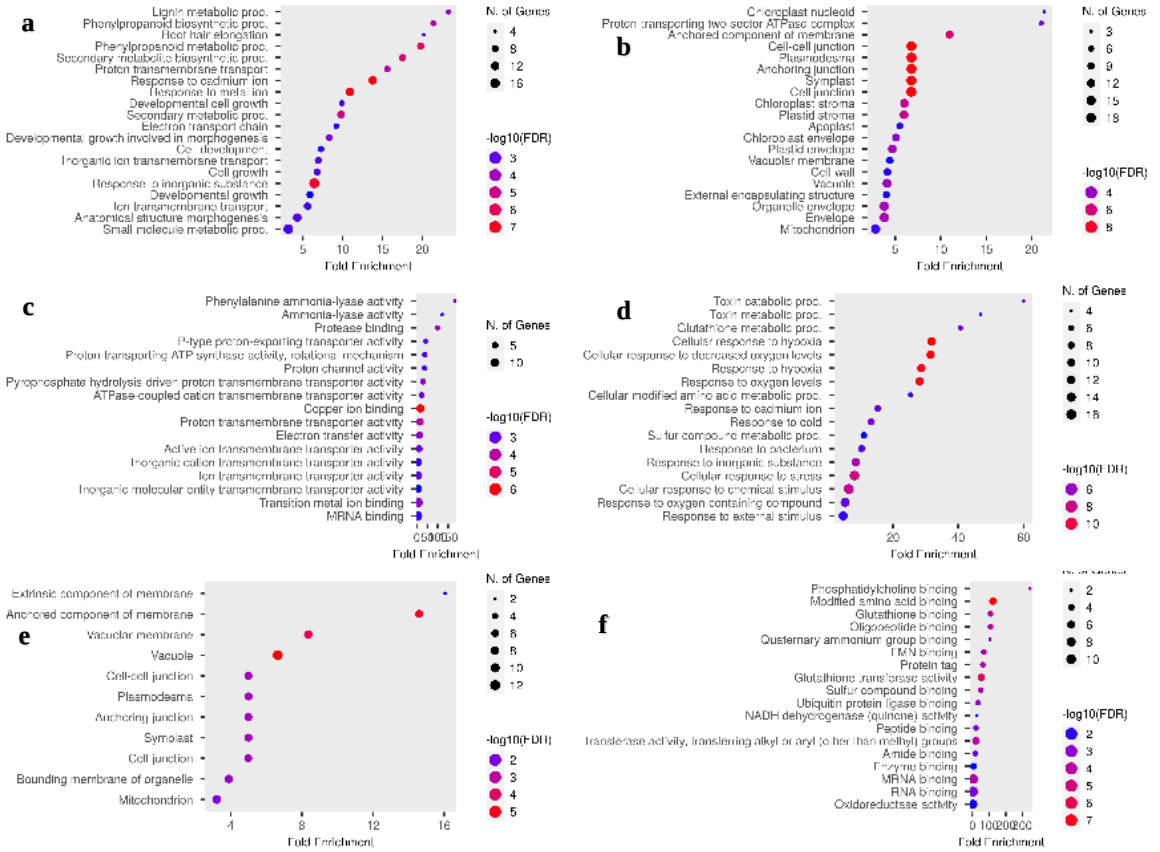

Figure 4.24. Significantly enriched GO terms in endodermis under 2B condition, a, b, c) BP, CC and MF for upregulated genes in endodermis, respectively, d, e, f) BP, CC and MF for downregulated genes in endodermis, respectively. BP: Biological process, CC: Cellular component, MF: Molecular Function

In root cap, top-ranked biological processes were response to hypoxia, cellular response to hypoxia, response to oxygen level and cellular response to decreased oxygen level Figure 4.26a.), top-ranked cellular components were protein-transporting ATP synthase complex and protein-transporting two sector ATPase complex (Figure 4.26b.), and top-ranked molecular functions were ligase activity (Figure 4.26c.) for upregulated genes. In this cluster, top-ranked biological processes were response to hypoxia, cellular response to hypoxia, response to oxygen level and cellular response to decreased oxygen level (Figure 4.26d.), and top-ranked cellular components were mitochondrion and vacuole (Figure

4.26e.), and top-ranked molecular functions were glutathione transferase activity and oxidoreductase (Figure 4.26f.) activity for downregulated genes.

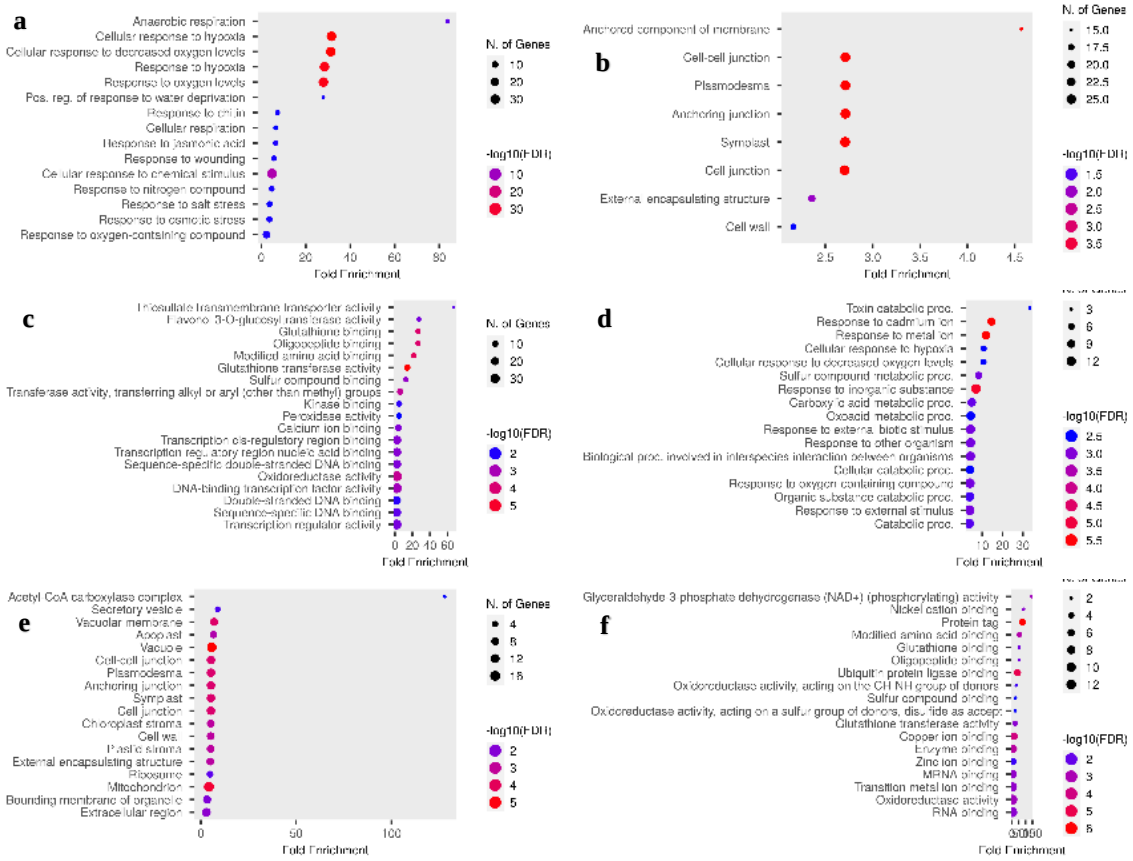

Figure 4.25. Significantly enriched GO terms in QC under 2B condition, a, b, c) BP, CC and MF for upregulated genes in QC, respectively, d, e, f) BP, CC and MF for downregulated genes in QC, respectively. BP: Biological process, CC: Cellular component, MF: Molecular Function

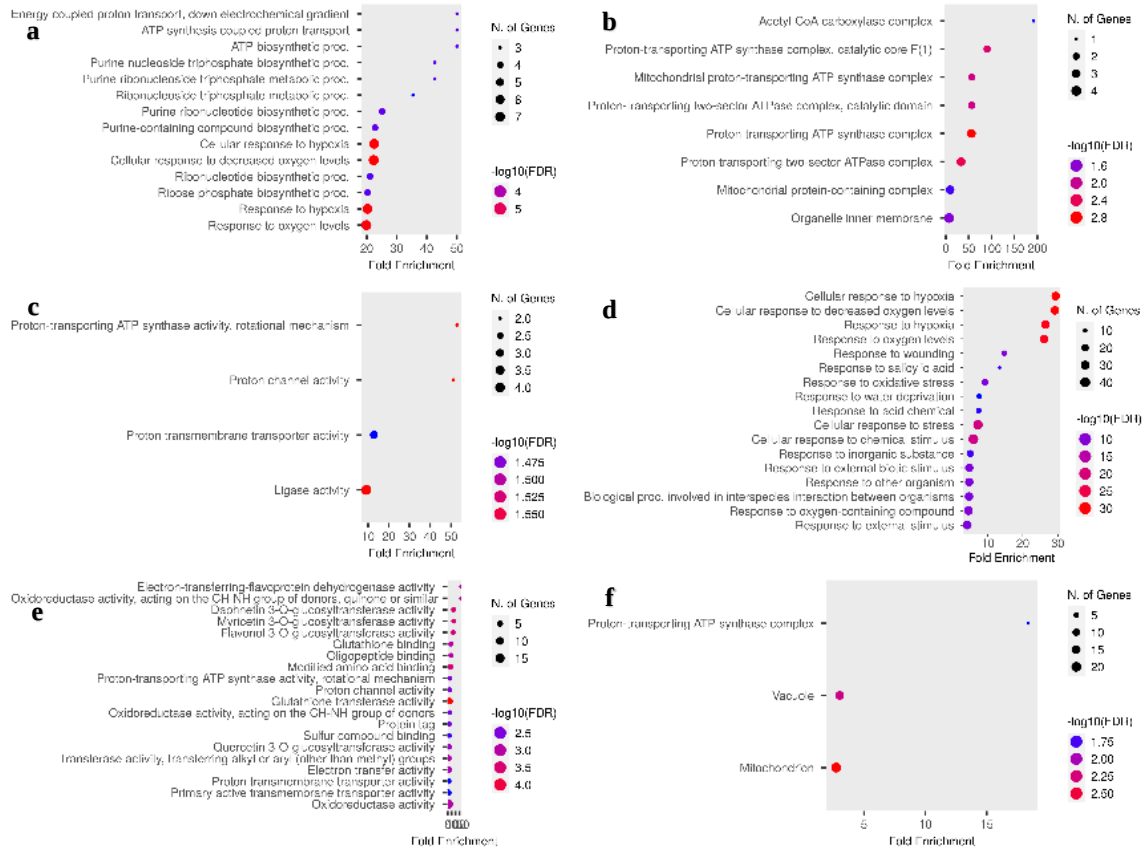

Figure 4.26. Significantly enriched GO terms in root cap under 2B condition, a, b, c) BP, CC and MF for upregulated genes in root cap, respectively, d, e, f) BP, CC and MF for downregulated genes in root cap, respectively. BP: Biological process, CC: Cellular component, MF: Molecular Function

To profile B toxicity responsive mechanisms at cell clusters, enrichment analyses of biological pathways defined by KO were conducted. KO analyses showed that under 1B, in columella, the upregulated DEGs were highly associated with ‘glutathione metabolism’, ‘autopathy’ and ‘sulfur metabolism’ (Figure 4.27a.). In endodermis, the upregulated DEGs were highly associated with pathways including ‘carbon fixation in photosynthetic organisms’, ‘glutathione metabolism’, ‘oxidative phosphorylation’, ‘phenylpropanoid biosynthesis’, ‘glycolysis/gluconeogenesis’, ‘carbon metabolism’ and ‘biosynthesis of amino acids’ (Figure 4.27b.), and the downregulated DEGs were highly associated with pathways including ‘ubiquitin mediated proteolysis’ (Figure 4.27c.). In root cap, the upregulated DEGs were highly associated with pathways such as ‘carbon fixation in photosynthetic organisms’, ‘glycolysis/gluconeogenesis’, ‘biosynthesis of amino acids’, ‘cysteine and methionine metabolism’ and ‘carbon metabolism’ (Figure 4.27d.), and the downregulated DEGs were highly associated with ‘glutathione metabolism’ (Figure 4.21e.).

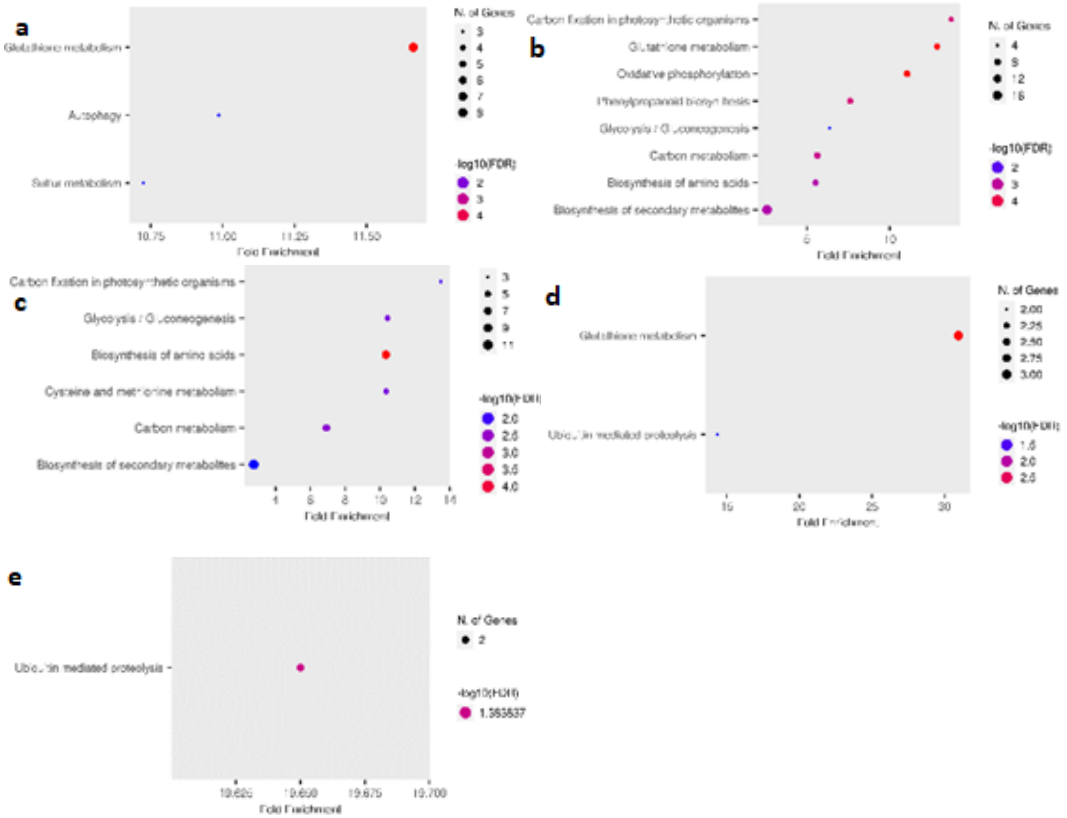

Figure 4.27. Significantly enriched pathway according to KEGG analysis under 1B condition, a) Upregulated genes in columella, b) Upregulated genes in endodermis c) Downregulated genes in endodermis, d) Upregulated genes in root cap, e) Downregulated genes in root cap

Under 2B treatment, in columella, the upregulated DEGs were highly associated with ‘glutathione metabolism’, ‘sulphur metabolism’ and ‘alanine, aspartate and glutamate metabolism’ (Figure 4.28a.). In endodermis, the upregulated DEGs were highly associated ‘stilbenoid, diaryheptanoid and gingerol biosynthesis (Figure 4.28b.), and the downregulated DEGs were highly associated with pathways including ‘glutathione metabolism’ (Figure 4.28c.). In QC, the upregulated DEGs were highly associated with pathways such as ‘glutathione metabolism’, ‘phenylpropanoid biosynthesis’, ‘plant-pathogen interaction’ and ‘MAPK signaling pathway-plant’ (Figure 4.28d.), and the downregulated DEGs were highly associated with pathways such as ‘arginine and proline metabolism’, ‘glutathione metabolism’ and ‘cysteine and methionine metabolism’ (Figure 4.28e.). In root cap, the upregulated DEGs were highly associated with pathways including ‘ribosome’, ‘carbon fixation in photosynthetic organisms’, ‘glycolysis/gluconeogenesis’, ‘biosynthesis of amino acids’, ‘cysteine and methionine metabolism’, ‘carbon metabolism’, ‘MAPK signaling pathway-plant’ and plant-pathogen interaction’ (Figure 4.28f.), and the downregulated DEGs were highly associated with pathways including ‘glutathione metabolism’ and ‘arginine and proline metabolism’ (Figure 4.28g.).

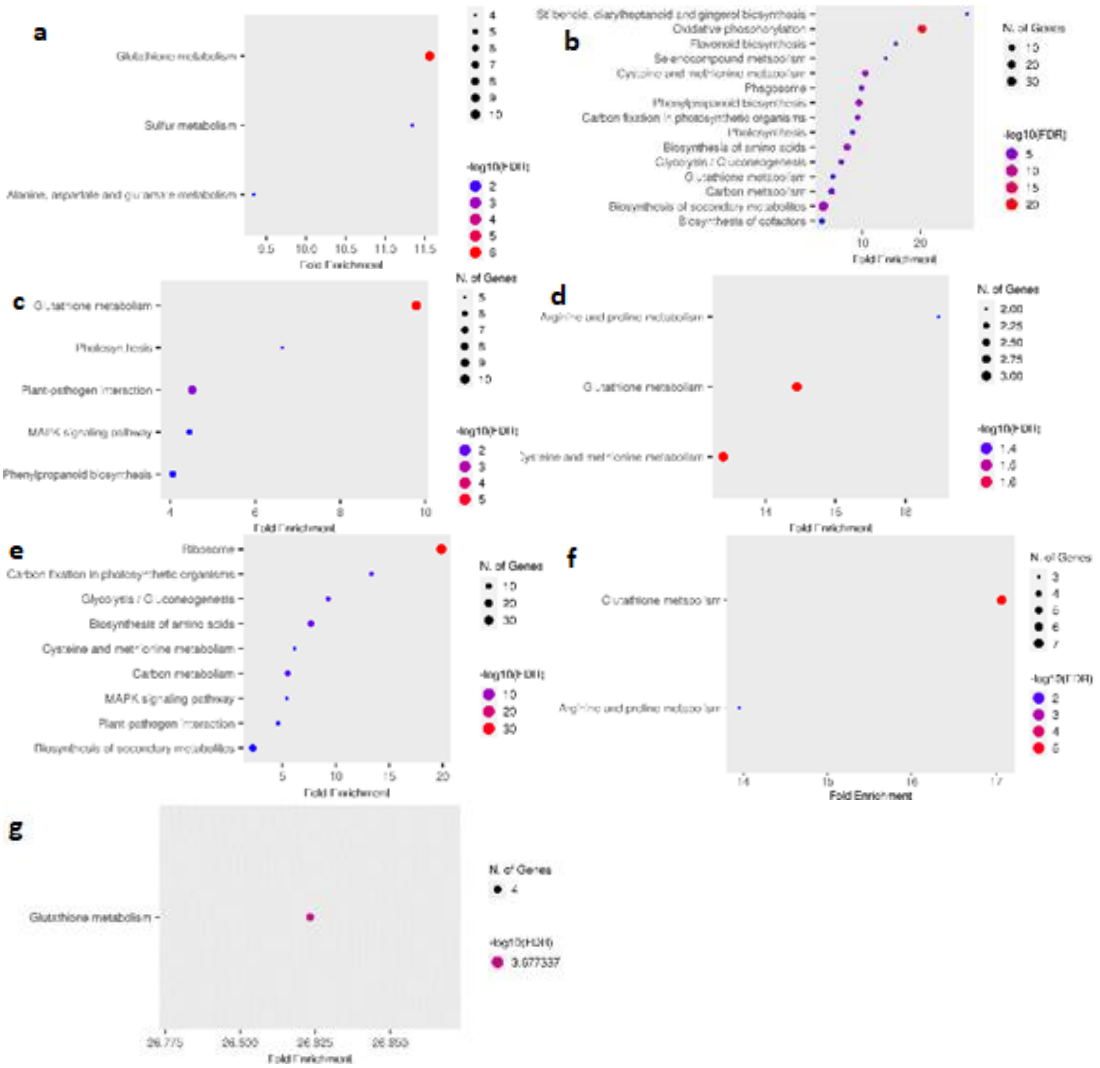

Figure 4.28. Significantly enriched pathway according to KEGG analysis under 2B condition, a) Upregulated genes in columella, b) Upregulated genes in endodermis c) Downregulated genes in endodermis, d) Upregulated genes in QC, e) Downregulated genes in QC, f) Upregulated genes in root cap, g) Downregulated genes in root cap

Glutathione metabolism was activated caused by B toxicity at different cell clusters in Arabidopsis root. Therefore, we carefully determined the genes related the glutathonine metabolism (Table 4.5.). Accordingly, under 1B condition, most significantly upregulated genes were *CICDH* and *GSTF10* in root cap, *GSTU25*, *GSTU24* and *GSTU7* in columella, and *GSTU26*, *GSTF10* and *GPX2* in endodermis. Moreover, most significantly downregulated genes were *GSTU25*, *GSTU19* and *GSTF8* in root cap (Table 4.5.). Under 2B condition, most significantly upregulated genes were *GSTU25*, *GPX2* and *GSTU5* in columella, *APX1*, *CICDH* and *GSTF10* in endodermis, and *GSTF2*, *GSTU17* and *GSTU11* in QC. On the other hand, most significantly downregulated genes were *GSTU25*, *GSTF8* and *GPX6* in root cap, *GSTF8*, *GSTU24* and *GSTU25* in endodermis, *GSTU24*, *GSTU25* and *GSTU19* in QC (Table 4.5.).

Table 4.5. The genes related to glutathione metabolism at each cluster under B toxicity in roots of *Arabidopsis thaliana*

Condition	Cluster	AGI Code	Gene Name		log_2 Fold Change	p- value
1B	Root cap	AT1G65930	*CICDH*	*CYTOSOLIC NAPD+-DEPENDENT ISOCITRATE DEHYDROGENASE*	2.545384	1.04E-10
		AT2G30870	*GSTF10*	*GLUTATHIONE S-TRANSFERASE PHI 10*	2.152333	4.83E-08
		AT1G17180	*GSTU25*	*GLUTATHIONE S-TRANSFERASE TAU 25*	-3.286	2.74E-10
		AT1G78380	*GSTU19*	*GLUTATHIONE S-TRANSFERASE TAU 19*	-0.68944	0.114121
		AT2G47730	*GSTF8*	*GLUTATHIONE S-TRANSFERASE PHI 8*	-0.03413	1
	Columella	AT1G17170	*GSTU24*	*GLUTATHIONE S-TRANSFERASE TAU 24*	2.976352	4.48E-15
		AT1G17180	*GSTU25*	*GLUTATHIONE S-TRANSFERASE TAU 25*	4.412456	9.83E-24
		AT1G78340	*GSTU22*	*GLUTATHIONE S-TRANSFERASE TAU 22*	2.714102	2.42E-09
		AT1G78380	*GSTU19*	*GLUTATHIONE S-TRANSFERASE TAU 19*	1.614958	7.43E-06
		AT2G29420	*GSTU7*	*GLUTATHIONE S-TRANSFERASE TAU 7*	3.963083	8.45E-21
		AT2G29450	*GSTU5*	*GLUTATHIONE S-TRANSFERASE TAU 5*	1.635258	0.000232
		AT2G47730	*GSTF8*	*GLUTATHIONE S-TRANSFERASE PHI 8*	1.139695	0.003358
		AT4G11600	*GPX6*	*GLUTATHIONE PEROXIDASE 6*	2.585115	2.75E-12
	Endodermis	AT1G07890	*APX1*	*ASCORBATE PEROXIDASE 1*	0.885448	0.710984
		AT1G17190	*GSTU26*	*GLUTATHIONE S-TRANSFERASE TAU 26*	1.876759	0.02203
		AT1G65930	*CICDH*	*CYTOSOLIC NAPD+-DEPENDENT ISOCITRATE DEHYDROGENASE*	1.022402	0.578257
		AT1G78380	*GSTU19*	*GLUTATHIONE S-TRANSFERASE TAU 19*	0.317051	1
		AT2G30870	*GSTF10*	*GLUTATHIONE S-TRANSFERASE PHI 10*	1.094846	0.461417
		AT2G31570	*GPX2*	*GLUTATHIONE PEROXIDASE 2*	1.665967	0.066977
		AT2G47730	*GSTF8*	*GLUTATHIONE S-TRANSFERASE PHI 8*	0.198198	1
2B	Root cap	AT1G07890	*APX1*	*ASCORBATE PEROXIDASE 1*	-0.33124	0.273624
		AT1G17180	*GSTU25*	*GLUTATHIONE S-TRANSFERASE TAU 25*	-1.80544	2.53E-10
		AT1G78380	*GSTU19*	*GLUTATHIONE S-TRANSFERASE TAU 19*	-0.56242	0.027762
		AT2G29420	*GSTU7*	*GLUTATHIONE S-TRANSFERASE TAU 7*	-0.86683	0.001082
		AT2G29450	*GSTU5*	*GLUTATHIONE S-TRANSFERASE TAU 5*	-0.5341	0.05444
		AT2G47730	*GSTF8*	*GLUTATHIONE S-TRANSFERASE PHI 8*	-1.15669	1.33E-06
		AT4G11600	*GPX6*	*GLUTATHIONE PEROXIDASE 6*	-1.19433	2.24E-06
	Columella	AT1G02930	*GSTF6*	*GLUTATHIONE S-TRANSFERASE PHI 6*	0.710635	0.024017
		AT1G17170	*GSTU24*	*GLUTATHIONE S-TRANSFERASE TAU 24*	1.824213	1.58E-19
		AT1G17180	*GSTU25*	*GLUTATHIONE S-TRANSFERASE TAU 25*	3.084355	2.73E-47
		AT1G78340	*GSTU22*	*GLUTATHIONE S-TRANSFERASE TAU 22*	1.704552	1.15E-14
		AT1G78380	*GSTU19*	*GLUTATHIONE S-TRANSFERASE TAU 19*	1.001175	4.50E-07
		AT2G29420	*GSTU7*	*GLUTATHIONE S-TRANSFERASE TAU 7*	2.535982	2.50E-37

Table 4.5. continued.

		AT2G29450	*GSTU5*	*GLUTATHIONE S-TRANSFERASE TAU 5*	0.059356	0.93561
		AT2G31570	*GPX2*	*GLUTATHIONE PEROXIDASE 2*	2.820802	2.22E-34
		AT2G47730	*GSTF8*	*GLUTATHIONE S-TRANSFERASE PHI 8*	0.454527	0.047744
		AT4G11600	*GPX6*	*GLUTATHIONE PEROXIDASE 6*	1.099918	1.64E-07
	Endodermis	AT1G07890	*APX1*	*ASCORBATE PEROXIDASE 1*	0.192205	0.784104
		AT1G65930	*CICDH*	*CYTOSOLIC NAPD+-DEPENDENT ISOCITRATE DEHYDROGENASE*	2.500977	6.95E-21
		AT2G30870	*GSTF10*	*GLUTATHIONE S-TRANSFERASE PHI 10*	0.97759	0.002349
		AT4G23100	*GSH1*	*GLUTAMATE-CYSTEINE LIGASE*	1.282175	5.76E-05
		AT1G17170	*GSTU24*	*GLUTATHIONE S-TRANSFERASE TAU 24*	-1.21126	0.006546
		AT1G17180	*GSTU25*	*GLUTATHIONE S-TRANSFERASE TAU 25*	-2.94772	2.94E-09
		AT1G78380	*GSTU19*	*GLUTATHIONE S-TRANSFERASE TAU 19*	-0.63674	0.208485
		AT2G47730	*GSTF8*	*GLUTATHIONE S-TRANSFERASE PHI 8*	-0.90056	0.031189
	QC	AT1G02930	*GSTF6*	*GLUTATHIONE S-TRANSFERASE PHI 6*	1.02617	0.000284
		AT1G07890	*APX1*	*ASCORBATE PEROXIDASE 1*	0.823161	2.60E-05
		AT1G10370	*GSTU17*	*GLUTATHIONE S-TRANSFERASE TAU 17*	3.137681	4.66E-25
		AT1G69930	*GSTU11*	*GLUTATHIONE S-TRANSFERASE TAU 11*	2.677485	8.94E-29
		AT2G29440	*GSTU6*	*GLUTATHIONE S-TRANSFERASE TAU 6*	2.517021	2.73E-38
		AT2G29450	*GSTU5*	*GLUTATHIONE S-TRANSFERASE TAU 5*	0.991123	6.62E-07
		AT2G30870	*GSTF10*	*GLUTATHIONE S-TRANSFERASE PHI 10*	0.029926	1
		AT2G47730	*GSTF8*	*GLUTATHIONE S-TRANSFERASE PHI 8*	0.733952	0.000203
		AT4G02520	*GSTF2*	*GLUTATHIONE S-TRANSFERASE PHI 2*	2.930031	9.04E-24
		AT4G11600	*GPX6*	*GLUTATHIONE PEROXIDASE 6*	0.284465	0.312405
		AT1G17170	*GSTU24*	*GLUTATHIONE S-TRANSFERASE TAU 24*	-0.38438	0.15589
		AT1G17180	*GSTU25*	*GLUTATHIONE S-TRANSFERASE TAU 25*	-1.74223	4.42E-13
		AT1G78380	*GSTU19*	*GLUTATHIONE S-TRANSFERASE TAU 19*	-0.18085	0.590017

To identify cell-specific transcription factors (TFs) in Arabidopsis root implicated in B toxicity, overlaps between TFs of *Arabidopsis thaliana* [125] and upregulated genes of each cluster of B toxicity conditions were determined by Venn diagram (https://bioinformatics.psb.ugent.be/webtools/Venn/). Accordingly, 13 TF families were found under B toxicity including ERF, NAC, C2H2, WRKY, NF-X1, Trihelix, bZIP, bHLH, MYB, C3H, HD-ZIP, LBD, and HSF (Table 4.6.). Under 1B condition, in columella total 14 genes belonging to 6 TF family including ERF, NAC, C2H2, WRKY, NF-X1, and Trihelix were upregulated. The most significantly upregulated TFs were *ANAC087* and *NFXL1* (Table 4.6). Under 2B condition, in columella, total 14 genes belonging to 7 TF family including NAC, ERF, LBD, WRKY, bZIP, NF-X1 and Trihelix were upregulated. The most significantly upregulated TFs were *NAC015* and *NAC083* (Table 4.6.). On the other hand, under this condition, in QC, total 33 genes belonging to 11 TF family including C2H2, ERF, bHLH, NAC, WRKY, HSF, MYB, C3H, WRKY, bZIP and HD-ZIP were upregulated. The most significantly upregulated TFs were *MYB15* and *MYB108* in QC (Table 4.6.). In root cap, total 12 genes belonging to 6 TF family including ERF, bHLH, C3H, NAC, WRKY and bZIP were upregulated. The most significantly upregulated TFs were *ERF59* and *ERF109* TFs in root cap (Table 4.6.).

4.4.4. Heatmap analysis of gene expression

We analysed DEGs via heatmap to visualize and interpret gene expression data at cell clusters in root tissues of *Arabidopsis thaliana* exposed to B toxicity (Figure 4.29.). Accordingly, under 1B condition, most significantly upregulated genes were *AT1G12080*, *AT4G22212* and *PDF2.3* in root cap, *AMC9* and *CEL3* in columella, *PME2*, *AIR1B* and *PER57* in endodermis, and *RPS7*, *RRN26* and *NAD2B* (Figure 4.29b., Table 4.7.). Under 2B condition, most significantly upregulated genes were *AGP31*, *DFC* and *RBG7* in root cap, *AT3G61930*, *PLP2* and *GLP9* in columella, *PER64*, *DIR9* and *AT1G71740* in endodermis, and *SCREW2*, *VBF* and *PP2B13* in QC (Figure 4.29c., Table 4.7.).

Table 4.6. Cell-specific TFs at each cluster under B toxicity in roots of *Arabidopsis thaliana*

Condition	Cluster	AGI Code	Gene name		TF Family	log_2 Fold Change	p- value
1B	Columella	AT5G05410	*DREB2A*	*DRE-BINDING PROTEIN 2A*	ERF	1.33004	0.000648
		AT5G08790	*ANAC081*	*ARABIDOPSIS NAC DOMAIN CONTAINING PROTEIN 81*	NAC	3.048772	6.11E-16
		AT5G59820	*ZAT12*	*ZINC FINGER PROTEIN ZAT12*	C2H2	1.292887	0.00155
		AT5G18270	*ANAC087*	*ARABIDOPSIS NAC DOMAIN CONTAINING PROTEIN 87*	NAC	4.458537	2.94E-18
		AT4G17490	*ERF6*	*ETHYLENE RESPONSIVE ELEMENT BINDING FACTOR 6*	ERF	1.267193	0.004468
			ERF020		ERF	2.991969	1.08E-13
		AT3G23240	*ERF1*	*ETHYLENE RESPONSIVE ELEMENT BINDING FACTOR 1*	ERF	3.078819	1.83E-13
		AT5G63790	*NAC102*	*NAC DOMAIN CONTAINING PROTEIN 102*	NAC	1.049346	0.009126
		AT1G62300	*WRKY6*	*ARABIDOPSIS THALIANA WRKY DNA-BINDING PROTEIN 6*	WRKY	3.028606	2.17E-15
		AT1G01720	*ANAC2*	*ARABIDOPSIS NAC DOMAIN CONTAINING PROTEIN 2*	NAC	0.565898	0.311588
		AT1G10170	*NFXL1*		NF-X1	4.390217	5.25E-14
		AT3G29035	*NAC3*	*NAC DOMAIN CONTAINING PROTEIN 3*	NAC	3.88046	1.20E-11
		AT3G50260	*CEJ1/ERF011*	*COOPERATIVELY REGULATED BY ETHYLENE AND JASMONATE 1*	ERF	3.847546	3.66E-12
		AT5G01380	*GT-3A*		Trihelix	2.29194	1.48E-06
2B	Columella	AT5G08790	*ANAC081*	*ARABIDOPSIS NAC DOMAIN CONTAINING PROTEIN 81*	NAC	0.999523	1.03E-06
		AT5G13180	*NAC083*	*NAC DOMAIN CONTAINING PROTEIN 83*	NAC	2.346609	2.84E-23
		AT3G23240	*ERF1*	*ETHYLENE RESPONSIVE ELEMENT BINDING FACTOR 1*	ERF	0.940751	2.22E-05
		AT4G37870	*PCK1*	*PEACOCK 1*	LBD	2.50318	4.95E-26
		AT5G64810	*WRKY51*	*ARABIDOPSIS THALIANA WRKY DNA-BINDING PROTEIN 51*	WRKY	0.325328	0.225352
		AT1G62300	*WRKY6*	*ARABIDOPSIS THALIANA WRKY DNA-BINDING PROTEIN 6*	WRKY	1.027372	1.18E-06
		AT2G40340	*DREB2C*	*DRE-BINDING PROTEIN 2C*	ERF	1.442235	1.08E-10
		AT5G49450	*BZIP1*	*BASIC LEUCINE-ZIPPER 1*	bZIP	0.242329	0.392172
		AT1G10170	*NFXL1*		NF-X1	2.148492	2.72E-26
		AT1G33280	*NAC015*	*NAC DOMAIN CONTAINING PROTEIN 15*	NAC	4.536568	1.18E-60
		AT3G29035	*NAC3*	*NAC DOMAIN CONTAINING PROTEIN 3*	NAC	1.662623	8.30E-13
		AT3G50260	*CEJ1/ERF011*	*COOPERATIVELY REGULATED BY ETHYLENE AND JASMONATE 1*	ERF	1.484669	1.68E-11
		AT5G01380	*GT-3A*		Trihelix	0.466754	0.066784
		AT5G64750	*ABR1*	*ABA REPRESSOR1*	ERF	0.887051	9.08E-05
	QC	AT1G27730	*ZAT10*	*ZINC FINGER PROTEIN ZAT10*	C2H2	1.78827	1.06E-20
		AT5G05410	*DREB2A*	*DEHYDRATION-RESPONSIVE ELEMENT BINDING PROTEIN 2*	ERF	0.799452	6.06E-05
		AT1G32640	*JAI1*	*JASMONATE INSENSITIVE 1*	bHLH	0.907001	2.44E-05
		AT5G08790	*ANAC081*	*ARABIDOPSIS NAC DOMAIN CONTAINING PROTEIN 81*	NAC	0.300075	0.250788
		AT5G59820	*ZAT12*	*ZINC FINGER PROTEIN ZAT12*	C2H2	1.1575	2.48E-09

Table 4.6. continued.

		AT1G80840	*WRKY40*	*ARABIDOPSIS THALIANA WRKY DNA-BINDING PROTEIN 40*	WRKY	2.069296	6.37E-26
		AT4G36990	*HSFB1*	*ARABIDOPSIS THALIANA CLASS B HEAT SHOCK FACTOR B1*	HSF	1.568176	2.56E-14
		AT5G49520	*WRKY48*	*ARABIDOPSIS THALIANA WRKY DNA-BINDING PROTEIN 40*	WRKY	2.087254	1.54E-22
			ERF020		ERF	1.269631	1.31E-10
		AT3G23240	*ERF1*	*ETHYLENE RESPONSE FACTOR 1*	ERF	0.35063	0.192383
		AT3G23250	*MYB15*	*MYB DOMAIN PROTEIN 15*	MYB	3.570997	1.33E-60
		AT1G78080	*WIND1/ERF59*	*WOUND INDUCED DEDIFFERENTIATION 1*	ERF	0.162198	0.619263
		AT2G40140	*SZF2*	*SALT-INDUCIBLE ZINC FINGER 2*	C3H	0.89684	5.67E-06
		AT5G64810	*WRKY51*	*ARABIDOPSIS THALIANA WRKY DNA-BINDING PROTEIN 51*	WRKY	0.749051	0.000504
		AT5G63790	*NAC102*	*AC DOMAIN CONTAINING PROTEIN 102*	NAC	0.859711	7.38E-06
		AT4G34410	*ERF109*	*ETHYLENE RESPONSE FACTOR 109*	ERF	1.628223	5.62E-18
		AT5G13080	*WRKY75*	*ARABIDOPSIS THALIANA WRKY DNA-BINDING PROTEIN 75*	WRKY	2.494932	7.80E-22
		AT2G46400	*WRKY46*	*ARABIDOPSIS THALIANA WRKY DNA-BINDING PROTEIN 46*	WRKY	1.485517	4.03E-11
		AT1G01720	*ANAC2*	*ARABIDOPSIS NAC DOMAIN CONTAINING PROTEIN 2*	NAC	0.547464	0.01137
		AT2G38470	*WRKY33*	*ARABIDOPSIS THALIANA WRKY DNA-BINDING PROTEIN 33*	WRKY	1.42071	6.21E-13
		AT3G62420	*BZIP53*	*BASIC REGION/LEUCINE ZIPPER MOTIF 53*	bZIP	0.753482	0.000677
		AT5G49450	*BZIP1*	*BASIC LEUCINE-ZIPPER 1*	bZIP	0.912309	1.92E-05
		AT3G06490	*MYB108*	*MYB DOMAIN PROTEIN 108*	MYB	3.978582	5.48E-50
		AT4G37790	*BHB3*	*BRASSINOSTEROID-RELATED HOMEOBOX 3*	HD-ZIP	1.803967	1.74E-17
		AT3G53600	*ZAT18*	*ZINC FINGER OF ARABIDOPSIS THALIANA 18*	C2H2	2.545192	2.86E-34
		AT3G15210	*ERF4*	*ETHYLENE RESPONSIVE ELEMENT BINDING FACTOR 4*	ERF	1.567611	8.90E-16
		AT3G19580	*ZF2*	*ZINC-FINGER PROTEIN 2*	C2H2	1.928208	1.59E-22
		AT2G37430	*ZAT11*	*ZINC FINGER OF ARABIDOPSIS THALIANA 11*	C2H2	2.860567	8.67E-37
		AT5G01380	*GT-3A*		Trihelix	1.28762	2.28E-10
		AT4G31800	*WRKY18*	*ARABIDOPSIS THALIANA WRKY DNA-BINDING PROTEIN 18*	WRKY	1.612479	1.76E-15
		AT3G55980	*SZF1*	*SALT-INDUCIBLE ZINC FINGER 1*	C3H	1.844753	2.42E-20
		AT5G64750	*ABR1*	*ABA REPRESSOR1*	ERF	0.557327	0.01849
		AT3G46080	*ZAT8*	*ZINC FINGER PROTEIN ZAT8*	C2H2	2.227168	1.45E-24
	Root cap	AT5G05410	*DREB2A*	*DEHYDRATION-RESPONSIVE ELEMENT BINDING PROTEIN 2*	ERF	0.029637	1
		AT1G32640	*JAI1*	*JASMONATE INSENSITIVE 1*	bHLH	0.92689	7.73E-05
		AT4G17490	*ERF6*	*ETHYLENE RESPONSIVE ELEMENT BINDING FACTOR 6*	ERF	1.104287	2.82E-07
		AT1G78080	*WIND1/ERF59*	*WOUND INDUCED DEDIFFERENTIATION 1*	ERF	1.174558	2.63E-08
		AT2G40140	*SZF2*	*SALT-INDUCIBLE ZINC FINGER 2*	C3H	0.3983210	0.112539
		AT5G63790	*NAC102*	*NAC DOMAIN CONTAINING PROTEIN 102*	NAC	0.189267	0.530659
		AT1G78080	*ERF58/RAP2.4*	*RELATED TO AP2 4*	ERF	1.188404	4.35E-07

Table 4.6. continued.

		AT4G34410	*ERF109*	*ETHYLENE RESPONSE FACTOR 109*	ERF	0.163791	0.599771
		AT1G01720	*ANAC2*	*ARABIDOPSIS NAC DOMAIN CONTAINING PROTEIN 2*	NAC	0.872182	6.41E-05
		AT2G38470	*WRKY33*	*ARABIDOPSIS THALIANA WRKY DNA-BINDING PROTEIN 33*	WRKY	0.61786	0.010357
		AT3G62420	*BZIP53*	*BASIC REGION/LEUCINE ZIPPER MOTIF 53*	bZIP	0.745991	0.00244
		AT4G31800	*WRKY18*	*ARABIDOPSIS THALIANA WRKY DNA-BINDING PROTEIN 18*	WRKY	0.415775	0.141632

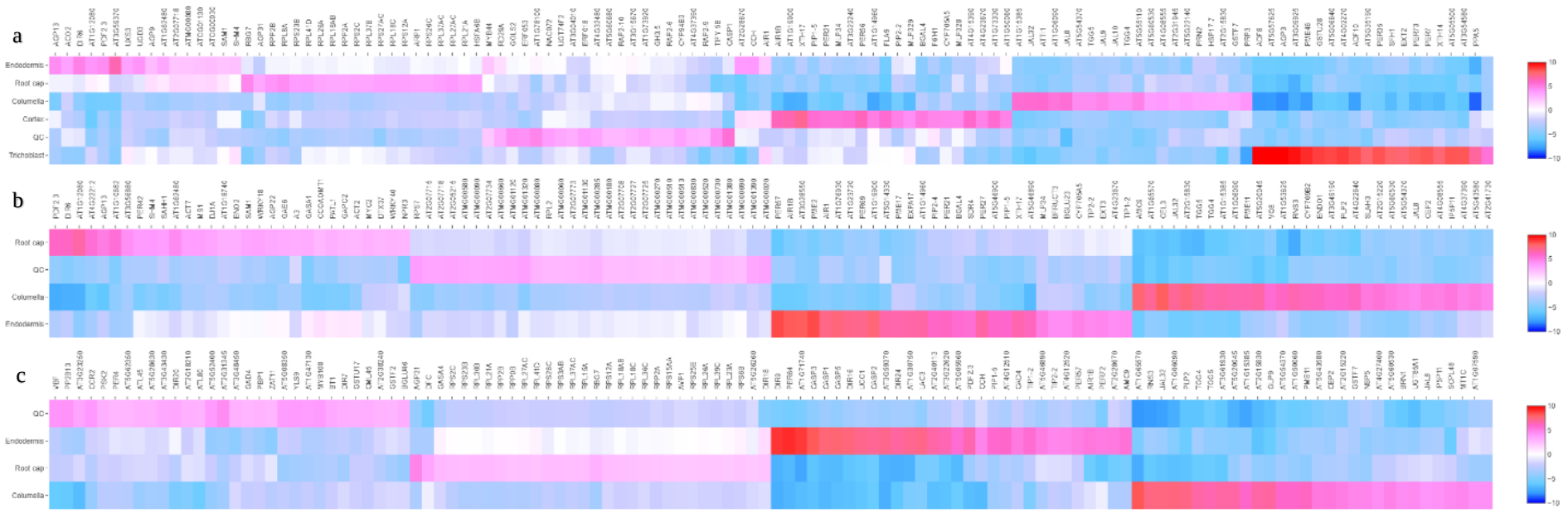

Figure 4.29. Heatmap visualization of the 50 most differentially expressed genes for each group, a) Control group, b) 1 mM boric acid treatment group, c) 2 mM boric acid treatment group.

Table 4.7. Most significantly upregulated genes at each cluster in root tissue *Arabidopsis thaliana* exposed to B toxicity

Condition	Cluster	AGI codes and Gene names	Gene Description	log_2 Fold Change	p- value
1B	Root cap	AT3G56880	VQ motif-containing protein	4.3917846	1.49E-22
		SORF1	a translated small open reading frame by ribosome profiling	5.6303147	5.20E-20
		AT1G12080	Vacuolar calcium-binding protein-like protein	6.7422076	1.16E-17
		AT4G22212	Defensin-like (DEFL) family protein	5.6691656	2.56E-14
		PDF2.3	a PR (pathogenesis-related) protein.	6.1448879	1.63E-20
	Columella	*AMC9*	Putative metacaspase.	7.791238	2.79E-16
		CEL3	Cellulase 3	8.1391948	9.85E-13
	Endodermis	*EXT1*	Extensin gene that belongs to cell-wall hydroxyproline-rich glycoproteins.	7.63621934	4.07E-09
		RUBY	RUBY encodes a secreted galactose oxidase involved in cell wall modification.	7.65414125	4.89E-09
		PME2	Pectin methylesterase involved in callus formation.	8.54310993	2.27E-11
		AIR1	possibly membrane spanning C-terminus.	7.34671272	2.98E-14
		AIR1B	Bifunctional inhibitor/lipid-transfer protein/seed storage 2S albumin superfamily protein	8.20776132	2.87E-16
		PER57	Peroxidase superfamily protein, overexpression increases ROS	8.58375192	1.39E-13
	QC	*RRN26*	Mitochondrial 26S ribosomal RNA protein	3.70384503	9.84E-28
		AT2G07718	Cytochrome b/b6 protein	3.54117733	9.28E-22
		NAD2B	Subunit of mitochondrial NAD(P)H dehydrogenase	3.77728766	6.06E-19
		RRN18	Mitochondrial 18S ribosomal RNA	3.5075893	1.12E-24
		RPS7	Chloroplast ribosomal protein S7	3.86357019	1.27E-21
		AT2G05215	Natural antisense transcript overlaps with AT5G01210	3.58999904	1.83E-15
2B	Root cap	*RBG7*	RNAse II-like 1	3.0793617	2.05E-34
		RPS26C	Cytoplasmic Ribosomal Protein Gene Family	2.6357764	1.68E-26
		AGP31	Atypical arabinogalactan protein	4.8605364	2.06E-77
		DFC	Pollen Ole e 1 allergen and extensin family protein	3.5201205	7.70E-39
		RPS3AB	Cytoplasmic Ribosomal Protein Gene Family	2.6131757	2.08E-28
	Columella	AT3G61930	hypothetical protein	6.7835861	3.51E-74
		PLP2	Lipid acyl hydrolase with wide substrate specificity	6.7829734	2.15E-34
		GLP9	Ethylene-activated signaling pathway, sulfur compound metabolic process	6.0615487	1.50E-25
	Endodermis	*PER64*	Peroxidase required for casparian strip lignification as well as partially required for SGN-dependent compensatory lignification	8.9009442	1.58E-16
		CASP5	Uncharacterized protein family (UPF0497)	7.5656635	3.00E-13
		DIR9	Disease resistance-responsive (dirigent-like protein) family protein	9.18316	9.19E-14
		CASP1	Membrane bound protein involved in formation of the casparian strip.	7.7349394	1.50E-19

Table 4.7. continued.

		CASP3	Uncharacterized protein family	7.6914378	6.51E-18
		AT1G71740	Nucleolar protein	8.2613672	3.68E-13
	QC	*VBF*	F-box protein that can functionally replace VirF, regulating levels of the VirE2 and VIP1 proteins via a VBF-containing SCF complex	4.1644483	4.20E-53
		AT5G08350	Mutants have decreased tolerance to cold and oxidative stress. Gene expression induced by drought and ABA	3.827626	2.84E-40
		AT1G47130	a purple acid phosphatase with phytase activity.	3.8003029	3.71E-54
		PP2B13	Phloem protein 2-B13	4.239493	2.93E-46
		MYB108	MYB transcription factor	3.9785818	5.48E-50
		YLS9	Arabidopsis non-race specific disease resistance gene (NDR1	3.9303027	6.07E-51
		SCREW2	Transmembrane protein	4.525303	7.73E-69
		CCR2	Cinnamoyl CoA reductase isoform. Involved in lignin biosynthesis	3.9981839	3.19E-51
		CYP715A1	Member of CYP715A	3.9206823	3.33E-51

5. DISCUSSION

B toxicity causes deterioration in developmental and metabolic activities of plants [126]. Several transcriptomic studies have been performed in plants, commonly using bulk methods such as microarray and RNA sequencing, to find the toxic B responsive regulations at molecular levels. [105, 127, 128, 129]. However, bulk methods are limited in detecting differentially expressed genes at different cell types. In addition, it is not possible to detect rare cell types with these methods. However, scRNA-seq solves these problems and profile gene expressions on a cell basis. Therefore, in this study, a scRNA-seq analysis was performed for Arabidopsis roots exposed to B toxicity at seedling stage to elucidate the molecular basis of the B tolerance mechanism at a high efficiency and single cell level.

We successfully generated high-resolution and highly reproducible single-cell transcriptomic maps of 1554 Arabidopsis root cells at seedling stage in the control and B toxicity treatment groups. We obtained the 6 clusters from the primary root representing some highly specific cell types, including QC, endodermis, root cap columella, cortex, and trichoblast. In B toxicity treatment groups, endodermis, QC, root cap and columella were identified Unannotated clusters may also be due to technical and/or computational constructs. Furthermore, scRNA-seq pipelines lack large cell size variability [130]. One such particularly examples were found with cortex cluster of the pooled only in the control group.

We identified changes in gene expression profiles in Arabidopsis roots under B toxicity for each cluster (Figure 4.17., 4.18.). Accordingly, the number of most significantly upregulated genes under 1B condition was determined in columella (Figure 4.17e.). However, they were seen in endodermis under 2B condition (Figure 4.17g.), Moreover, the number of most significantly downregulated genes under 1B condition and 2B condition were seen in root cap (Figure 4.17f., 4.17h.). These results showed that columela, endodermis and root cap might have a critical role against severe B toxicity conditions.

To determine and classify functions of DEGs, we performed GO enrichment analyses on the complete set of DEGs. Analysing the enrichment of functional categories within identified clusters enabled us to perform deeper functional discoveries (Figure 4.19., 4.23.). Interestingly, in columella, in the category of molecular functions, “serine type endopeptidase inhibitor activity”, “peptidase inhibitor activity”, “endopeptidase inhibitor activity” and “peptidase regulator activity” were the top enriched GO terms among upregulated genes of in both 1B and 2B toxicity conditions. Likewise, it was found that the well-represented molecular functions were peptidase and endopeptidase inhibitor activity for upregulated genes in roots of two contrasting wheat cultivars [3].

To find which metabolic pathways were affected under B toxicity, KO analyses were performed with ShinyGO (v.0.76.3) (Table 4.27., 4.28.). Accordingly, we found that under B toxicity conditions, the DEGs were significantly enriched in 22 KEGG pathways, including pathways associated with ‘glutathione metabolism’, ‘autopathy’, ‘sulphur metabolism’, ‘alanine, aspartate and glutamate metabolism, ‘carbon fixation in photosynthetic organisms’, ‘β alanine metabolism’, ‘arginine and proline metabolism’, ‘glycolysis/gluconeogenesis’, ‘cysteine and methionine metabolism’, ‘carbon metabolism’, ‘biosynthesis of secondary metabolites’, ‘oxidative phosphorylation’, ‘phenylpropanoid biosynthesis’, ‘stilbenoid, diaryheptanoid’, ‘gingerol biosynthesis’, ‘Photosynthesis ’, plant-pathogen interaction’, ‘MAPK signalling pathway-plant’, ribosome’, ‘cyanoamino acid metabolism’, ‘ubiquitin mediated proteolysis’, ‘arginine and proline metabolism’ (Figure 4. 27., 4.28.). Similar to the results in our study, in a recent study [131], it was shown that the highest number of DEGs in *Triticum zhukovskyi* under B toxicity were determined in ‘biosynthesis of secondary metabolites’, ‘plant–pathogen interaction, metabolic pathways’, ‘phenylpropanoid biosynthesis’, ‘RNA transport’, and ‘MAPK signalling pathway’. Moreover, the importance of phenylpropanoid pathways found to play a key role in the compartmentalization of B in vacuoles in *Arabidopsis thaliana* [101]. Additionally, in another study, Kayıhan et al., [3] showed that in sensitive and tolerant wheat cultivars, the majority of differentially expressed genes related to protein metabolism were involved in protein degradation in response to B toxicity and the numbers of these genes were higher in root tissues of sensitive wheat cultivars than tolerant wheat cultivar under B toxicity.

Under both 1B and 2B toxicity conditions, upregulated genes were highly associated with ‘glutathione and ‘sulfur metabolism’ (Figure 4.27a., 4.28a.). It has been suggested that B-anthocyanin complexes in vacuoles are an internal mechanism of tolerance to B toxicity [132]. Anthocyanin–glutathione or – glutathione –S transferase (GST) complexes can temporarily bind to metal or metalloid ions. In this way, GST-anthocyanin-metal complexes are formed and/or glutathionylanthocyanin metal complexes are vacuolated sequestered [132]. In our study, in columella, *GSTU24, GSTU25*, *GSTU22*, *GSTU19*, *GSTU7*, *GSTU5*, *GSTF8* and *GPX6* under 1B condition *GSTF6, GSTU24, GSTU25, GSTU22*, *GSTU19, GSTU7*, *GSTU5, GPX2, GSTF8 and GPX6* under 2B condition were found to be enriched among upregulated genes in functions associated with glutathione and metabolism (Table 4.5.). Moreover, in this cluster, AT1G55920, AT4G04610, AT4G21990 under 1B condition (Figure 4.27a.), and AT1G55920 AT1G62180, AT4G04610 and AT4G21990 under 2B condition (Figure 4.28a.) were revealed to be enriched among upregulated genes in functions associated with ‘sulfur metabolism’. These results might indicate the importance of GST related to an internal B tolerance mechanism in columella cell cluster in Arabidopsis root.

Moreover, Kayıhan et al., 2021 [101] examined toxic B-treated *Arabidopsis thaliana* to determine the gene expression levels related to anthocyanin biosynthesis and transport, and TFs under B toxicity. Accordingly, 3 mM boric acid treatment induced *4CL3* and *C4H* anthocyanin biosynthesis genes, *MYB75* and *MYB114* TFs an *TT13* and *TT19* anthocyanin transporter genes [101]. In our study, we found that *C4H* was commonly upregulated between endodermis and QC under 2B condition. Furthermore, under 2B condition, AT1G14540 AT1G61820 AT1G80820 AT2G30490 AT2G37040 AT4G34230 AT5G39580 were revealed to be enriched among upregulated genes in functions associated with ‘phenylpropanoid biosynthesis’ in QC (Figure 4.28d.). On the other hand, cysteine biosynthesis is involved in fixing inorganic sulphur and thus provides the sulphide source for the generation of glutathione and methionine [133]. Accordingly, KEGG analysis showed that in root cap, *SAM1*, *SAMDC1*, *SAHH1* and *MS1* under 1B condition (Figure 4.27d.), and *SAT1*, *SAM2*, *SAHH1* and *MS1* under 2B condition (Figure 4.22f.) were revealed to be enriched among upregulated genes in functions associated with ‘cysteine and methionine metabolism’. On the other hand, in QC, *TAT3*, *SAMDC1* and *MS1* under 2B condition (Figure 4.28e.) were revealed to be enriched among downregulated genes in functions associated with ‘cysteine and methionine metabolism’. These results may indicate that cysteine and methionine metabolism play a key role in the formation of GST-anthocyanin-

metal complexes related to the B tolerance mechanism by contributing to sulphur uptake in the root cap and QC.

Toxic B also cause impairment of metabolic process including photosynthesis due to decreasing the rate of content of chlorophyll, photosynthesis, and electron transport rate, and this can result in over accumulation of ROS in the plant [134]. KEGG analysis showed that in QC, ATCG00020, ATCG00130, ATCG00340, ATCG00470 and ATCG00720 under 2B condition (Figure 4.28d.) were revealed to be enriched among upregulated genes in functions associated with 'Photosynthesis'. Moreover, when toxic B binds with molecules such as ATP and NADPH [135], may limit the free energy required for carbohydrate biosynthesis and thus cause alterations in the sugar content [136, 137]. Interestingly, KEGG analyses showed that in root cap, *GAPC2*, *GAPC1* and *FBA8* under 1B condition (Figure 4.27d.), and *GAPC2*, *GAPC1*, *FBA8*, *CTIMC* and *PCKA* under 2B condition (Figure 4.28f.) were revealed to be enriched among upregulated genes in functions associated with 'carbon fixation in photosynthetic organisms. Moreover, AT1G04410, AT1G13440, AT1G65930, AT3G04120, AT3G14940, AT3G52930, AT3G55440 and AT4G14880 under 1B condition were revealed to be enriched among upregulated genes in functions associated with 'carbon fixation in photosynthetic organisms' (Figure 4.27d.), and also *GAPC2*, *GAPC1*, *FBA8* and *MS1* under 1B condition (Figure 4.27d.), *GAPC2*, *GAPC1*, *FBA8*, *CTIMC* and *PCKA* under 2B conditions (Figure 4.28f.) were revealed to be enriched among upregulated genes in functions associated with 'carbon metabolism'. Moreover, in endodermis, AT1G13440, AT3G04120, AT3G14940, AT3G52930 and AT3G55440 under 1B condition were revealed to be enriched among upregulated genes in functions associated with 'carbon metabolism' (Figure 4.27b). This might be due to toxic level B forming complexes with molecules such as ATP and NADPH [135]. This interaction limits the availability of free energy required for carbohydrate biosynthesis and thus, change in sugar content and partitioning [136, 137]. Furthermore, in root cap, *GAPC2*, *ENO2*, *GAPC1* and *FBA8* under 1B condition (Figure 4.27d.), and *GAPC2*, *ENO2*, *GAPC1*, *FBA8*, *CTIMC* and *PCKA* under 2B condition (Figure 4.28d) were revealed to be enriched among upregulated genes in functions associated with 'glycolysis/gluconeogenesis', and in endodermis, AT1G13440, AT3G04120, AT3G52930 and AT3G55440 under 1B condition (Figure 27b.), were revealed to be enriched among upregulated genes in functions associated with 'glycolysis/gluconeogenesis'.

We also showed significantly changing transcripts unique to B toxicity for each cluster (Figure 4.16., 4.17.). Interestingly, *GDH1* which activity known to be increased under B toxicity [138], was specifically upregulated in columella under 1B and 2B conditions and downregulated between endodermis and QC under 2B condition (Figure 4.16., 4.17.). Jasmonic acid (JA) related genes are an important late response to B toxicity. Differentially expression profiles showed that the barley transcriptome profile and signalling and molecular network responses alter under B toxicity [139]. Accordingly, AT3G56880 and *AGP31* was specifically upregulated in root cap in both 1B and 2B conditions (Figure 4.17e., 4.18c.). Furthermore, *NOI5* and *PSK2* were specifically upregulated in QC under 2B condition (Figure 4.17e., 4.18e) and *ABCG40* was specifically upregulated in columella under 1B and 2B conditions (Figure 4.17e., 4.18g.).

Several plant TFs involved in B toxicity have been known including WRKY, ERF, NAC, MYB [140, 141, 100, 142, 127]. In our study, we identified 13 TF families including ERF, NAC, C2H2, WRKY, NF-X1, Trihelix, bZIP, bHLH, MYB, C3H, HD-ZIP, LBD and HSF (Table 4.6.) at cell clusters under B toxicity conditions. In columella, TFs upregulation was seen in under all B toxicity conditions. In relation to transcription factors, genes related to ERF, NAC, C2H2, WRKY, NF-X1, Trihelix, LBD and bZIP TFs were upregulated in columella under B toxicity. Particularly, *ANAC081* gene was commonly upregulated in columella under all B toxicity conditions (Table 4.6.). Furthermore, *WRKY6*, *NFXL1*, *ERF1*, *GT-3A* and *ERF011* genes were also commonly upregulated in columella at seedling stage. On the other hand, the greatest number of TF expression was seen in QC. Accordingly, genes related to C2H2, ERF, bHLH, NAC, WRKY, HSF, MYB, C3H, bZIP, HD-ZIP and Trihelix TF families were upregulated in QC (Table 4.6.). These results show that QC and columella might be involved in TF regulation under B toxicity. NAC TFs are involved in the regulation of B toxicity [139]. Accordingly, in our study, 7 significantly upregulated genes from the NAC gene family were identified at cell clusters under toxic level B conditions, especially in columella (Figure 4.6.). Particularly, *ANAC081*, *ANAC2* and *NAC102* genes related to NAC TF family were highly upregulated under B toxicity conditions. Moreover, ERF TF family genes play a key role responding to abiotic stress. ERF TFs help activating ethylene and abscisic acid-dependent and independent stress-responsive genes [143]. In our study, 10 significantly upregulated genes from the ERF gene family were identified at cell clusters under toxic level B conditions (Figure 4.6.).

6. CONCLUSION

We successfully generated high-resolution and highly reproducible single-cell transcriptomic maps of 1554 Arabidopsis root cells at seedling stage in the control and B toxicity treatment groups. We obtained the 6 clusters from the primary root representing some highly specific cell types, including QC, endodermis, root cap columella, cortex, and trichoblast. The number of most significantly upregulated genes under 1B condition was determined in columella. However, they were seen in endodermis under 2B condition (On the other hand, the number of most significantly downregulated genes under 1B condition and 2B condition were seen in root cap

The pathways already presented in the literature related to B toxicity were found and many new genes specific to cell type were identified. Interestingly, predetermined B toxicity and JA association and genes involved in this context were identified as a cell-type basis. On the other hand, the role of anthocyanins and GSTs related to the B tolerance mechanism was identified at cell specific basis. In this context, GO and KO analysis were performed under B toxicity treatment in the columella. The results point to vacuoles and GST being the most altered gene groups in this cluster, suggesting that the internal B tolerance mechanism was effectively columella. Furthermore, QC and columella are highly involved in TF regulation under B toxicity. The further analysis of these genes and pathways at cell type basis and further analysis of related clusters are crucial to clarify B toxicity tolerance mechanism in plants more accurately and precisely.

Moreover, we identified cell specific 13 TF families under B toxicity including ERF, NAC, C2H2, WRKY, NF-X1, Trihelix, bZIP, bHLH, MYB, C3H, HD-ZIP, LBD and HSF. Our study showed that QC and columella are highly involved in TF regulation under B toxicity. However, the functions of TFs should be examined in the relevant clusters in more detail.

This study can impact on the potential transgenic and marker assisted breeding strategies to improve the boron tolerant cultivars against boron toxicity in plants.

REFERENCES

[1] W. D. Loomis and R. W. Durst, "Chemistry and biology of boron," *BioFactors,* vol. 3, pp. 229-239, 1992.

[2] R. J. Reid, J. E. Hayes, A. Post, J. C. R. Stangoulis and R. D. Graham, "A critical analysis of the causes of boron toxicity in plants," *Plant Cell Environ.*, vol. 27, pp. 1405-1414, 2004.

[3] C. Kayıhan, M. T. E. F. Y. M. Öz and H. A. Öktem, "Physiological, Biochemical, and Transcriptomic Responses to Boron Toxicity in Leaf and Root Tissues of Contrasting Wheat Cultivars," *Plant Mol Biol Rep,* vol. 25, pp. 97-109, 2017.

[4] E. Z. Macosko, A. Basu, R. Satija, J. Nemesh, K. Shekhar, M. Goldman, I. Tirosh, A. R. Bialas, N. Kamitaki, E. M. Martersteck, J. J. Trombette, D. A. Weitz, J. R. S. A. K. Shalek, A. Regev and S. A. McCarroll, "Highly parallel genome-wide expression profiling of individual cells using nanoliter droplets," *Cell,* vol. 161, pp. 1202-1214, 2015.

[5] C. Ziegenhain, B. Vieth, S. Parekh, B. Reinius, A. Guillaumet-Adkins, M. Smets, H. Leonhardt, H. Heyn, I. Hellmann and W. Enard, "Comparative analysis of single-cell RNA sequencing methods," *Mol Cell,* vol. 65, pp. 631-643, 2017.

[6] A. Wagner, A. Regev and N. Yosef, "Revealing the vectors of cellular identity with single-cell genomics," *Nature Biotechnology 34, 1145-1160.*, vol. 34, pp. 1145-1160, 2016.

[7] E. Lieckfeldt, U. Simon-Rosin, F. Kose, D. Zoeller, M. Schliep and J. Fisahn, "Gene expression profiling of single epidermal, basal and trichome cells of Arabidopsis thaliana," *J Plant Physiology,* vol. 165, pp. 1530-1544, 2008.

[8] P. Brennecke, S. Anders, J. K. Kim, A. A. Kołodziejczyk, X. Zhang, V. Proserpio, B. Baying, V. Benes, S. A. Teichmann, J. C. Marioni and M. G. Heisler, "Accounting for technical noise in single-cell RNA-seq experiments," *Nat Methods,* vol. 10, pp. 1093-1095, 2013.

[9] I. Efroni, P. L. Ip, T. Nawy, A. Mello and K. Birnbaum, "Quantification of cell identity from single-cell gene expression profiles," *Genome Biology,* vol. 16, no. 9, 2015.

[10] M. H. Frank and M. J. Scanlon, "Cell-specific transcriptomic analyses of three-dimensional shoot development in the moss Physcomitrella patens," *Plant J.*, vol. 83, pp. 743-751, 2015.

[11] I. Efroni and K. D. Birnbaum, "The potential of single-cell profiling in plants," *Genome Biology,* vol. 17, no. 65, 2016.

[12] M. Libault, L. Pingault, P. Zogli and J. Schiefelbein, "Plant systems biology at the single-cell level," *Trends Plant Sci,* vol. 22, pp. 949-960, 2017.

[13] A. Bruex, R. M. Kainkaryam, Y. Wieckowski, Y. H. Kang, C. Bernhardt, Y. Xia, X. Zheng, J. Y. Wang, M. M. Lee, P. Benfey, P. J. Woolf and J. Schiefelbein, "A gene regulatory network for root epidermis cell differentiation in Arabidopsis," *PLoS Genetics,* vol. 8, no. e1002446, 2012.

[14] S. Li, M. Yamada, X. Han, U. Ohler and B. P. N, "High-resolution expression map of the Arabidopsis root reveals alternative splicing and lincRNA regulation," *Dev Cell,* vol. 39, pp. 508-500, 2016.

[15] G. X. Zheng, J. M. Terry, B. P., R. P., Z. W. Bent, R. Wilson, S. B. Ziraldo, T. Wheeler, G. P. McDermot and J. Zhu, "Massively parallel digital transcriptional profiling of single cells," *Nat coomun,* vol. 8, no. 14049, 2017.

[16] U. Krämer, "Planting molecular functions in an ecological context with Arabidopsis thaliana," *eLife,* vol. 4, no. e06100, 2015.

[17] D. M. Maarten Koornneef, "The development of Arabidopsis as a model plant," *The Plant Journal,* vol. 61, no. 6, pp. 909-921, 2010.

[18] W. A. Rensink and C. R. Buell, "Arabidopsis to Rice. Applying Knowledge from a Weed to Enhance Our Understanding of a Crop Species," *Plant Physiology,* vol. 135, no. 2, pp. 622-629, 2004.

[19] A. Platt, M. Horton, Y. S. Huang, Y. Li, A. E. Anastasio, N. W. Mulyati, J. Agren, O. Bossdorf, D. Byers, K. Donohue, M. Dunning, E. B. Holub, A. Hudson, V. L.

Corre, O. Loudet, F. Roux and N. Warthm, "The scale of population structure in Arabidopsis thaliana," *PLoS Genetics,* vol. 6, no. 2, 2010.

[20] The, Arabidopsis, Genome and Initiative, "Analysis of the genome sequence of the flowering plant Arabidopsis thaliana," *Natura,* vol. 408, no. 6814, pp. 796-815, 2000.

[21] C.-Y. Cheng, V. Krishnakumar, A. P. Chan, F. Thibaud-Nissen, S. Schobel and C. D. Town, "Araport11: a complete reannotation of the Arabidopsis thaliana reference genome," *The Plant Journal,* vol. 89, no. 4, pp. 789-804, 2018.

[22] L. R. Hogge, D. W. Reed, E. W. Underhill and G. W. Haughn, "HPLC Separation of Glucosinolates from Leaves and Seeds of Arabidopsis thaliana and Their Identification Using Thermospray Liquid Chramatography/Mass Spectrometry," *Chromatographic Science,* vol. 26, no. 11, pp. 551-556, 1988.

[23] N. J. Provart, J. Alonso, S. M. Assmann, D. Bergmann, S. M. Brady, J. Brkljacic, J. Browse, C. Chapple, V. Colot, S. Cutler, J. Dangl, D. Ehrhardt, J. D. Friesner, W. B. Frommer, E. Grotewold, E. Meyerowitz, J. Nemhauser, M. Nordborg and C. Pikaard, "50 years of Arabidopsis research: highlights and future directions," *New Phytologist* , vol. 209, no. 3, pp. 921-944, 2016.

[24] G. Lussac, J. Louis and L. J. Thénard, "Sur la décomposition et la recomposition de l'acide boracique," *Ann. Chim. Phys.*, vol. 68, pp. 169-174, 1808.

[25] F. S. Kot, "Boron sources, speciation and its potential impact on health," *Environmental Science and Bio/Technology,* vol. 8, pp. 3-28, 2009.

[26] R. Thompson, Inorganic boron chemistry: an introduction and background. In:, New York: Longman, 1980.

[27] H. W. Roesky, Clusters, and Polymers of Main Group and Transition Elements, Ars: Elsevier Science Limited, 1989.

[28] M. A. Soriano-Ursua, B. C. Das and J. G. Trujillo-Ferrara, "Boron-containing compounds: chemico-biological properties and expanding medicinal potential in prevention, diagnosis and therapy," *Expert Opin. Ther. Patents,* vol. 24, no. 5, 2014.

[29] A. Earnshaw and N. N. Greenwood, Chemistry of the Elements (Vol 60), Oxford: Butterworth-Heinemann, 1997.

[30] H. Steinberg, "Boron-oxygen and boron-sulfur," in *Organoboron Chemistry*, vol. 1, New York, 1964.

[31] H. Reeves, "The origin of the light elements in the early Universe," in *The Century of Space Science*, Dordrecht, Springer, 2001.

[32] P. Power and W. G. Woods, "The chemistry of boron and its speciation in plants," *Plant Soil,* vol. 193, pp. 1-13, 1997.

[33] E. Meydan, "BORON COMPOUNDS WITH MAGNETIC PROPERTIES AND THEIR APPLICATION AREAS IN INDUSTRY," *Journal of Scientific Perspectives,* vol. 3, no. 1, pp. 11-20, 2019.

[34] L. Bolaños, K. Lukaszewski, I. Bonilla and D. Blevins, "Why boron?," *Plant Physiology and Biochemistry,* vol. 42, no. 11, pp. 907-912, 2004.

[35] P. H. Brown, N. Bellaloui, M. A. Wimmer, E. S. Bassil, J. Ruiz, H. Hu, H. Pfeffer, F. Dannel and V. Römheld, "Boron in plant biology," *Plant Biology*, vol. 4, no. 2, pp. 205-223, 2002.

[36] K. Warington, "The effect of boric acid and borax on the broad bean and certain other plants," *Ann. Bot.,* vol. 37, pp. 629-672, 1923.

[37] H. E. Goldbach, Q. Yu, R. Wingender, M. Schulz, M. Wimmer, P. Findeklee and F. Baluska, "Boron in plants and animals: is there a role beyond cell-wall structure?," *J Plant Nutr Soil Sci.,* vol. 164, pp. 173-181, 2001.

[38] M. A. O'Neill, T. Ishii, P. Albersheim and A. G. Darvill, " Rhamnogalacturonan II: structure and function of a borate cross-linked cell wall pectic polysaccharide," *Annu. Rev. Plant Biol.,* vol. 55, pp. 109-139, 2004.

[39] M. Pičmanová and B. L. Møller, "Apiose: One of nature's witty games," *Glycobiology,* vol. 26, no. 5, pp. 430-442, 2016.

[40] M. Kobayashi, T. Matoh and J. Azuma, "Two chains of rhamnogalacturonan II are cross-linked by borate-diol ester bonds in higher plant cell walls," *Plant Physiol.,* vol. 110, pp. 1017-1020, 1996.

[41] H. Hu, P. H. Brown and J. H. Labavitch, "Species variability in boron requirement is correlated with cell wall pectin," *J. Exp. Bot.,* vol. 47, pp. 227-232, 1996.

[42] P. Marschner, Marschner's Mineral Nutrition of Higher, USA: Elsevier, Academic Press, 2012.

[43] Y. Oiwa, K. Kitayama, M. Kobayashi and T. Matoh, "Boron deprivation immediately causes cell death in growing roots of Arabidopsis thaliana (L.) Heynh," *Soil Sci. Plant Nutr.,* vol. 59, no. 4, pp. 621-627, 2013.

[44] A. Fleischer, C. Title and R. Ehwald, "The boron requirement and cell wall properties of growing- and stationary-phase suspensioncultured Chenopodium album L. cells," *Plant Physiology,* vol. 117, pp. 1401-1410, 1988.

[45] A. Fleischer, M. A. O'Neil and R. Ehwald, "The pore size of non-graminaceous plant cell walls is rapidly decreased by borate ester cross-linking of the pectic polysaccharide Rhamnogalacturonan II," *Plant Physiology,* vol. 121, pp. 829-836, 1999.

[46] A. Voxeur and S. C. Fry, "Glycosylinositol phosphorylceramides from Rosa cell cultures are boron-bridged in the plasma mem brane and form complexes with rhamnogalacturonan II," *Plant J,* vol. 79, no. 1, pp. 139-149, 2014.

[47] N. Wang, C. Yang, Z. Pan, Y. Liu and S. Peng, "Boron defciency in woody plants: various responses and tolerance mechanisms," *Front Plant Sci.*, vol. 6, p. 916, 2015.

[48] I. Cakmak, H. K. and H. Marschner, *Physiologia Plant,* vol. 95, pp. 11-18, 1995.

[49] C. Dordas and P. H. Brown, "Boron deficiency affects cell viability, phenolic leakage and oxidative burst in rose cell cultures," *Plant Soil,* vol. 268, pp. 293-301, 2005.

[50] J. Blaser-Grill, D. Knoppik, A. Amberger and H. Goldbach, " Influence of boron on the membrane potential in Elodea densa and Helianthus annuus roots and H+ extrusion of suspension cultured Daucus carota cells.," *Plant Physiol. ,* vol. 90, pp. 280-284, 1989.

[51] B. Alberts, D. Bray, J. Lewis, M. Raff, K. Roberts and J. D. Watson, in *Molecular Biology of the Cell. (Ed.)*, New York, Garland Publishers, 1998, p. 503.

[52] J. M. Davis, D. C. Sanders, P. Nelson, L. Lengnick and W. J. Sperry, "Boron improves growth, yield, quality, and nutrient content of tomato," *J. Am. Soc. Hort. Sci.,* vol. 128, pp. 441-446, 2003.

[53] M. K. Schon, D. G. Blevins and A. Novacky, "Boron: from cell membranes to soybean branching.," in *D. D. Randall; D. G Blevins; C. D. Miles (Ed.) Current Topics in Plant Biochem. and Physiol. Vol. 10,* Columbus, 1991, pp. 230-239.

[54] B. Dell and L. Huang, "Physiological response of plants to low boron," *Plant Soil,* vol. 193, pp. 103-120, 1997.

[55] J. Takano, M. Wada, U. Ludewig, G. Schaaf, N. V. W. and T. Fujiwara, "The Arabidopsis major intrinsic protein NIP5; 1 is essential for efficient boron uptake and plant development under boron limitation," *Plant Cell,* vol. 18, pp. 1498-1509, 2006.

[56] E. M. Martín-Rejano, J. J. Camacho-Cristóbal, M. B. Herrera-Rodríguez, J. Rexach, M. T. Navarro-Gochicoa and A. González-Fontes, "Auxin and ethylene are involved in the responses of root system architecture to low boron supply in Arabidopsis seedlings," *Physiol. Plant,* vol. 140, p. 170–178, 2011.

[57] J. Camacho-Cristóbal, E. M. Martín-Rejano, M. B. Herrera-Rodríguez, M. T. Navarro-Gochicoa, J. Rexach and A.González-Fontes, "Boron deficiency inhibits root cell elongation via an ethylene/auxin/ROS dependent pathway in Arabidopsis seedlings," *J. Exp. Bot.,* vol. 66, pp. 3831-3840, 2015.

[58] C. G. Sherrel, "Boron deficiency and response in white and red clovers and lucerne," *New Zeal. J. Agric. Res.,* vol. 26, pp. 197-203, 1983.

[59] Q. L. Wang, L. D. Lu, X. Q. Wu, Y. Q. Li and J. X. Lin, "Boron influences pollen germination and pollen tube growth in Picea meyeri," *Tree Physiology,* vol. 23, pp. 345-351, 2003.

[60] S. Lordkaew, S. Konsaeng, J. Jongjaidee, B. Dell, B. Rer-kasem and S. Jamjod, "Variation in responses to boron in rice," *Plant Soil,* vol. 363, pp. 287-295, 2013.

[61] K. C. Berger, "Boron in soils and crops," in *Norman AG (Ed.). Advances in Agronomy*, New York, Academic Press, 1949.

[62] H. G. Gauch and W. M. Dugger, "The role of boron in the translocation of sucrose," *Physiol. Plant,* vol. 28, p. 457, 1953.

[63] M. Gomez-Rodriguez, J. L. d. Castillo and M. Alvarez-Tinaut, "he evolution of glucose-6P-dehydrogenase and 6P-gluconate-dehydrogenase activities and the ortho-diphenolic content of sunflower leaves cultivated under different boron treatments," *J. Plant Nutr.*, vol. 10, pp. 2211-2229, 1987.

[64] J. A. Heyes, P. J. White and B. C. Loughman, "The role of boron in some membrane characteristics of plant cells and protoplasts," in *Current Topics in Plant Biochem. and Physiol., vol 10*, Columbus, University Missouri, 1991, pp. 179-194.

[65] U. Weser, "Aktivitat shemmung der hefe-alcohol-dehydrogenase in gegenwart von germanat und borat.," *Hoppe-Seyler's Zeit. Physiol. Chem.,* vol. 349, pp. 1479-1482, 1968.

[66] K. W. Smith and S. L. Johnson, "Borate inhibition of yeast alcohol dehydrogenase," *Biochem. ,* vol. 15, pp. 560-565, 1976.

[67] L. Bolanos, N. J. Brewin and I. Bonilla, "Effects of boron on Rhizobium-legume cell-surface interactions and nodule development," *Plant Physiology,* vol. 110, pp. 1249-1256, 1996.

[68] I. Abreu, M. E. Cerda, M. P. d. Nanclares, I. Baena, J. Lloret, I. Bonilla, L. Bolanos and M. Reguera, "Reguera Boron deficiency affects rhizobia cell surface polysaccharides important for suppression of plant defense mechanisms during legume recognition and for development of nitrogen-fixing symbiosis," *Plant Soil,* vol. 361, pp. 385-395, 2012.

[69] L. Hamilton, K. F. M. R. E. M. A. Leach and J. Brockwell, "Boron deficiency in pasture based on subterranean clover (Trifolium subterraneum L.) is linked to symbi otic malfunction," *Crop & Pasture Sci.*, vol. 68, pp. 1197-1212, 2017.

[70] H. E. Goldbach and M. A. Wimmer, "Boron in plants and animals: is there a role beyond cell-wall structure?," *J. Plant Nutr. Soil Sci. ,* vol. 170, pp. 39-48, 2007.

[71] J. J. Camacho-Crist´obal, M. B. Herrera-Rodr´ıguez, V. M. Beato, M. T. Rexach, N.-. Gochicoa, J. M. Maldonado and A. González-Fontesa, "The expression of several

cell wall- related genes in Arabidopsis roots is down-regulated under boron deficiency," *Env. Exp. Bot.* , vol. 63, pp. 351-358, 2008.

[72] A. G. Gunes, G. Soylemezoglu, A. Inal, E. Bagci, S. Çoban and O. Şahin, "Antioxidant and stomatal responses of grapevine (Vitis vinifera L.) to boron toxicity," *Scientia Horticulturae,* vol. 110, p. 279–284, 2006.

[73] J. Z. Wang, S. T. Tao, K. J. Qi, J. Wu, H. Q. Wu and S. L. Zhang, "Changes in photosynthetic properties and antioxidative system of pear leaves to boron toxicity," *Afr. J. Biotecnology,* vol. 10, pp. 19693-19700, 2011.

[74] U. Yermiyahu, A. Ben-Gal, R. Keren and R. J. Redi, "Combined effect of salinity and boron on plant growth and yield," *Plant Soil,* vol. 304, pp. 73-87, 2008.

[75] M. Brdar-Jokanovi´c, "Boron Toxicity and Deficiency in Agricultural Plants," *Int. J. Mol. Sci.,* vol. 21, no. 1, pp. 1424-1443, 2020.

[76] U. Gupta, Y. W. Jame, C. A. Campbell, A. J. Leyshon and W. Nicholaichuck, "Boron toxicity and deficiency," *Can. J. Soil Sci.*, vol. 65, pp. 381-409, 1985.

[77] R. O. Nable, G. S. Bañuelos and J. Paull, "Boron toxicity," *Plant Soil,* vol. 193, pp. 181-198, 1997.

[78] M. Tanaka and T. Fujiwara, "Physiological roles and transport mechanisms of boron: perspectives from plants," *Eur. J. Physiology,* vol. 456, pp. 671-677, 2008.

[79] S. K. Ya and M. C. Saxena, "Variation in growth, development, and yield of durum wheat in response to high soil boron I. Average effects," *Australian Journal of Agricultural Research,* vol. 48, no. 7, pp. 945-950, 1997.

[80] J. J. Christensen, "Non-parasitic leaf spots of barley," *Phytopathology,* vol. 24, pp. 726-742, 1934.

[81] F. M. Eaton, "Deficiency, toxicity and accumulation of boron in plants," *J. Agric. Res.*, vol. 69, pp. 237-277, 1944.

[82] B. Cartwright, B. A. Zarcinas and A. H. Mayfield, "Toxic concentrations of boron in a red-brown earth at Gladstone, South Australia. Aust.," *J. Soil Res.,* vol. 22, pp. 261-272, 1984.

[83] R. O. Nable, "Resistance to boron toxicity amongst several barley and wheat cultivars: A preliminary examination of the resistance mechanism," *Plant Soil,* vol. 112, pp. 45-52, 1988.

[84] J. G. Paull, B. Cartwright and A. J. Rathjen, "Responses of wheat and barley genotypes to toxic concentrations of soil boron," *Euphytica,* vol. 39, pp. 137-144, 1988.

[85] J. G. Paull, A. J. R. B. C. and R. O. Nable, "Selection parameters for assessing the tolerance of wheat to high concentrations of boron," in *Genetic Aspects of Plant Mineral Nutrition; N. El Bassam; M. Dambroth; B. C. Loughman* , Dordrecht, The Netherlands, Kluwer Academic Publisher, 1990, p. 361–369..

[86] V. Mahalakshmi, S. K. Yau, J. R. and J. M. P. , "Boron toxicity in barley (Hordeum vulgare L.) seedlings in relation to soil temperature," *Plant Soil,* vol. 177, pp. 151-156, 1995.

[87] S. K. Yau, M. M. Nachit, J. Ryan and J. Hamblin, "Phenotypic variation in boron toxicity tolerance at seedling stage in durum wheat (Triticum durum)," *Euphytica,* vol. 83, pp. 185-191, 1995.

[88] G. S. Bañuelos, H. A. A. L. Caceres and D. Dyer, "Germination responses and boron accumulation in germplasm from Chile and the United States grown with boron-enriched water," *Ecotoxicol. Environ. Saf.,* vol. 43, pp. 62-67, 1999.

[89] S. Rehman, T. I. P. Y. J. K. Z. W. S. and S. J. Y. , "Inverse relationship between boron toxicity tolerance and boron contents of barley seed and root," *J. Plant Nutr.,* vol. 26, pp. 1779-1789, 2006.

[90] A. A. Torun., A. Yazici., H. Erdem and I. Çakmak, "Genotypic variation in tolerance to boron toxicity in 70 durum wheat genotypes," *Turk. J. Agric. For.,* vol. 30, pp. 49-58, 2006.

[91] P. H. Brown and H. Hu, "Phloem mobility of boron is species dependent: evidence for phloem mobility in sorbitol-rich species," *Ann. Bot.,* vol. 77, pp. 497-505, 1996.

[92] P. H. Brown and B. J. Shelp, "Boron mobility in plants," *Plant Soil,* vol. 193, pp. 85-101, 1997.

[93] L. M. Cervilla, M. A. Rosales, M. M. Rubio-Wilhelmi, E. Sanchez-Rodrıguez, B. Blasco and J. J. Ríos, "Involvement of lignifcation and membrane permeability in the tomato root response to boron toxicity," *Plant Sci.,* vol. 176, pp. 545-552, 2009.

[94] D. Liu, W. Jiang, L. Zhang and L. Li, "Effects of boron ions on root growth and cell division of broadbean (Vicia faba L.)," *Isr J Plant Sci,* vol. 48, no. 1, pp. 47-51, 2000.

[95] C. J. Lovatt and L. M. Bates, "Early effects of excess boron on photosynthesis and growth of Cucurbita pepo," *Journal of Experimental Botany ,* vol. 35, pp. 297-305, 1984.

[96] E. Karabal, M. Yücel and H. A. Öktem, "Antioxidant responses of tolerant and sensitive barley cultivars to boron toxicity," *Plant Science ,* vol. 164, pp. 925-933, 2003.

[97] I. Bonilla, C. Cadahia, O. Carpena and V. Hernando, "Effects of boron on nitrogen metabolism and sugar levels of sugar beet," *Plant Soil,* vol. 57, pp. 3-9, 1980.

[98] R. Kastori and N. Petrovic, "Effect of boron on nitrate reductase activity in young sunflower plants," *J. Plant Nutr.,* vol. 12, pp. 621-627, 1989.

[99] R. Deshmukh, H. Sonah, G. Patil, W. Chen, S. Prince, R. Mutava, T. Wuong, B. Valliyodan and H. T. Nguyen, "Integrating omic approaches for abiotic stress tolerance in soybean," *Frontiers in Plant Science,* vol. 5, 2014.

[100] C. Kayıhan, M. T. Oz, F. Eyidogan, M. Yücel and H. A. Oktem, "Physiological, biochemical, and transcriptomic responses to boron toxicity in leaf and root tissues of contrasting wheat cultivars.," *Plant Mol. Biol.,* vol. 35, pp. 97-105, 2016.

[101] C. Kayıhan, "The involvement of the induction of anthocyanin biosynthesis and transport in toxic boron responsive regulation in Arabidopsis thaliana," *Turkish Journal of Botany,* vol. 45, no. 3, pp. 181-191, 2021.

[102] J.-H. Huang, Y.-P. Qi, S.-X. Wen, P. Guo, X.-M. Chen and L.-S. Chen, "Illumina microRNA profiles reveal the involvement of miR397a in Citrus adaptation to long-term boron toxicity via modulating secondary cell-wall biosynthesis," *Scientific Reports,* vol. 6, p. 22900, 2016.

[103] J. H. Huang, X. J. Lin, L. Y. Zhang, X. D. Wang, G. C. Fan and L. S. Chen, "MicroRNA Sequencing Revealed Citrus Adaptation to Long-Term Boron Toxicity through Modulation of Root Development by miR319 and miR171," *International journal of molecular sciences*, vol. 20, no. 6, p. 1422, 2019.

[104] D. Kayıhan, C. Kayıhan and Y. Ö. Çiftçi, "Moderate level of toxic boron causes differential regulation of microRNAs related to jasmonate and ethylene metabolisms in Arabidopsis thaliana," *Turkish Journal of Botany*, vol. 43, no. 2, pp. 167-172, 2019.

[105] Y. Feng, R. Cui, Y. Huang, L. Shi, S. Wang and F. Xu, "Repression of transcription factor AtWRKY47 confers tolerance to boron toxicity in Arabidopsis thaliana," *Ecotoxicology and Environmental Safety*, vol. Volume 220, p. 112406, 2021.

[106] C. Trapnell, D. Cacchiarelli, J. Grimsby, P. Pokharel, S. Li, M. Morse, K. J. L. N. J. Lennon, T. S. Mikkelsen and J. L. Rinn, "The dynamics and regulators of cell fate decisions are revealed by pseudotemporal ordering of single cells," *Nat Biotechnol*, vol. 32, pp. 381-386, 2014.

[107] L. Wen and F. Tang, "Boosting the power of single-cell analysis," *Nat Biotechnol.*, vol. 36, no. 5, pp. 408-409, 2018.

[108] B. Artegiani, A. Lyubimova, M. Muraro, J. H. v. Es, A. v. Oudenaarden and H. Clevers, "A single-cell RNA sequencing study reveals cellular and molecular dynamics of the hippocampal neurogenic niche," *Cell Rep.*, vol. 21, pp. 3271-3284, 2017.

[109] A. C. Villani, R. Satija, G. Reynolds, S. Sarkizova, K. Shekhar, J. Fletcher, M. Griesbeck, A. Butler, S. Zheng, S. Lazo, L. Jardine, D. Dixon, E. Stephenson, E. Nilsson, I. Grundberg, D. McDonald, A. Filby, W. Li, P. L. D. Jager and O. Rozenblatt-Rosen, "Single-cell RNA-seq reveals new types of human blood dendritic cells, monocytes, and progenitors," *Science*, vol. 21, no. 356(6335):eaah4573, 2017.

[110] L. L. Glass, F. J. Calero-Nieto, W. Jawaid, P. Larraufie, R. G. Kay, B. Göttgens, F. Reimann and F. M. Gribble, "Single-cell RNA-sequencing reveals a distinct population of proglucagon-expressing cells specific to the mouse upper small intestine," *Mol. Metab.*, vol. 6, p. 1296–1303, 2017.

[111] A. K. Shalek, R. Satija, X. Adiconis, R. S. Gertner, J. T. Gaublomme, R. Raychowdhury, S. Schwartz, N. Yosef, C. Malboeuf, D. Lu, J. J. Trombetta, D. Gennert, A. Gnirke, A. Goren, N. Hacohen, J. Z. Levin, H. Park and A. Regev, "Single-cell transcriptomics reveals bimodality in expression and splicing in immune cells," *Nature* , vol. 498, p. 236–240, 2013.

[112] B. Mahata, X.Zhang, A. A. Kolodziejczyk, V. Proserpio, L. Haim-Vilmovsky, A. E. Taylor, D. Hebenstreit, F. A. Dingler, V. Moignard, B. Göttgens, W. Arlt, A. N. J. McKenzie and S. A. Teichmann, "Single-cell RNA sequencing reveals T helper cells synthesizing steroids de novo to contribute to immune homeostasis," *Cell Rep.*, vol. 7, pp. 1130-1142, 2014.

[113] A. K. Shalek, R. Satija, J. Shuga, J. J. Trombetta, D. Gennert, D. Lu, P. Chen, R. S. Gertner, J. T. Gaublomme, N. Yosef, S. Schwartz, B. Fowler, S. Weaver, J. Wang, X. Wang, R. Ding, R. Raychowdhury, N. Friedman, N. Hacohen, H. Park, A. P. May and A. Regev, "Single-cell RNA-seq reveals dynamic paracrine control of cellular variation," *Nature,* vol. 510, pp. 363-369, 2014.

[114] D. Grün, A. Lyubimova, L. Kester, K. Wiebrands, O. Basak, N. Sasaki, H. Clevers and A. v. Oudenaarden, "A Single-cell messenger RNA sequencing reveals rare intestinal cell types," *Nature,* vol. 525, pp. 251-255, 2015.

[115] E. Torre, H. Dueck, S. Shaffer, J. Gospocic, R. Gupte, R. Bonasio, J. Kim, J. Murray and A. Raj, "Rare cell detection by single-cell RNA sequencing as guided by single-molecule RNA FISH," *Cell Systems,* vol. 6, pp. 171-179, 2018.

[116] X. Zhao, S. Gao, Z. Wu, S. Kajigaya, X. Feng, Q. Liu, D. M. Townsley, J. Cooper, J. Chen, K. Keyvanfar, M. D. P. F. Ibanez, X. Wang and N. S. Young, "Single-cell RNA-seq reveals a distinct transcriptome signature of aneuploid hematopoietic cells," *Blood,* vol. 130, pp. 2762-2773, 2017.

[117] B. Treutlein, D. G. Brownfield, A. R. Wu, N. F. Neff, G. L. Mantalas, F. H. Espinoza, T. J. Desai, M. A. Krasnow and S. R. Quake, "Reconstructing lineage hierarchies of the distal lung epithelium using single-cell RNA-seq," *Nature,* vol. 509, p. 371–375, 2014.

[118] X. Qiu, Q. Mao, Y. Tang, L. Wang, R. Chawla, H. A. Pliner and C. Trapnell, "Reversed graph embedding resolves complex single-cell trajectories," *Nat Methods,* vol. 14, pp. 979-982, 2017.

[119] K. H. Ryu, L. Huang, H. M. Kang and J. Schiefelbein, "Single-Cell RNA Sequencing Resolves Molecular Relationships Among Individual Plant Cells," *Plant Physiol.,* vol. 179, no. 4, pp. 1444-1456, 2019.

[120] F. Apelt, E. Mavrothalassiti, S. Gupta, F. Machin, J. J. Olas, M. G. Annunziata, D. Schindelasch and F. Kragler, "Shoot and root single cell sequencing reveals tissue- and daytime-specific transcriptome profiles," *Plant phsiology,* vol. 188, pp. 861-878, 2022.

[121] K. Birnbaum, J. W. Jung, J. Y. Wang, G. M. Lambert, J. A. Hirst, D. W. Galbraith and P. N. Benfey, "Cell type-specific expression profiling in plants via cell sorting of protoplasts from fluorescent reporter lines," *Nat Methods,* vol. 2, pp. 615-619, 2015.

[122] A. Butler, P. Hoffman, P. Smibert, E. Papalexi and R. Satija, "Integrating single-cell transcriptomic data across different conditions, technologies, and species," *Nature Biotechnology,* vol. 36, pp. 411-420, 2018.

[123] S. X. Ge, D. Jung and R. Yao, "ShinyGO: a graphical gene-set enrichment tool for animals and plants," *Bioinformatics,* vol. 36, no. 8, pp. 2628-2629, 2020.

[124] S. De Smet, A. Cuypers, J. Vangronsveld and T. Remans, "Gene Networks Involved in Hormonal Control of Root Development in Arabidopsis thaliana: A Framework for Studying Its Disturbance by Metal Stress," *International Journal of Molecular Sciences,* vol. 16, no. 8, pp. 19195-19224, 2015.

[125] J. Jin, F. Tian, D. C. Yang, M. Y. L. Kong, J. C. Luo and G. Gao, "PlantTFDB 4.0: toward a central hub for transcription factors and regulatory interactions in plants.," *Nucleic Acids Research,* vol. 45, pp. 1040-1045, 2017.

[126] K. Mengel and E. A. Kirkby, Principles of plant nutrition, Springer Science & Business Media, 2012.

[127] F. Chen, J. Gao, W. Li and P. Fang, "Transcriptome profiles reveal the protective role of seed coating with zinc against boron toxicity in maize (Zea mays L.)," *Journal of Hazardous Materials,* vol. 423, 2022.

[128] A. Pandey, M. Kamran Khan, M. Hamurcu, M. Brestic, A. Topal and S. Gezgin, "Insight into the Root Transcriptome of a Boron-Tolerant Triticum zhukovskyi Genotype Grown under Boron Toxicity," *Agronomy,* vol. 12, no. 10, p. 2421, 2022.

[129] B. Wu, J. Zhang, W. Huang, L. Yang, Z. Huang, J. W. J. Guo and L. Chen, "Molecular mechanisms for pH-mediated amelioration of aluminum-toxicity revealed by conjoint analysis of transcriptome and metabolome in Citrus sinensis roots," *Chemosphere,* vol. 299, no. 134335, 2022.

[130] R. Shaw, X. Tian and J. Xu, "Single-cell transcriptome analysis in Plants: Advances and Challenges," *Mol. Plant,* vol. 14, no. 1, pp. 115-126, 2021.

[131] A. Pandey, M. K. Khan, M. Hamurcu, M. Brestic, A. Topal and S. Gezgin, "Insight into the Root Transcriptome of a Boron-Tolerant Triticum zhukovskyi Genotype Grown under Boron Toxicity," *Agronomy,* vol. 12, no. 10, p. 2421, 2022.

[132] M. Landi, M. Tattini and K. S. Gould, "Multiple functional roles of anthocyanins in plant-environment interactions," *Environ Exp Bot.,* vol. 119, pp. 4-17, 2015.

[133] E. R. Bonner, R. E. Cahoon, S. M. Knapke and j. M. Jez, "Molecular basis of cysteine biosynthesis in plants: structural and functional analysis of O-acetylserine sulfhydrylase from Arabidopsis thaliana," *J Biol Chem,* vol. 280:, no. 46, pp. 38803-13, 2005.

[134] C. Antonopoulou and C. Christos Chatzissavvidis, "Impact of boron and its toxicity on photosynthetic capacity of plants," in *Boron in Plants and Agriculture,* London, Academic Press, 2022, pp. 169-186.

[135] L. M. Cervilla, B. Blasco, J. J. Ríos, M. A. Rosales, M. M. Rubio-Wilhelmi, E. Sánchez-Rodríguez, L. Romero and J. M. Ruiz, "Response of nitrogen metabolism to boron toxicity in tomato plants," *Plant Biology,* vol. 11, pp. 671-677, 2009.

[136] U. Roessner, J. Patterson, M. G. F. G. Forbes, P. Langridge and A. Bacic, "An investigation of boron toxicity in barley using metabolomics," *Plant Physiol.,* vol. 142, no. 3, pp. 1087-1101, 2006.

[137] I. E. Papadakis, P. I. Tsiantas, G. Tsaniklidis, M. Landi, M. Psychoyou and C. Fasseas, "Changes in sugar metabolism associated to stem bark thickening partially assist young tissues of Eriobotrya japonica seedlings under boron stress," *Plant Physiol.,* vol. 231, pp. 337-345, 2018.

[138] H. Mahboobi, M. Yucel and H. A. Oktem, "Nitrate reductase and glutamate dehydrogenase activities of resistant and sensitive cultivars of wheat and barley under boron toxicity," *J. Plant Nutr.,* vol. 25, pp. 1829-1837, 2002.

[139] M. T. Öz, R. Yılmaz and F. G. L. D. Eyidoğan, "Microarray Analysis of Late Response to Boron Toxicity in Barley (Hordeum vulgare L.) Leaves," *Turkish Journal of Agriculture and Forestry,* vol. 33, no. 2, pp. 191-202, 2009.

[140] F. Aquea, F. Federici, C. Moscoso, A. Vega, P. Jullian, J. Haseloff and P. Arce-Johnson, "A molecular framework for the inhibition of Arabidopsis root growth in response to boron toxicity," *Plant Cell Environ.,* vol. 35, no. 4, pp. 719-734, 2012.

[141] H. Tombuloglu, G. Kekec, S. M. S and T. Unver, "Transcriptome-wide identification of R2R3-MYB transcription factors in barley with their boron responsive expression analysis," *Mol Genet Genomics,* vol. 288, pp. 141-155, 2013.

[142] Y. Hua, Y. Feng, T. Zhou and F. Xu, "Genome-scale mRNA transcriptomic insights into the responses of oilseed rape (Brassica napus L.) to varying boron availabilities," *Plant Soil,* vol. 416, pp. 205-225, 2017.

[143] Z. Xie, T. M. Nolan, H. Jiang and Y. Yin, "AP2/ERF Transcription Factor Regulatory Networks in Hormone and Abiotic Stress Responses in Arabidopsis," *Front. Plant Sci.,* 2019.